NUMERICAL ANALYSIS AND PHENOMENOLOGY OF HOMOGENEOUS, ISOTROPIC TURBULENCE GENERATED BY HIGHER ORDER MODELS OF TURBULENCE

by

Monika Neda

B.S. in Mechanical Engineering - Engineer for Development, Technical Faculty "Mihajlo Pupin", University of Novi Sad, 2001

Submitted to the Graduate Faculty of
the Department of Mathematics in partial fulfillment
of the requirements for the degree of
Doctor of Philosophy

University of Pittsburgh

2007

UNIVERSITY OF PITTSBURGH

MATHEMATICS DEPARTMENT

This dissertation was presented

by

Monika Neda

It was defended on

May 4th 2007

and approved by

Prof. William J. Layton, University of Pittsburgh

Prof. Beatrice Riviere, University of Pittsburgh

Prof. Ivan Yotov, University of Pittsburgh

Prof. Noel Walkington, Carnegie Mellon University

Dissertation Director: Prof. William J. Layton, University of Pittsburgh

NUMERICAL ANALYSIS AND PHENOMENOLOGY OF HOMOGENEOUS, ISOTROPIC TURBULENCE GENERATED BY HIGHER ORDER MODELS OF TURBULENCE

Monika Neda, PhD

University of Pittsburgh, 2007

Turbulence appears in many processes in the nature and it is connected with many engineering, biophysical and climate applications. Therefore, the accurate, efficient and reliable simulation of turbulent flows is an essential difficulty in many current applications. Fundamental and universal (i.e. mathematical) insights into fluid structures will enable such simulations.

To that end, we apply the phenomenology of homogeneous, isotropic turbulence to a family of Large Eddy Simulation (LES) models, the so-called family of Approximate Deconvolution Models (ADM). We establish that the models themselves have an energy cascade with two asymptotically different inertial ranges. Delineation of these gives insight into the resolution requirements of using ADM.

A correct prediction of a $3D$ turbulent flow means getting the energy balance and rotational structures correct, i.e., it means (in the large) matching the energy and helicity statistics. Thus, we consider the prediction of energy and helicity statistics of the family of Approximate Deconvolution Models of turbulence. We show that the family of ADM has a helicity cascade that it is linked to its energy cascade and predicted correctly over the large/resolved scales.

Turbulent flows are very rich in scales and to be able to capture all of them, we need to use a very fine mesh. Unfortunately, even with the amazing development of the computer power, we are not able to perform such simulations. Thus, many numerical regularization

(aiming to truncate the small scales) have been explored in computational fluid dynamics. We investigated one of such regularization, called the Time Relaxation Model (TRM). We apply the phenomenology of homogeneous, isotropic turbulence to understand how the time relaxation term, by itself, acts to truncate solution scales and to use this understanding to give insight into coefficient selection.

We also study the stability and convergence analysis of a finite element discretization of TRM. Next we complement this with an experimental study of the convergence rates and of the effect the time relaxation term has on the large scales of a flow near a transitional point.

Acknowledgements

I would like to thank everyone who has helped me scientifically and personally to write this thesis. The work would not have been possible without their support during these hard times and at the same time beautiful years as a graduate student and the years before that as well.

I am forever thankful to my advisor, Prof. William Layton, for his support, encouragement, guidance and inspiration over the last few years. He spent a lot of time teaching me the beautiful and challenging mathematics of the Navier-Stokes equations.

I would like to express my appreciation to Professors Beatrice Riviere, Ivan Yotov and Noel Walkington for teaching and preparing me for research and for their helpful consultations and discussions.

A major part of this work was influenced by Professors William Layton and Vincent Ervin, as well as my friends/colleagues Dr. Carolina Manica and Dr. Leo Rebholz. I would like to thank them for a continuous time of joint effort and work presented in Chapters 4, 5, 6 and 7 and in [39, 37, 38, 58]. I would like to thank the *FreeFem++* team, for making their software available and especially Prof. Frederich Hecht, for some suggestions. I also thank Professor Constantine Magda for being a great mathematical and personal support during my graduate studies at University of Pittsburgh.

A warm and special thank you goes to my parents and my sister for putting up with me during the difficult times and for their invaluable support and love.

Last but not least, I would like to thank my husband, Milan Jevtic, for his endless love, encouragement and great understanding. His support means more than I can ever put into words. I appreciate everything that he has done for me.

To my husband, Milan, and my parents, Ana and George

TABLE OF CONTENTS

LIST OF TABLES

LIST OF FIGURES

1.0 INTRODUCTION

Turbulence is part of everyday life and it is all around us. Turbulence controls the drag on cars, aeroplanes and bridges. It also dictates the weather forecast through its influence on atmospheric and oceanic flows and it is also important in geophysics. Turbulent convection in the core of the earth is what maintains the earth's magnetic field despite the natural forces decay. Turbulence has a great impact on many engineering and biophysical applications. For example, the flow of the coolant in the core of a nuclear reactor is turbulent. Regarding the biophysical applications, the air flowing in and out of our lungs and the circulation of blood in arteries are turbulent processes. Scientists have studied turbulence for years and turbulent motion has been extensively discussed in literature (see [20, 47, 15]) but the essence of this complex phenomenon is still lacking sufficient understanding and clearness. One common way to describe turbulence is by listing its characteristics. Based on [6] we give a summary here:

irregularity: main reason why it is problematic and difficult to describe turbulent motion as a function of time and space coordinates. Sensitive dependence on the initial and boundary conditions makes fluid flow irregular both in time and in space so that a statistical description (averaging) is needed;

diffusivity: causes rapid mixing and increased rates of momentum, heat and mass transfer. It is the single most important feature from the practical point of view;

Reynolds number: turbulent flows often originate as an instability of laminar flows as the Reynolds number becomes too large;

three dimensional vorticity: vorticity cannot be created or destroyed within the interior of a flow. It can spread (by diffusion) and it can be moved from place to place (by

advection). The implication is that vorticity is generated in boundary layers and then released into the turbulent flow which is a spatially distribution of vorticity. Thus it is impossible to imagine irrotational turbulent flow;

dissipation: turbulent flows are always dissipative. The turbulent motion decays if there is no external source of energy to make up for this kinetic energy loss. Viscous effects will result in the conversion of kinetic energy of the flow into heat;

continuum: even the smallest scales are far larger than any molecular length scale.

The flow of water over a simple smooth object, such as a sphere, at very low speeds is laminar, i.e., the flow is smooth (though it may involve vortices on a large scale). As the speed increases, at some point the transition is made to turbulent ("chaotic") flow. In turbulent flow, unsteady vortices appear on many scales and interact with each other. Drag due to boundary layer friction increases. The structure and location of boundary layer separation often changes, sometimes resulting in a reduction of overall drag. The Navier-Stokes equations (NSE), named after Claude-Louis Navier (French engineer and physicist) and George Gabriel Stokes (Irish mathematician and physicist), are derived directly from conservation laws and are the governing equations that describe the complex motion of turbulence. The NSE are nonlinear partial differential equations and the nonlinearity makes most problems difficult or impossible to solve and is part of the cause of turbulence. Despite the fact that the governing equations have been known for one and a half centuries, there is still surprisingly little we can predict with certainty. The intricacy with these equations that we encounter is that, except for some very simple flows, there is no analytical solution. Therefore, understanding turbulence continues to be a great challenge for scientists. A million dollar prize was offered in May 2000 by the Clay Mathematics Institute to whoever makes preliminary progress toward a mathematical theory which will help in the understanding of this phenomenon. Since turbulence is inherently a multi-disciplinary phenomena, each area can bring interesting and useful insights to its development. Not being able to find the analytical solution directs us to the approach to compute the numerical approximation directly by using a discretization of the NSE such that all the persistent eddies are resolved. But the difficulty with this is that

"It must be admitted that the problems are too vast to be solved by a direct computational attack"

J. von Neumann, 1949.

This is still true today for simulation of turbulent flows and provides the motivation for the development and mathematical analysis of turbulence models. These models should lead to an economical computable flow (i.e. flow that requires a much smaller number of degrees of freedom for its computation) but still contains important properties of the original turbulent flow governed by the NSE. Thus, to begin, we consider the incompressible Navier-Stokes equations in a periodic box in $\mathbb{R}^3$

$$\begin{aligned} \mathbf{u}_t + \mathbf{u}\cdot\nabla\mathbf{u} - Re^{-1}\triangle\mathbf{u} + \nabla p &= \mathbf{f} \quad \text{in } \Omega = (0,L)^3,\ t>0, \\ \nabla\cdot\mathbf{u} &= 0 \quad \text{in } (0,L)^3, \end{aligned} \tag{1.1}$$

subject to periodic (with zero mean) conditions

$$\begin{aligned} \mathbf{u}(\mathbf{x}+L\mathbf{e}_j,t) &= \mathbf{u}(\mathbf{x},t) \quad j=1,2,3 \quad \text{and}, \\ \int_\Omega \phi\, d\mathbf{x} &= 0 \ \text{ for } \ \phi = \mathbf{u},\ \mathbf{u}_0,\ \mathbf{f},\ p. \end{aligned} \tag{1.2}$$

where $\mathbf{u}$ is the velocity of fluid flow, p is the pressure, $\mathbf{f}$ is the external body force. The Navier-Stokes equations (1.1) representing the conservation of momentum and mass are in the non-dimensional form with Reynolds number Re being the control parameter of the flow. It is named after British fluid dynamics engineer, Osborne Reynolds ($1842-1912$), who proposed it in 1883. From the physical point of view, Re represents the ratio of the inertial forces ($U\rho$) and the viscous forces (μ/L) and is given by

$$Re = \frac{\rho UL}{\mu} = \frac{UL}{\nu}$$

where

U - characteristic velocity,

L - characteristic length,

ρ - fluid density,

μ - dynamic viscosity,

$\nu := \frac{\mu}{\rho}$ - kinematic viscosity.

In the mathematical setting of the Navier-Stokes equations, the Reynolds number makes the difference between laminar and turbulent flow. Laminar flow occurs at low Reynolds numbers, where viscous forces are dominant, and is characterized by smooth, constant fluid motion, while turbulent flow, on the other hand, occurs at high Reynolds numbers and is dominated by inertial forces, producing random eddies, vortices and other flow fluctuations. A few representative values of Re are given in Table 1.

1 cm sphere moving 1 cm/s in water	$Re = 100$
cars (characteristic speed 3 m/s)	$Re = 6 \times 10^5$
airplanes (characteristic speed 30m/s)	$Re = 2 \times 10^7$
atmospheric flows	$Re = 10^{20}$

Table 1: Representation values of Re

In this respect, based on Table 1 and present computational resources, the Direct Numerical Simulation (DNS) of turbulent flows are not economical or even feasible!

1.1 CHAPTER DESCRIPTION

One promising approach to the simulation of turbulent flows is to develop turbulence models that are predicting the large/resolved scales (i.e. the scales bigger than the averaging radius, usually denoted by δ). The large scales are believed to be deterministic and the small scales (accepting Kolmogorov's description) have a universal structure so, in principle, their mean effects on the large scales should be model-able. The crudest estimate of cost is

$$\Delta x = \Delta y \ = \Delta z = O(\delta),$$

with thus $O(\delta^{-3})$ storage required in space per time step. On the other hand, it is entirely possible that the computational mesh must be smaller than $O(\delta)$ to predict the $O(\delta)$

structures correctly. It is also entirely possible that, since turbulence models are themselves inexact and uncertain, solutions to a model contain persistent energetic structures smaller than $O(\delta)$. The nonlinear interactions and the sensitivity to perturbations of the models might also introduce unintended and persistent small scales. To that end, the core of this thesis is about the predictions of energy and helicity statistics, i.e. their cascade and derivation of the micro-scale (i.e. the scale of the smallest persistent structures in the models' solution) for turbulence models. Another aspect that also deserves attention is the classical numerical analysis of algorithms of turbulence models. These topics are addressed in the thesis with a following outline.

In Chapter 2 the energy and helicity for the Navier-Stokes equations are presented. The Kolmogorov 1941 theory, known as K41, is summarized too. Chapter 3 is focused on proving preliminary properties of the approximate deconvolution operator that is used for the closure problem of the family of ADM and for driving the unresolved fluctuations to zero in simulation governed by TRM.

Chapter 4 and 6 investigate the following questions for the family of ADM and TRM: *What is the length scale of the smallest persistent eddy in the models' solution?* (This length scale corresponds to the Kolmogorov dissipation length scale for a turbulent flow.) *Do solutions of the models exhibit an energy cascade and, if so, what are its details? How do the models act to truncate the small eddies?* Inspired by Muschinsky's study of the Smagorinsky model [46], the answers to these questions will come from two simple but powerful tools: a precise proof of the energy balance for the models themselves and Kolmogorov's similarity theory, suitably adapted. In particular, the ADM's energy balance contains both an enhanced energy dissipation and a modification to the kinetic energy that induce a secondary energy cascade and acceleration of scale truncation. The aim of the time relaxation study is to drive the unresolved fluctuations in a computational simulation to zero exponentially fast by an appropriate choice of its coefficient. We show that TRM can truncate the scales up to the filter length-scale by a specific selection of the time relaxation coefficient.

In Chapter 5 the accuracy of flow statistics (and thus the physical fidelity) related to rotational structures in turbulent flows is considered. In other words, we consider statistically stationary, homogeneous, isotropic turbulence predicted by the ADM, develop the helicity

and time-averaged helicity statistics predicted by the ADM and evaluate their accuracy up to the cutoff frequency / filter length scale. The models' energy and helicity cascade at the correct rate (rate of the NSE) over the resolved scales and a faster rate over the underresolved scales. Supported by a strong physical reasoning that scales with no energy should not be rotational, we show that the inertial range of helicity is contained in the inertial range of energy (which means that the smallest active helical scales are bigger than the energetic micro-scales).

In Chapter 7 a classical analysis for a fully discretized continuous finite element scheme of Time Relaxation Model is developed. We prove the existence of the discrete finite element solution together with a stability bound and derived optimal error estimates. Besides the computational investigation of the theoretical obtained rates, a flow very close to its transition from one regime to another (from equilibrium to time dependent via shedding of eddies behind the forward-backward step) is studied.

Finally, Chapter 8 consists of conclusions and future research.

2.0 ENERGY AND HELICITY IN TURBULENCE

2.1 ENERGY BALANCE

The key idea in making progress in the mathematical understanding of turbulent flows governed by the Navier-Stokes equations is the notion of energy balance. Energy balance is a systematic presentation of energy flows and transformations in a fluid. Theoretical basis for an energy balance is the first law of thermodynamics according to which energy cannot be created or destroyed, only modified in form.

If $\mathbf{u}, p$ is a smooth solution of (1.1) then multiplying the momentum equation by $\mathbf{u}$, integrating over $\Omega = (0, L)^3$, integrating by parts and integrating in time gives

$$\begin{aligned} \frac{1}{2}\int_\Omega |\mathbf{u}(\mathbf{x},t)|^2 d\mathbf{x} \;\; &+ \;\; \int_0^t Re^{-1} \int_\Omega |\nabla \mathbf{u}(\mathbf{x},t')|^2 d\mathbf{x}\, dt' \\ &= \;\; \frac{1}{2}\int_\Omega |\nabla \mathbf{u}(\mathbf{x},0)|^2 d\mathbf{x} \; + \; \int_0^t \int_\Omega \mathbf{f}(\mathbf{x},t') \cdot \mathbf{u}(\mathbf{x},t')\, d\mathbf{x}\, dt' \end{aligned} \tag{2.1}$$

Looking at the energy equality, there are three terms involved:

$$\begin{aligned} &\text{The kinetic energy:} \quad E(\mathbf{u})(t) := \frac{1}{2}\frac{1}{L^3}\int_\Omega |\mathbf{u}(\mathbf{x},t)|^2 d\mathbf{x}\,, \\ &\text{The energy dissipation rate:} \quad \varepsilon(\mathbf{u})(t) := \frac{Re^{-1}}{L^3}\int_\Omega |\nabla \mathbf{u}(\mathbf{x},t)|^2 d\mathbf{x}\,, \\ &\text{Power input via body forces:} \quad P(\mathbf{u})(t) := \frac{1}{L^3}\int_\Omega \mathbf{f}(\mathbf{x},t)\cdot \mathbf{u}(\mathbf{x},t)\, d\mathbf{x}\,. \end{aligned}$$

With the above definitions (2.1) is equivalent to

$$E(\mathbf{u})(t) \; + \; \int_0^t \varepsilon(\mathbf{u})(t')\, dt' = E(\mathbf{u})(0) + \int_0^t P(\mathbf{u})(t')\, dt'\,.$$

Thus, the energy equality (2.1) describes the evolution of the kinetic energy in a fluid's flow and has the following physical interpretation:

$$\begin{aligned} \text{kinetic energy(t)} \quad &+ \quad \text{total energy dissipated} \\ &= \quad \text{kinetic energy(0)} + \text{total energy input by body forces.} \end{aligned}$$

2.1.1 Spectral Representation of the Kinetic Energy

Recall that we impose the zero mean condition and thus we can expand the fluid velocity in a Fourier series

$$\mathbf{u}(\mathbf{x},t) = \sum_{\mathbf{k}} \widehat{\mathbf{u}}(\mathbf{k},t) e^{-i\mathbf{k}\cdot\mathbf{x}}, \text{ where } \mathbf{k} = \frac{2\pi\mathbf{n}}{L} \text{ is the wave-number and } \mathbf{n} \in \mathbb{Z}^3. \tag{2.2}$$

The Fourier coefficients are given by

$$\widehat{\mathbf{u}}(\mathbf{k},t) = \frac{1}{L^3}\int_\Omega \mathbf{u}(\mathbf{x},t) e^{-i\mathbf{k}\cdot\mathbf{x}} d\mathbf{x}.$$

Magnitudes of $\mathbf{k}, \mathbf{n}$ are defined by

$$\begin{aligned} |\mathbf{n}| &= \{|n_1|^2 + |n_2|^2 + |n_3|\}^{\frac{1}{2}}, |\mathbf{k}| = \frac{2\pi|\mathbf{n}|}{L}, \\ |\mathbf{n}|_\infty &= \max\{|n_1|, |n_2|, |n_3|\}, |\mathbf{k}|_\infty = \frac{2\pi|\mathbf{n}|_\infty}{L}. \end{aligned}$$

The length-scale of the wave-number $\mathbf{k}$ is defined by $l = \frac{2\pi}{|\mathbf{k}|_\infty}$. Parseval's equality implies that the energy in the flow can be decomposed by wave-number as follows. For $\mathbf{u} \in L^2(\Omega)$,

$$\frac{1}{L^3}\int_\Omega \frac{1}{2}|\mathbf{u}(\mathbf{x},t)|^2 d\mathbf{x} = \sum_{\mathbf{k}} \frac{1}{2}|\widehat{\mathbf{u}}(\mathbf{k},t)|^2 =$$

$$= \sum_k \left(\sum_{|\mathbf{k}|=k} \frac{1}{2}|\widehat{\mathbf{u}}(\mathbf{k},t)|^2 \right), \text{where } \mathbf{k} = \frac{2\pi\mathbf{n}}{L} \text{ is the wave-number and } \mathbf{n} \in \mathbb{Z}^3.$$

Let $< \cdot >$ denote long time averaging (e.g., Reynolds, [50])

$$< \phi > (\mathbf{x}) := \lim_{T\to\infty} \sup \frac{1}{T}\int_0^T \phi(\mathbf{x},t) dt. \tag{2.3}$$

Definition 2.1. *The kinetic energy distribution functions are defined by*

$$\begin{aligned} E(k,t) &= \frac{L}{2\pi}\sum_{|\mathbf{k}|=k}\frac{1}{2}|\widehat{\mathbf{u}}(\mathbf{k},t)|^2, \text{ and} \\ E(k) &:= < E(k,t) >, \end{aligned}$$

Parseval's equality thus can be rewritten as

$$\begin{aligned} \frac{1}{L^3}\int_\Omega \frac{1}{2}|\mathbf{u}(\mathbf{x},t)|^2 d\mathbf{x} = \frac{2\pi}{L}\sum_k E(k,t), \text{ and} \\ < \frac{1}{L^3}\int_\Omega \frac{1}{2}|\mathbf{u}(\mathbf{x},t)|^2 d\mathbf{x} >= \frac{2\pi}{L}\sum_k E(k). \end{aligned}$$

2.2 A SYNOPSIS OF K41 PHENOMENOLOGY

Turbulent flows consist of three dimensional eddies of various sizes. In 1941, I. Kolmogorov gave a remarkable, universal description of the eddies in turbulent flow by combining a judicious mix of physical insight, conjecture, mathematical analysis and dimensional analysis, e.g., Frisch [20], Pope [47]. In his description, the largest eddies are deterministic in nature. Those below a critical size are dominated by viscous forces, and die very quickly due to these forces. This critical length scale (the Kolmogorov micro-scale) is $\eta = O(Re^{-3/4})$ [1] in $3D$. From this estimate, it follows that direct numerical simulation of a $3D$ flow thus requires $\Delta x = \Delta y = \Delta z = O(Re^{-3/4})$ giving $O(Re^{+9/4})$ mesh points in space per time step, and thus is often not computationally economical or even feasible. This estimate is based upon existence of an energy cascade in turbulent flow problems and Kolmogorov's estimate of the micro-scale at the bottom of the energy cascade. Since this energy cascade theory is extended herein beyond the Navier-Stokes equations, the answers to important questions about it must be reviewed.

Why do solutions of the Navier-Stokes equations exhibit an energy cascade? And, should it be expected that solutions of turbulence models have their own energy cascade? The answer to the first question has been understood since the work of L. F. Richardson and I.

[1] The length scale of the smallest persistent eddy is traditionally denoted by η rather than l.

Kolmogorov. We shall briefly review the answer because its answer also contains the answer to the second question that we are interested in. The Navier-Stokes equations and their solutions have the following well-known features:

- If $\nu = 0$ the total kinetic energy of the flow is exactly conserved [2]:

$$E(\mathbf{u})(t) = E(\mathbf{u})(0) + \int_0^t P(\mathbf{u})(t')\, dt'.$$

- The nonlinearity conserves energy globally (since $\int_\Omega \mathbf{u}\cdot\nabla\mathbf{u}\cdot\mathbf{u}d\mathbf{x} = 0$) but acts to transfer energy to smaller scales by breaking down eddies into smaller eddies (for example, if $\mathbf{u} \simeq (U\sin(\frac{\pi x_1}{l}), 0, 0)^{tr}$ has wave length l and frequency $\frac{\pi}{l}$ then $\mathbf{u}\cdot\nabla\mathbf{u} \simeq \frac{U^2\pi}{2l}(\sin(\frac{\pi x_1}{l/2}), 0, 0)^{tr}$ has shorter wave length $\frac{l}{2}$).

- If $\nu > 0$, them the viscous terms dissipate energy from the flow globally:

$$E(\mathbf{u})(t) + \int_0^t \varepsilon(\mathbf{u})(t')dt' = E(\mathbf{u})(0) + \int_0^t P(\mathbf{u})(t')\, dt', \text{ where } \varepsilon(\mathbf{u})(t') \geq 0.$$

- For Re large the energy dissipation due to the viscous terms is negligible except on very small scales of motion. For example, if $\mathbf{u} \simeq (U\sin(\frac{\pi x_1}{l}), 0, 0)^{tr}$ then (considering the dimensional NSE)

$$\begin{aligned} \text{viscous term on this scale} &= -\nu\triangle\mathbf{u} \simeq \pi^2\frac{\nu U}{l^2}(\sin(\frac{\pi x_1}{l}), 0, 0)^{tr}, \text{from which:} \\ \text{energy dissipation on this scale} &= \varepsilon(\mathbf{u}) \simeq \frac{C}{L^3}\frac{\nu U}{l^2}. \end{aligned}$$

  Thus the nonlinear term dominates and the viscous term is negligible if

$$\frac{U^2}{l} >> \frac{\nu U}{l^2} \;\Rightarrow\; \frac{lU}{\nu} >> 1 \text{ , i.e., } Re >> 1.$$

- The forces driving the flow input energy persistently into the largest scales of motion.

[2] For the physical reasoning in this section it is perhaps appropriate to suppose that the energy equality holds and sidestep the deeper questions concerning weak vs. strong solutions and energy equality vs. energy inequality, e.g., [21], [22].

The picture of the energy cascade that results from these effects is thus: *energy is input into the largest scales of the flow. There is an intermediate range in which nonlinearity drives this energy into smaller and smaller scales and conserves the global energy because dissipation is negligible. Eventually, at small enough scales dissipation is nonnegotiable and the energy in those smallest scales is driven to zero exponentially fast.* This is the physical reasoning behind Richardson's famous description:

> "Big whirls have little whirls
> That feed on their velocity,
> And little whirls have lesser whirls,
> And so on to viscosity."

Inspired by this description, in 1941 I. Kolmogorov gave a quantitative and universal characterization of the energy cascade (often called the K-41 theory). The most important components of the K-41 theory are the time (or ensemble) averaged energy dissipation rate, ε, and the distribution of the flows averaged kinetic energy across wave-numbers, $E(k)$. Given the velocity field of a particular flow, $\mathbf{u}(\mathbf{x}, t)$, the (time averaged) energy dissipation rate of that flow is defined to be

$$\varepsilon := < \frac{1}{L^3} \int_{\Omega} \nu |\nabla \mathbf{u}(\mathbf{x}, t)|^2 d\mathbf{x} > . \tag{2.4}$$

Further, the K-41 theory states that at high enough Reynolds numbers there is a range of wave-numbers known as the inertial range, beyond which the kinetic energy in a turbulent flow is negligible, and in this range

$$E(k) = \alpha \varepsilon^{\frac{2}{3}} k^{-\frac{5}{3}}, \tag{2.5}$$

where α is the universal Kolmogorov constant whose value is generally believed to be between 1.4 and 1.7 (for example, Wyngaard and Pao [61] found a value of $\alpha = 1.62$ in studies of atmospheric turbulence), k is the wave-number and ε is the particular flow's energy dissipation rate. The energy dissipation rate ε is the only parameter which differs from one flow to another. Indeed, in Pope [47], figure 6.14 page 235 in [47], the power spectrums of 17 different turbulent flows taken from Saddoughi and Veeravalli [53] (which also contains the references to the particular experiments) are plotted on log-log plots. The slope of the

linear region in this plot has the universal value of $-\frac{5}{3}$ for all 17 turbulent flows, exactly corresponding to the $k^{-\frac{5}{3}}$ law.

We review this argument of Kolmogorov, which is adapted in our work. It begins with a physical conjecture that:

Conjecture 2.1. *The time averaged kinetic energy only depends on the time averaged energy dissipation rate ε and the wave-number k.*

Beginning with this, postulate a simple power law dependency of the form

$$E(k) \simeq C\varepsilon^a k^b. \tag{2.6}$$

If this relation is to hold the units, denoted by $[\cdot]$ on the LHS must be the same as the units on the RHS, $[LHS] = [RHS]$. The three quantities in the above have the units

$$[k] = \frac{1}{length},\ [\varepsilon] = \frac{length^2}{time^3},\ [E(k)] = \frac{length^3}{time^2}.$$

Inserting these units into the above relation gives

$$\begin{aligned} \frac{length^3}{time^2} &= \frac{length^{2a}}{time^{3a}}\frac{1}{length^b} = length^{2a-b}time^{-3a},\ \text{giving} \\ 3a &= 2, 2a-b = 3,\ \text{or}\ a = \frac{2}{3}, b = -\frac{5}{3}. \end{aligned}$$

Thus, Kolmogorov's law follows

$$E(k) = \alpha\varepsilon^{\frac{2}{3}}k^{-\frac{5}{3}},\ \text{over the inertial range}\ 0 < k \leq C(LRe^{-\frac{3}{4}})^{-1}.$$

The above estimate $\eta \sim LRe^{-\frac{3}{4}}$ for the Kolmogorov micro-scale (i.e. the end of the inertial range) is derived by similar physical reasoning. Let the reference large scale velocity and length (which are used in the definition of the Reynolds number) be denoted by U, L. At the scales of the smallest persistent eddies (the bottom of the inertial range) we shall denote the smallest scales of velocity and length by v_{small}, η. We form two Reynolds numbers:

$$Re = \frac{UL}{\nu},\ \ Re_{small} = \frac{v_{small}\eta}{\nu}.$$

The global Reynolds number measures the relative size of viscosity on the large scales and when Re is large the effects of viscosity on the large scales are then negligible. The smallest

scales Reynolds number similarly measures the relative size of viscosity on the smallest persistent scales. Since it is non-negligible we must have

$$Re_{small} \simeq 1, \text{ equivalently } \frac{v_{small}\eta}{\nu} \simeq 1.$$

Next comes an assumption of statistical equilibrium:

Energy input at large scales = Energy dissipation at smallest scales.

The largest eddies have energy which scales like $O(U^2)$ and associated time scale $\tau = O(\frac{L}{U})$. The rate of energy transfer/energy input is thus $O(\frac{U^2}{\tau}) = O(\frac{U^3}{L})$. The small scales energy dissipation from the viscous terms scales like

$$\varepsilon_{small} \simeq \nu|\nabla u_{small}|^2 \simeq \nu(\frac{v_{small}}{\eta})^2.$$

Thus we have the second ingredient:

$$\frac{U^3}{L} \simeq \nu(\frac{v_{small}}{\eta})^2.$$

Solving the first equation for v_{small} gives $v_{small} \simeq \frac{\nu}{\eta}$. Inserting this value for the small scales velocity into the second equation, solving for the length-scale η and rearranging the result in terms of the global Reynolds number gives the following estimate for η which determines the above estimate for the highest wave-number in the inertial range:

$$\eta = \eta_{Kolmogorov} \simeq Re^{-\frac{3}{4}}L\,.$$

This estimate for the size of the smallest persistent solution scales is the basis for the estimates of $O(Re^{\frac{9}{4}})$ mesh-points in space per time step for DNS of turbulent flows.

2.3 HELICITY FOR THE NAVIER-STOKES EQUATIONS

The study of helicity in fluid flow and turbulence has only recently begun. It was not until 1961 that helicity's inviscid invariance was discovered by Moreau [45]. Moffatt and Tsoniber [44] gave a good summary of the early results. Later Moffatt [43] showed that helicity is nonzero if and only if the flow field is not rotationally symmetric. This topological characterization lead to the commonly accepted interpretation: helicity measures the degree to which the vortex lines are knotted and intertwined. If $\mathbf{u}, p$ is a smooth solution of (1.1) then multiplying the momentum equation by $\nabla \times \mathbf{u}$, integrating over $\Omega = (0, L)^3$, integrating by parts and integrating in time gives

$$H(\mathbf{u})(t) + \int_0^t \gamma(\mathbf{u})(t')\, dt' = H(\mathbf{u})(0) + \int_0^t \frac{1}{L^3} \int_\Omega \mathbf{f}(\mathbf{x}, t') \cdot \nabla \times \mathbf{u}(\mathbf{x}, t)\, d\mathbf{x}\, dt' \,. \tag{2.7}$$

where:

$$\text{The helicity: } H(\mathbf{u})(t) := \frac{1}{L^3} \int_\Omega \mathbf{u}(\mathbf{x}, t) \cdot (\nabla \times \mathbf{u}(\mathbf{x}, t)) d\mathbf{x}\,,$$

$$\text{The helicity dissipation rate: } \gamma(\mathbf{u})(t) := \frac{Re^{-1}}{L^3} \int_\Omega \nabla \times \mathbf{u}(\mathbf{x}, t) \cdot (\nabla \times)^2 \mathbf{u}(\mathbf{x}, t)\, d\mathbf{x}\,.$$

Based on its above mathematical definition helicity is a rotational meaningful quantity

Therefore, based on (2.1) and (2.7), both energy and helicity are conserved by the Euler equations and dissipated (primarily at the small scales) by viscosity. There is considerable evidence that both energy and helicity exhibit cascades and the details of their respective cascades are intertwined, e.g. André and Lesieur [5]. Recent theoretical studies, which have been experimentally confirmed by Bourne and Orszag [8], have suggested that for homogeneous, isotropic turbulence averaged fluid velocities exhibit a joint energy and helicity cascade through the inertial range of wave-numbers given by

$$E(k) = C_E \epsilon^{2/3} k^{-5/3}, \qquad H(k) = C_H \gamma \epsilon^{-1/3} k^{-5/3}, \tag{2.8}$$

where k is wave-number, ϵ the time averaged energy dissipation rate, and γ the time averaged helicity dissipation rate, see Q. Chen, S. Chen and Eyink [11], Q. Chen, S. Chen, Eyink and Holm [12], Ditlevsen and Giuliani [16]. The cascades are referred to as "joint" because they

travel with the same speed through wave space (i.e. the exponents of k are equal). The energy cascade given in (2.8) is the famous Kolmogorov cascade, and Q. Chen, S. Chen and Eyink [11] showed that the helicity cascade in (2.8) is consistent for wave-numbers up to the standard Kolmogorov wave-number, $k_E = \nu^{-3/4}\epsilon^{1/4}$.

2.3.1 Spectral Representation of Helicity

Each Fourier mode $\hat{\mathbf{w}}(\mathbf{k},t)e^{i\mathbf{k}\cdot\mathbf{x}}$ has three degrees of freedom. Given a Fourier mode, we can calculate

$$\nabla\cdot(\hat{\mathbf{w}}(\mathbf{k},t)e^{i\mathbf{k}\cdot\mathbf{x}}) = i\mathbf{k}\cdot\hat{\mathbf{w}}(\mathbf{k},t)e^{i\mathbf{k}\cdot\mathbf{x}}\,,$$

and

$$\nabla\times(\hat{\mathbf{w}}(\mathbf{k},t)e^{i\mathbf{k}\cdot\mathbf{x}}) = i\mathbf{k}\times\hat{\mathbf{w}}(\mathbf{k},t)e^{i\mathbf{k}\cdot\mathbf{x}}.$$

Incompressibility implies the constraint $\mathbf{k}\cdot\hat{\mathbf{w}}(\mathbf{k},t)=0$ for all $\mathbf{k}$ leaving two remaining degrees of freedom in the Fourier mode. These two are most conveniently expressed (following Q.Chen, S.Chen and Eyink [11] and Waleffe [59]) as helical modes, defined next.

Definition 2.2. *For any given* $\mathbf{k}$*, the helical modes* $\mathbf{h}_\pm$ *are associated with orthogonal eigenvectors of the curl operator via* $i\mathbf{k}\times\mathbf{h}_\pm = \pm k\mathbf{h}_\pm$*:*

$$\nabla\times(\mathbf{h}_\pm(\mathbf{k})e^{i\mathbf{k}\cdot\mathbf{x}}) = \pm k\mathbf{h}_\pm(\mathbf{k})e^{i\mathbf{k}\cdot\mathbf{x}}.$$

We can thus write a Fourier mode's coefficient as

$$\hat{\mathbf{w}}(\mathbf{k},t) = a_+(\mathbf{k},t)\mathbf{h}_+ + a_-(\mathbf{k},t)\mathbf{h}_-.$$

The Fourier series (2.2) for the model's velocity can be further split, using the above, as

$$\mathbf{w}(\mathbf{x},t) = \sum_k \sum_{|\mathbf{k}|=k} \sum_{s=\pm} a_s(\mathbf{k},t)\mathbf{h}_s(\mathbf{k})e^{i\mathbf{k}\cdot\mathbf{x}}\,. \tag{2.9}$$

Using the above helical mode we can easily calculate, for example,

$$(\nabla\times)\mathbf{w}(\mathbf{x},t) = \sum_k \sum_{|\mathbf{k}|=k} \sum_{s=\pm} sk a_s(\mathbf{k},t)\mathbf{h}_s(\mathbf{k})e^{i\mathbf{k}\cdot\mathbf{x}}\,. \tag{2.10}$$

Similarly,

$$(\nabla\times)^n\mathbf{w}(\mathbf{x},t)=\sum_k\sum_{|\mathbf{k}|=k}\sum_{s=\pm}s^nk^na_s(\mathbf{k},t)\mathbf{h}_s(\mathbf{k})e^{i\mathbf{k}\cdot\mathbf{x}}. \tag{2.11}$$

Since the helical mode expansions (2.9) and (2.10) are themselves Fourier series, (2.9),(2.10) and Parseval's equality can be used exactly as for energy to give a modal decomposition of helicity and helicity dissipation as

$$H(\mathbf{w})(t) = \frac{2\pi}{L}\sum_k H(k,t), \text{ where} \tag{2.12}$$

$$H(k,t) := \frac{L}{2\pi}\sum_{|\mathbf{k}|=k}\sum_{s=\pm}sk\left|a_s(\mathbf{k},t)\right|^2. \tag{2.13}$$

and

$$\gamma(\mathbf{w})(t)=\frac{2\pi}{L}\sum_k\gamma(k,t), \text{ with} \tag{2.14}$$

$$\gamma(k,t):=\nu\frac{L}{2\pi}\sum_{|\mathbf{k}|=k}\sum_{s=\pm}k^2H(k,t). \tag{2.15}$$

The exact interpretation of helicity is not clear as clear as energy since both helicity and helicity dissipation can have two signs. We would like to have the result that when $H(\mathbf{w})(t)\geq 0$ then $\gamma(\mathbf{w})(t)\geq 0$ and when $H(\mathbf{w})(t)\leq 0$ then $\gamma(\mathbf{w})(t)\leq 0$. Based on the definitions of the helicity (2.12) and helicity dissipation (2.14), this is exactly true. In particular, the global positive and negative components of helicity, $H_+(\mathbf{w})(t)=\sum_k k\sum_{|\mathbf{k}|=k}\sum_{s=+}s\left|a_s(\mathbf{k},t)\right|^2$ and $H_-(\mathbf{w})(t)=\sum_k k\sum_{|\mathbf{k}|=k}\sum_{s=-}s\left|a_s(\mathbf{k},t)\right|^2$ are non-increasing functions of time based on summation.

3.0 APPROXIMATE DECONVOLUTION OPERATOR AND APPROXIMATE DECONVOLUTION MODELS

The deconvolution problem is central in both image processing, (see Bertero and Boccacci [7]) and turbulence modeling in Large Eddy Simulation, (see Berselli, Iliescu and Layton [6] and Geurts [24]). The basic problem in approximate deconvolution is: given $\overline{\mathbf{u}}$ find a *useful* approximations of $\mathbf{u}$. In other words, solve the following equation for an approximation which is appropriate for the application at hand

$$G\mathbf{u} = \overline{\mathbf{u}}, \text{ solve for } \mathbf{u}. \tag{3.1}$$

For most averaging operators, G is symmetric and positive semi-definite. Typically, G is not invertible or at least not stably invertible due to small divisor problems. Thus, this deconvolution problem is ill-posed.

Many spacial averaging operators associated with a length-scale δ are possible, e.g., Berselli, Iliescu and Layton [6], John [30] and Sagaut [54]. For specificity, we choose a simple differential filter, Germano [23] :given an L-periodic $\mathbf{u}$, its average $\overline{\mathbf{u}}$ is the unique L-periodic solution of

$$-\delta^2 \triangle \overline{\mathbf{u}} + \overline{\mathbf{u}} = \mathbf{u}, \text{ in } \Omega. \tag{3.2}$$

This filtering operation is often denoted $\overline{\phi} = G\phi$ with $G := (-\delta^2 \triangle + I)^{-1}$.

3.0.2 The van Cittert Algorithm

The deconvolution algorithm we consider was studied by van Cittert in 1931 and its use in LES pioneered by Stolz and Adams [2, 3]. For each $N = 0, 1, ...$ it computes an approximate

solution $\mathbf{u}_N$ to the deconvolution equation (3.1) by N steps of a fixed point iteration for the fixed point problem (see Bertero and Boccacci [7]):

$$\text{given } \overline{\mathbf{u}} \quad \text{solve } \mathbf{u} = \mathbf{u} + \{\overline{\mathbf{u}} - G\mathbf{u}\} \quad \text{for } \mathbf{u}.$$

The deconvolution approximation is then computed as follows.

Algorithm 3.1 (van Cittert approximate deconvolution algorithm)**.** $\mathbf{u}_0 = \overline{\mathbf{u}}$,

for n=1,2,...,N-1, perform

$\mathbf{u}_{n+1} = \mathbf{u}_n + \{\overline{\mathbf{u}} - G\mathbf{u}_n\}$

Call $\mathbf{u}_N = G_N\overline{\mathbf{u}}$.

By eliminating the intermediate steps, it is easy to find an explicit formula for the N^{th} deconvolution operator G_N

$$G_N\overline{\mathbf{u}} := \sum_{n=0}^{N}(I - G)^n\overline{\mathbf{u}}\,. \tag{3.3}$$

For example, the approximate deconvolution operator corresponding to $N = 0, 1, 2$ are:

$$\begin{aligned} G_0\overline{u} &= \overline{u}, \\ G_1\overline{u} &= 2\overline{u} - \overline{\overline{u}}, \\ G_2\overline{u} &= 3\overline{u} - 3\overline{\overline{u}} + \overline{\overline{\overline{u}}}. \end{aligned}$$

The corresponding transfer functions are:

$$\begin{aligned} \widehat{G_0}(k) &= 1, \\ \widehat{G_1}(k) &= 2 - \frac{1}{\delta^2k^2+1} = \frac{2\delta^2k^2+1}{\delta^2k^2+1}, \\ \widehat{G_2}(k) &= 1 + \frac{\delta^2k^2}{\delta^2k^2+1} + (\frac{\delta^2k^2}{\delta^2k^2+1})^2. \end{aligned}$$

It is insightful to plot the transfer functions, Figure 1.

The large scales are associated with the smooth components and with the wave-numbers near zero (i.e., $|\mathbf{k}|$ small). Thus, the fact that G_N is a very accurate solution of the deconvolution problem for the large scales is reflected in the above graph in that the transfer functions $\widehat{G_N}(k)$ have high order contact with $\frac{1}{1+\delta^2k^2}$ (i.e., exact deconvolution) near $k = 0$.

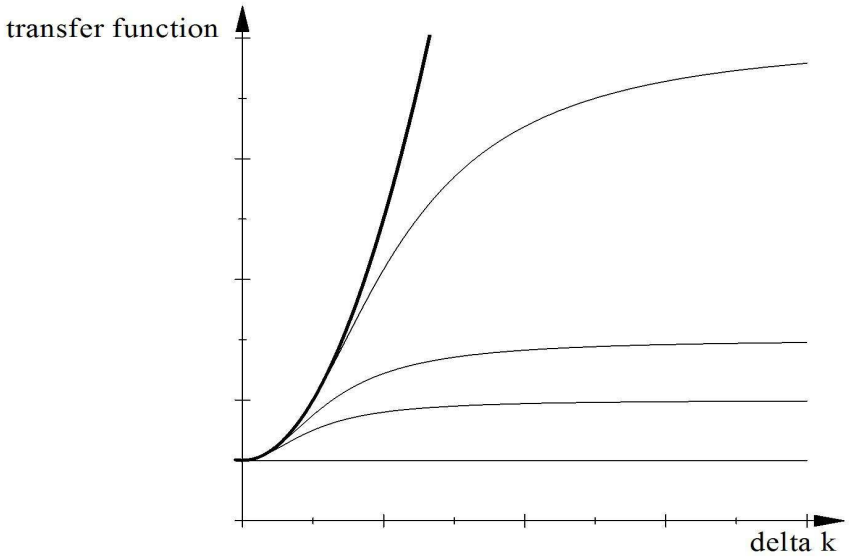

Figure 1: **Exact** and approximate deconvolution operators for N=0,1,2 and 7.

3.1 PROPERTIES OF APPROXIMATE DECONVOLUTION OPERATOR

The $L^2(\Omega)$ norm and inner product will be denoted by $\|\cdot\|$ and $(\cdot,\cdot)$. Likewise, the $L^p(\Omega)$ norms and the Sobolev $W_p^k(\Omega)$ norms are denoted by $\|\cdot\|_{L^p}$ and $\|\cdot\|_{W_p^k}$, respectively. For the semi-norm in $W_p^k(\Omega)$ we use $|\cdot|_{W_p^k}$. H^k is used to represent the Sobolev space W_2^k, and $\|\cdot\|_k$ denotes the norm in H^k. For functions $v(\mathbf{x},t)$ defined on the entire time interval $(0,T)$, we define

$$\|v\|_{\infty,k} := \sup_{0<t<T} \|v(t,\cdot)\|_k\,, \qquad \text{and} \qquad \|v\|_{m,k} := \left(\int_0^T \|v(t,\cdot)\|_k^m\, dt\right)^{1/m}.$$

We begin by reviewing a result of Stolz, Adams and Kleiser [56] and Dunca and Epshteyn [18].

Lemma 3.1. *[Error in approximate deconvolution] For any $\phi \in L^2(\Omega)$,*

$$\begin{aligned} \phi - G_N\overline{\phi} &= (I-G)^{N+1}\phi \\ &= (-1)^{N+1}\delta^{2N+2}\triangle^{N+1}G^{(N+1)}\phi\,. \end{aligned}$$

Proof. Let $B = I - G$. Since $\overline{\phi} = G\phi$, $\overline{\phi} = (I - B)\phi$. Since $G_N := \sum_{n=0}^{N} B^n$, a geometric series calculation gives

$$(I - B)G_N\overline{\phi} = (I - B^{N+1})\overline{\phi}.$$

Subtraction gives

$$\phi - G_N\overline{\phi} = G^{-1}B^{N+1}\overline{\phi} = B^{N+1}G^{-1}\overline{\phi} = B^{N+1}\phi.$$

Finally, $B = I - G$, so rearranging terms gives the claimed result

$$\begin{aligned} \phi - G_N\overline{\phi} &= (G^{-1} - I)^{N+1}G^{(N+1)}\phi \\ &= G^{(N+1)}((-1)^{N+1}\delta^{2N+2}\triangle^{N+1})\phi. \end{aligned}$$

□

Lemma 3.2. *G is a self-adjoint positive definite operator with eigenvalues*

$$\lambda(G) = \frac{1}{\delta^2 k^2 + 1}, \quad \textit{for } k = 1, 2, \ldots$$

Proof. The Laplacian operator is self-adjoint positive definite, and so are $-\delta^2\triangle + I$ and its inverse, G. Similarly, the eigenvalues of G are the inverse of the eigenvalues of $-\delta^2\triangle + I$. □

Lemma 3.3. *[Stability of approximate deconvolution] G_N is a self-adjoint, positive definite operator on $L_2(\Omega)$ with norm*

$$||G_N|| := \sup_{\phi \in L_2(\Omega)} \frac{||G_N\phi||}{||\phi||} = N + 1\,.$$

Proof. We summarize the proof from Berselli, Iliescu and Layton [6] for completeness. Since G_N is a function of G, it is also self-adjoint. Recall from Lemma 3.2 that the eigenvalues of G are between zero and one, accumulating at zero. By the spectral mapping theorem

$$\lambda(G_N) = \sum_{n=0}^{N} \lambda(I - G)^n = \sum_{n=0}^{N} (1 - \lambda(G))^n, \text{ and}$$

$$0 < \lambda(G) \leq 1 \text{ by the definition of operator G.}$$

Thus, $1 \leq \lambda(G_N) \leq N+1$, i.e., $\lambda(G_N) > 0$, so G_N is positive definite. Since G_N is self-adjoint, the operator norm $||G_N||$ is also easily bounded by the spectral mapping theorem by

$$||G_N|| = \sum_{n=0}^{N} \lambda_{max}(I-G)^n = \sum_{n=0}^{N} (1-\lambda_{min}(G))^n = N+1\,.$$

□

Definition 3.1. *The deconvolution weighted inner product and norm are*

$$(\phi,\psi)_N := (\phi, G_N\psi) \quad \textit{and} \quad ||\phi||_N = \sqrt{(\phi, G_N\phi)} \quad \textit{for } \phi,\psi \in L^2(\Omega)\,.$$

Remark 3.1. *Based on Lemma 3.3, the deconvolution weighted inner product and norm are well-defined.*

Lemma 3.4. *Consider the approximate deconvolution operator G_N as defined above. Then*

$$||\phi||^2 \leq ||\phi||_N \leq (N+1)||\phi||^2,\ \forall \phi \in L^2(\Omega)\ .$$

Proof. Recall that $1 \leq \lambda(G_N) \leq N+1$ from the proof of Lemma 3.3. Since G_N is a self-adjoint operator and its eigenvectors form an orthonormal basis of $L^2(\Omega)$, this proves the above equivalence of norms. □

The analysis of Time Relaxation Model involves information on the action of the operator H_N defined below.

Lemma 3.5. *Let the bounded linear operator $H_N : L^2(\Omega) \to L^2(\Omega)$ be defined by $H_N\phi = G_N G\phi$. Then, H_N and $I - H_N$ are both self-adjoint, positive semi-definite operators on $L^2(\Omega)$. For $\mathbf{u} \in L^2(\Omega)$*

$$\int_\Omega (\mathbf{u} - H_N\mathbf{u})\cdot\mathbf{u}\,d\mathbf{x} \geq 0 \quad \textit{and} \quad \int_\Omega (H_N\mathbf{u})\cdot\mathbf{u}\,d\mathbf{x} \geq 0.$$

Proof. H_N is a function of the self-adjoint positive definite operator G so self-adjointness is immediate and positivity is easily established in the periodic case by a direct calculation using Fourier series. To begin, expand $\mathbf{u}(\mathbf{x},t) = \sum_{\mathbf{k}} \widehat{\mathbf{u}}(\mathbf{k},t)e^{-i\mathbf{k}\cdot\mathbf{x}}$, where $\mathbf{k} = \frac{2\pi\mathbf{n}}{L}$ is the wave-number and $\mathbf{n} \in \mathbb{Z}^3$. Then, by direct calculation using Parseval's equality

$$\begin{aligned}\frac{1}{2L^3}\int_\Omega (H_N\mathbf{u})\cdot\mathbf{u}\,d\mathbf{x} &= \frac{2\pi}{L}\sum_k \widehat{H}_N(k)E(k)\ , \text{ where}\\ \widehat{H}_N(k) &= \frac{1}{1+z^2}\sum_{n=0}^{N}(1-\frac{1}{1+z^2})^n\ , \text{ where } z=\delta k.\end{aligned}$$

The expression for $\widehat{H}_N(k)$ can be simplified by summing the geometric series. This gives

$$\widehat{H}_N(k) = 1 - (\frac{z^2}{1+z^2})^{N+1}\ , \text{ where } z = \delta k\ .$$

Since z is real, $0 \le \frac{z^2}{1+z^2} \le 1$, and $0 \le 1 - (\frac{z^2}{1+z^2})^{N+1} \le 1$. Thus we have shown

$$0 \le \int_\Omega (H_N\mathbf{u})\cdot\mathbf{u}\,d\mathbf{x} \le \int_\Omega |\mathbf{u}|^2\,d\mathbf{x}.$$

Similarly, we show $0 \le 1 - \widehat{H}_N(k) \le 1$ and

$$0 \le \int_\Omega (\mathbf{u} - H_N\mathbf{u})\cdot\mathbf{u}\,d\mathbf{x} \le \int_\Omega |\mathbf{u}|^2\,d\mathbf{x},$$

which completes the proof. □

It is insightful to plot the transfer function $\widehat{H}_N(k) = 1 - (\frac{z^2}{1+z^2})^{N+1}$ for a few values of N. We do so in Figure 2 for $N = 5, 10, 100$.

Examining these graphs, we observe that $H_N(\mathbf{u})$ is very close to $\mathbf{u}$ for the low frequencies/largest solution scales and that $H_N(\mathbf{u})$ attenuates small scales/high frequencies. The breakpoint between the low frequencies and high frequencies is somewhat arbitrary. The following is convenient for our purposes and fits our intuition of a spectral cutoff operator.

Definition 3.2 (Cutoff-Frequency)**.** *The cutoff frequency of H_N is*

$$k_c := \textit{greatest integer}(H_N^{-1}(\frac{1}{2})).$$

In other words, the frequency for which H_N most closely attains the value $\frac{1}{2}$.

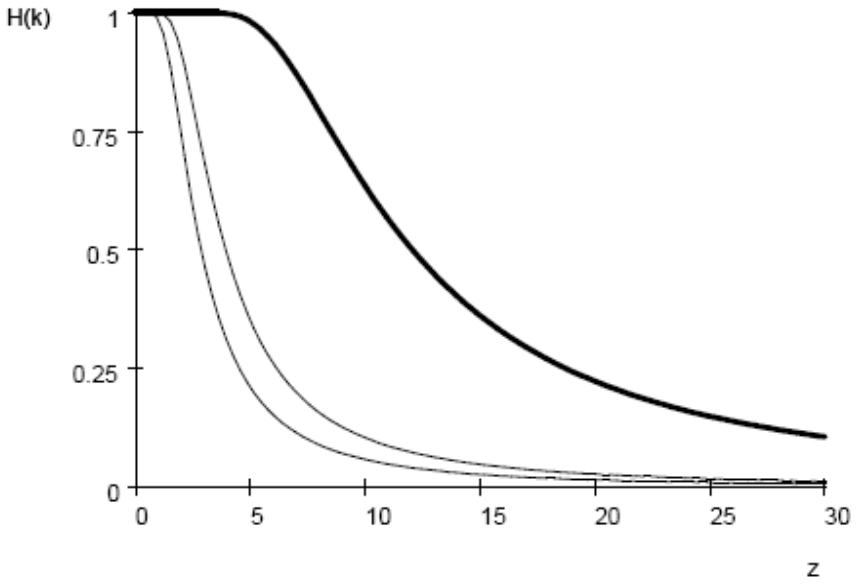

Figure 2: Transfer function $\hat{H}_N$, for $N = 5, 10, 100$.

From the above explicit formulas and Figure 2, it is easy to verify that the cutoff frequency grows to infinity slowly as $N \to \infty$ for fixed δ and as $\delta \to 0$ for fixed N. Other properties of the operator $H_N(\cdot)$ follow similarly easily from its transfer function.

Proposition 3.1. *H_N is a compact operator. Let Π_N denote the orthogonal L^2 projection into span$\{e^{i\mathbf{k}\cdot\mathbf{x}} : |\mathbf{k}| \leq k_c\}$. For all $\mathbf{u} \in L^2(\Omega)$:*

$$\begin{aligned} (H_N\mathbf{u}, \mathbf{u})_{L^2(\Omega)} &\geq C||\Pi_N\mathbf{u}||^2, \\ (\mathbf{u} - H_N\mathbf{u}, \mathbf{u})_{L^2(\Omega)} &\geq C||(I - \Pi_N)\mathbf{u}||^2. \end{aligned} \tag{3.4}$$

Proof. Compactness follows since $\widehat{H}_N(k) \to 0$ as $k \to \infty$. The second and third claims follow from the definition of the cutoff frequency, the explicit formula for the transfer function and a calculation. □

3.2 APPROXIMATE DECONVOLUTION MODELS

Averaging the NSE (meaning: applying G to (1.1)) gives the exact space filtered NSE for $\overline{\mathbf{u}}$

$$\begin{aligned} \overline{\mathbf{u}}_t + \overline{\mathbf{u}\cdot\nabla\mathbf{u}} - \nu\triangle\overline{\mathbf{u}} + \nabla\overline{p} &= \overline{\mathbf{f}} \text{ and} \\ \nabla\cdot\overline{\mathbf{u}} &= 0. \end{aligned}$$

This is not closed since (noting that $\overline{\mathbf{u}\cdot\nabla\mathbf{u}} = \nabla\cdot(\overline{\mathbf{u}\,\mathbf{u}})$)

$$\overline{\mathbf{u}\,\mathbf{u}} \neq \overline{\mathbf{u}}\,\overline{\mathbf{u}}.$$

There are many closure models used in LES, see [54], [30], [6] for a surveys. Since $G_N\overline{\mathbf{u}}$ approximates $\mathbf{u}$ to accuracy $O(\delta^{2N+2})$ in the smooth flow regions it is justified to consider the closure approximation

$$\overline{\mathbf{u}\,\mathbf{u}} = \overline{G_N\overline{\mathbf{u}}G_N\overline{\mathbf{u}}} + O(\delta^{2N+2}). \tag{3.5}$$

Using this closure approximation (3.5) results in an LES model whose solutions are intended to approximate the true flow averages, $\mathbf{w} \approx \overline{\mathbf{u}}$, $q \approx \overline{p}$. The resulting models, introduced by Stolz and Adams [1, 2, 3], are given by

$$\mathbf{w}_t + \nabla\cdot(\overline{G_N\mathbf{w}\;G_N\mathbf{w}}) - \nu\triangle\mathbf{w} + \nabla q + \chi\,(\mathbf{w} - \overline{\mathbf{w}}) = \overline{\mathbf{f}}, \text{ and } \nabla\cdot\mathbf{w} = 0,\ N = 0, 1, 2, \ldots. \tag{3.6}$$

The time relaxation term $\chi\,(\mathbf{w} - \overline{\mathbf{w}})$ is included in numerical simulations of (3.6) to damp strongly the temporal growth of the fluctuating component of w driven by noise, numerical errors, inexact boundary conditions and so on. It can be used as a numerical regularization in any model and is studied in Stolz and Adams [1], Pruett[48], [38, 58]. In this chapter we study the parameter-free deconvolution model that results by setting $\chi = 0$.

In the simplest (and least accurate) $N = 0$ case, the operator G_N reduces to $G_0\overline{\mathbf{u}} = \overline{\mathbf{u}}$ and thus the Zeroth Order ADM is

$$\mathbf{w}_t + \nabla\cdot(\overline{\mathbf{w}\mathbf{w}}) - \nu\Delta\mathbf{w} + \nabla q = \overline{f}, \quad \nabla\cdot\mathbf{w} = 0\,. \tag{3.7}$$

Approximate Deconvolution Models, studied herein, are used, with success, in many simulations of turbulent flows, e.g., Stolz and Adams [1, 2, 3]. They are among the most

accurate of turbulence models and one of the few for which a mathematical confirmation of their effectiveness is known. Lewandowski and Layton in [40] proved the existence and uniqueness of strog solutions, developed regularity of solutions of the Zeroth Order ADM and gave a rigorous bound on the modeling error $\|\overline{\mathbf{u}} - \mathbf{w}\|$. This analysis has been extended for the Nth order ADM by Dunca and Epshteyn in [18]. Also, Lewandowsky and Layton in [41] showed analytically by using the $-5/3$ Kolmogorov's law that the time averaged consistency error of the Nth ADM, i.e. time average of $G_N(\overline{\mathbf{u}})G_N(\overline{\mathbf{u}}) - \mathbf{uu}$, converges to zero following a law as the cube root of the averaging radius and independently of the Reynolds number.

4.0 A SIMILARITY THEORY OF APPROXIMATE DECONVOLUTION MODELS OF TURBULENCE

We start this chapter with a clear energy balance of ADM that enable us to develop a strong mathematical platform for the similarity theory of this family of models.

4.1 ENERGY BALANCE OF APPROXIMATE DECONVOLUTION MODELS

Proposition 4.1. *Suppose* $\chi = 0$ *in the ADM (3.6). Then, if* $\mathbf{w}$ *is a strong solution of (3.6),* $\mathbf{w}$ *satisfies*

$$\frac{1}{2}\left[||\mathbf{w}(t)||_N^2 + \delta^2||\nabla\mathbf{w}(t)||_N^2\right] + \int_0^t \nu||\nabla\mathbf{w}(t')||_N^2 + \nu\delta^2||\triangle\mathbf{w}(t')||_N^2\, dt' = \\ = \frac{1}{2}\left[||\mathbf{w}_0||_N^2 + \delta^2||\nabla\mathbf{w}_0||_N^2\right] + \int_0^t (\mathbf{f}(t')\,, \mathbf{w}(t'))_N\, dt'.$$

Proof. Let $(\mathbf{w}, q)$ denote a periodic solution of the Nth order model with $\chi = 0$. Multiplying (3.6) by $G^{-1}G_N\mathbf{w}$ and integrating over the flow domain Ω gives

$$\int_\Omega \left\{\mathbf{w}_t \cdot G^{-1}G_N\mathbf{w} + \nabla\cdot(\overline{G_N\mathbf{w}\ G_N\mathbf{w}})\cdot G^{-1}G_N\mathbf{w} - \nu\triangle\mathbf{w}\cdot G^{-1}G_N\mathbf{w} + \nabla q\cdot G^{-1}G_N\mathbf{w}\right\}\, d\mathbf{x} \\ = \int_\Omega \overline{\mathbf{f}}\cdot G^{-1}G_N\mathbf{w}\, d\mathbf{x}\,.$$

The nonlinear term vanishes exactly because

$$\begin{aligned}\int_\Omega \nabla\cdot(\overline{G_N\mathbf{w}\ G_N\mathbf{w}})\cdot G^{-1}G_N\mathbf{w}\, d\mathbf{x} &= \int_\Omega G(\nabla\cdot(G_N\mathbf{w}\ G_N\mathbf{w}))\cdot G^{-1}G_N\mathbf{w}\, d\mathbf{x} \\ &= \int_\Omega \nabla\cdot(G_N\mathbf{w}\ G_N\mathbf{w})\cdot G_N\mathbf{w}\, d\mathbf{x} = 0.\end{aligned}$$

Integrating by parts the remaining terms gives

$$\frac{d}{dt}\frac{1}{2}\left[||\mathbf{w}(t)||_N^2+\delta^2||\nabla\mathbf{w}(t)||_N^2\right]+\nu\left[||\nabla\mathbf{w}(t)||_N^2+\delta^2||\triangle\mathbf{w}(t)||_N^2\right]=(\mathbf{f}(t)\cdot\mathbf{w}(t))_N\,.$$

The results follows by integrating this from 0 to t. □

Remark 4.1. *We can clearly identify three physical quantities of kinetic energy, energy dissipation rate and power input. These are given by*

$$\textit{Model's energy:}\qquad E_{model}(\mathbf{w})(t):=\frac{1}{2L^3}\{||\mathbf{w}(t)||_N^2+\delta^2||\nabla\mathbf{w}(t)||_N^2\},\tag{4.1}$$

$$\textit{Model's dissipation rate:}\qquad \varepsilon_{model}(\mathbf{w})(t):=\frac{\nu}{L^3}\{||\nabla\mathbf{w}(t)||_N^2+\delta^2||\triangle\mathbf{w}(t)||_N^2\},\tag{4.2}$$

$$\textit{Model's power input:}\qquad P_{model}(\mathbf{w})(t):=\frac{1}{L^3}(\mathbf{f}(t),\mathbf{w}(t))_N.\tag{4.3}$$

Remark 4.2. *The ADM thus has two terms which reflect extraction of energy from resolved scales. The energy dissipation in the model (4.2) is enhanced by the extra term which is equivalent to* $\nu\delta^2\left\|\triangle\mathbf{w}(t)\right\|^2$ *(by Lemma 3.4). Thus, this term dissipates energy locally where large curvatures in the velocity* $\mathbf{w}$ *occur, rather than large gradients. This term thus acts as an irreversible energy drain localized at large local fluctuations. The second term, which is uniformly equivalent to* $\delta^2\left\|\nabla\mathbf{w}(t)\right\|^2$*, (by Lemma 3.4) occurs in the models kinetic energy given by (4.1). The true kinetic energy (*$\frac{1}{2}\left\|\mathbf{w}(t)\right\|^2$*) in regions of large deformations is thus extracted, conserved and stored in the kinetic energy penalty term* $\delta^2\left\|\nabla\mathbf{w}(t)\right\|^2$*. Thus, this reversible term acts as a kinetic "Energy sponge". Both terms have to have an obvious regularizing effect.*

Lemma 4.1. *As* $\delta\to 0$*,*

$$\begin{aligned}
E_{model}(\mathbf{w})(t) &\to E(\mathbf{w})(t)=\frac{1}{2L^3}||\mathbf{w}(t)||^2,\\
\varepsilon_{model}(\mathbf{w})(t) &\to \varepsilon(\mathbf{w})(t)=\frac{\nu}{2L^3}||\nabla\mathbf{w}(t)||^2,\ \textit{and}\\
P_{model}(\mathbf{w})(t) &\to P(\mathbf{w})(t)=\frac{1}{L^3}(\mathbf{f}(t),\mathbf{w}(t)).
\end{aligned}$$

Proof. As $\delta\to 0$ all the δ^2 terms drop out in the definitions above, $G_N\to I$ and $||\phi||_N\to||\phi||$. □

4.2 ENERGY CASCADES OF APPROXIMATE DECONVOLUTION MODELS

From the previous section we know that the ADM conserve the energy based on the energy balance and therefore we have a solid physical platform for developing a similarity theory for the family of ADM. We start by checking the important features of the NSE (that are making the existence of the energy cascade likely to happen) for the family of ADM. If we apply G^{-1} to the model (3.6) (with $\chi = 0$) it becomes:

$$\frac{\partial}{\partial t}\left[\mathbf{w} - \delta^2 \triangle \mathbf{w}\right] + G_N(\mathbf{w}) \cdot \nabla G_N(\mathbf{w}) - \nu\left[\triangle \mathbf{w} - \delta^2 \triangle^2 \mathbf{w}\right] + \nabla P = \mathbf{f}\,, \qquad \text{in } \Omega \times (0,T).$$

Since G_N is spectrally equivalent to the identity (uniformly in k, δ, nonuniformly in N) the nonlinear interaction $G_N(\mathbf{w}) \cdot \nabla G_N(\mathbf{w})$ (like those in the NSE) will pump energy from large scales to small scales. The viscous terms in the above equation will damp energy at the small scales (more strongly than in the NSE in fact). Lastly, when $\nu = 0$, $f \equiv 0$ the model's kinetic energy is exactly conserved (Remark 4.1 and Proposition 4.1)

$$E_{model}(\mathbf{w})(t) = E_{model}(\mathbf{w}_0).$$

Thus, (3.6) satisfies all the requirements for the existence of a Richardson - like energy cascade for E_{model}. We thus proceed to develop a similarity theory for ADM's (paralleling the K-41 theory of turbulence) using the Π-theorem of dimensional analysis, recalled next. We stress that the Π-theorem is a rigorous mathematical theorem. The only phenomenology or physical intuition involved is the selection of variables and assumptions of dimensional homogeneity.

Theorem 4.1 (The Π-theorem)**.** *If it is known that a physical process is governed by a dimensionally homogeneous relation involving n dimensional parameters, such as*

$$x_1 = f(x_2, x_3, ...x_n), \tag{4.4}$$

where the x's are dimensional variables, there exists an equivalent relation involving a smaller number, $(n-k)$, of dimensionless parameters, such that

$$\Pi_1 = F(\Pi_2, \Pi_3, ..., \Pi_{n-k}), \tag{4.5}$$

where the Π*'s are dimensionless groups constructed from the* x*'s. The reduction,* k*, is usually equal, but never more than, the number of fundamental dimensions involved in the* x*'s.*

Proof. The proof can be found in Daugherty and Franzini [14]. □

The kinetic energy distribution of ADM in physical space (at the point $\mathbf{x}$ in space) is given by (4.1). We will similarly define a distribution in wave-number space using Fourier expansion.

Definition 4.1. *The kinetic energy distribution functions are defined by*

$$E_{model}(k,t) := \frac{L}{2\pi}\sum_{|\mathbf{k}|=k}\frac{1}{2}\left(\widehat{G_N}(k)+\delta^2k^2\widehat{G_N}(k)\right)|\widehat{\mathbf{w}}(k,t)|^2 \tag{4.6}$$

$$E_{model}(k) =< E_{model}(k,t) > \tag{4.7}$$

The units of a variable will be denoted by $[\cdot]$. Thus, for example, [velocity] $= lenght/time$. We start the dimensional analysis for the approximate deconvolution model following Kolmogorov's analysis of the NSE by selecting the variables:

- E_{model} - energy spectrum of model with $[E_{model}(k)] = length^3time^{-2}$,
- ε_{model} - time averaged energy dissipation rate of the model's solution with $[\varepsilon_{model}(k)] = length^2time^{-3}$,
- k - wave-number with $[k] = length^{-1}$ and
- δ - averaging radius with $[\delta] = length$.

Choosing the set of fundamental or primary dimensions $mass$, $length$ and $time$ we then work with 2 dimensionless ratios, Π_1 and Π_2. Choosing ε and k for the repeating variables (note that ε and k cannot form a dimensionless group) we obtain $\Pi_1 = \varepsilon_{model}^a k^b E_{\ model}$ and $\Pi_2 = \varepsilon_{model}^c k^d \delta$ for some a, b, c, d real numbers. Equating the exponents of the corresponding dimensions in both dimensionless groups gives

$$\Pi_1 = \varepsilon_{model}^{-2/3}k^{5/3}E_{\ model} \quad \text{and} \quad \Pi_2 = k\delta$$

The Π-theorem implies that there is a functional relationship between Π_1 and Π_2 , i.e., $\Pi_1 = f(\Pi_2)$, or

$$E_{\ model}\varepsilon_{model}^{-2/3}k^{5/3} = f(k\delta) \text{ or } E_{\ model} = \varepsilon_{model}^{2/3}k^{-5/3}f(k\delta).$$

The simplest case[1] is when $f(\Pi_2) = \alpha_{model}$. In this case we have

$$E_{model}(k) = \alpha_{model}\varepsilon_{model}^{2/3}k^{-5/3}.$$

It is not surprising that, since the ADM is dimensionally consistent with the Navier-Stokes equations, dimensional analysis would reveal a similar energy cascade for the model's kinetic energy. However, interesting conclusions result from the difference between $E(\mathbf{w})(t)$ and $E_{model}(\mathbf{w})(t)$.

$$\begin{aligned} E_{model}(\mathbf{w})(t) := \ &< \frac{1}{2L^3}(||\mathbf{w}||_N^2 + \delta^2||\nabla\mathbf{w}||_N^2) > \\ &\simeq < \frac{1}{2L^3}[||\mathbf{w}||^2 + \delta^2||\nabla\mathbf{w}||^2] > \quad \text{by Lemma (3.4)} \\ &\simeq \sum_k (1+\delta^2\,k^2)E(k) \quad \text{using Parseval's equality.} \end{aligned}$$

Further, since $E_{model}(k) \simeq \alpha_{model}\varepsilon_{model}^{2/3}k^{-5/3}$ we have

$$E(k) \simeq \frac{\alpha_{model}\varepsilon_{model}^{2/3}k^{-5/3}}{1+\delta^2k^2}. \tag{4.8}$$

Equation (4.8) gives precise information about how small scales are truncated by the ADM. Indeed, there are two wave-number regions depending on which term in the denominator is dominant: 1 or δ^2k^2. The transition point is the cutoff wave-number $k = \frac{1}{\delta}$. We thus have

$$\begin{aligned} E(k) &\simeq \alpha_{model}\varepsilon_{model}^{2/3}k^{-5/3}, \quad \text{for} \quad k \le \frac{1}{\delta}, \\ E(k) &\simeq \alpha_{model}\varepsilon_{model}^{2/3}\delta^{-2}k^{-11/3}, \quad \text{for } k \ge \frac{1}{\delta}\ . \end{aligned}$$

This asymptotic behavior is depicted in Figure 3.

[1] We shall show in subsection (4.2.1) that this case is implied by Kraichnan's dynamic argument.

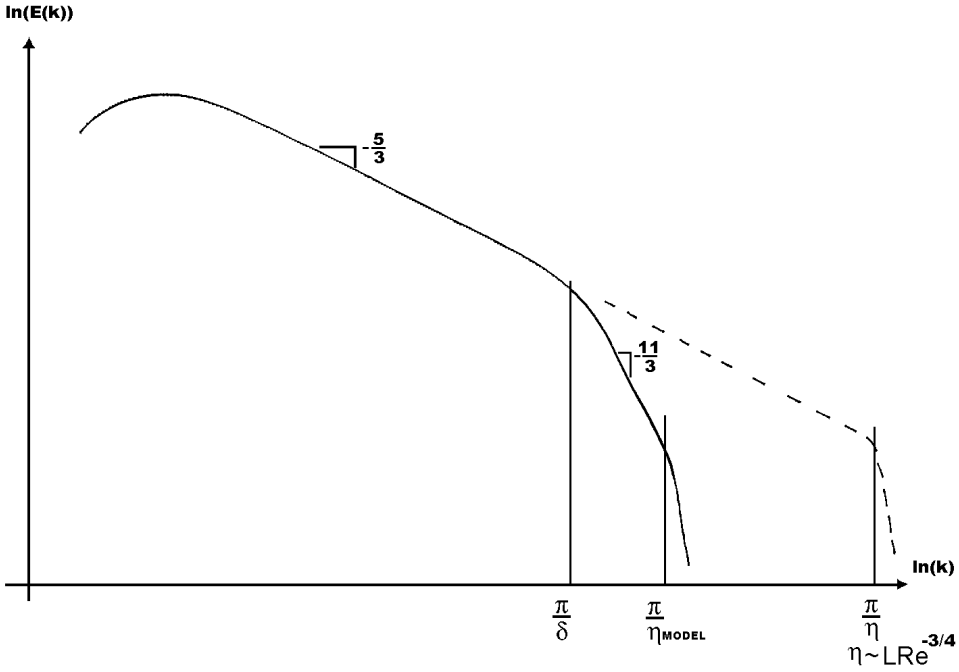

Figure 3: Kinetic energy spectrum of the model

4.2.1 Kraichnan's Dynamic Analysis Applied to ADM's

The energy cascade will now be investigated more closely using the dynamical argument of Kraichnan, [34]. Let $\Pi_{model}(k)$ be defined as the total rate of energy transfer from all wave-numbers $< k$ to all wave-numbers $> k$. Following Kraichnan [34] we assume that $\Pi_{model}(k)$ is proportional to the total energy ($kE_{model}(k)$) in wave-numbers of the order k and to some effective rate of shear $\sigma(k)$ which acts to distort flow structures of scale $1/k$. That is:

$$\Pi_{model}(k) \simeq \sigma(k)\, k\, E_{model}(k) \tag{4.9}$$

Furthermore, we expect

$$\sigma(k)^2 \simeq \int_0^k p^2 E_{model}(p) dp \tag{4.10}$$

The major contribution to (4.10) is from $p \simeq k$, in accord with Kolmogorov's localness assumption, [33]. This is because all wave-numbers $\leq k$ should contribute to the effective

mean-square shear acting on wave-numbers of order k, while the effects of all wave-numbers $\gg k$ can plausibly be expected to average out over the scales of order $1/k$ and over times the order of the characteristic distortion time $\sigma(k)^{-1}$.

We shall say that there is an energy cascade if in some "inertial" range, $\Pi_{model}(k)$ is independent of the wave-number, i.e., $\Pi_{model}(k) = \varepsilon_{model}$. Using the equations (4.9) and (4.10) we get

$$E_{model}(k) \simeq \varepsilon_{model}^{2/3} k^{-5/3}$$

Then, using the relation $E_{model}(k) \simeq (1 + \delta^2 k^2) E(k)$ we have:

$$\begin{aligned} E(k) &\simeq \varepsilon_{model}^{2/3} k^{-5/3}, \text{ for } k \leq \frac{1}{\delta}, \\ E(k) &\simeq \varepsilon_{model}^{2/3} \delta^{-2} k^{-11/3}, \text{ for } k \geq \frac{1}{\delta}. \end{aligned}$$

This is consistent with our previous derived result using dimensional analysis.

4.2.2 The Micro-scale of Approximate Deconvolution Models

The models' Reynolds number represents the ratio of nonlinearity to viscous terms action, i.e.

$$Re_{model} \simeq \frac{|\nabla \cdot \overline{G_N \mathbf{w}\, G_N \mathbf{w}}|}{|\nu \triangle \mathbf{w}|} \tag{4.11}$$

Then, with respect to the models' largest and smallest scales Re_{model} is given by

$$\text{Large scales:} \qquad Re_{model-large} = \frac{UL}{\nu(1 + (\frac{\delta}{L})^2)} (\sum_{n=0}^{N} (1 - \frac{1}{1 + (\delta/L)^2})^n)^2$$

$$\text{Small scales:} \qquad Re_{model-small} = \frac{w_{small} \eta_{model}}{\nu(1 + (\frac{\delta}{\eta_{model}})^2)} (\sum_{n=0}^{N} (1 - \frac{1}{1 + (\delta/\eta_{model})^2})^n)^2.$$

where w_{small} represents the velocity scale of the smallest persistent eddies in the ADM's solution and η_{model} is the ADM's micro-scale being the length scale of the ADM's smallest persistent eddies.

As in the Navier-Stokes equations, the ADM's energy cascade is halted by viscosity grinding down eddies exponentially fast when

$$Re_{model-small} \simeq O(1), \text{ i.e., when}$$
$$\frac{w_{small}\eta_{model}}{\nu(1+(\frac{\delta}{\eta_{model}})^2)}(\sum_{n=0}^{N}(1-\frac{1}{1+(\delta/\eta_{model})^2})^n)^2 \simeq 1.$$

This last equation allows us to determine the characteristic velocity of the models' smallest persistent eddies w_{small} and eliminate it from subsequent equations. This gives

$$w_{small} \simeq \frac{\nu}{\eta_{model}}(1+(\frac{\delta}{\eta_{model}})^2)(\sum_{n=0}^{N}(1-\frac{1}{1+(\delta/\eta_{model})^2})^n)^{-2}.$$

The second important equation determining the models' micro-scale comes from matching energy in to energy out. The rate of energy input to the largest scales is the energy over the associated time scale

$$\frac{E_{model}}{(\frac{L}{U})} = \frac{U^2(1+(\frac{\delta}{L})^2)(\sum_{n=0}^{N}(1-\frac{1}{1+(\delta/L)^2})^n)}{(\frac{L}{U})} = \frac{U^3}{L}(1+(\frac{\delta}{L})^2)(\sum_{n=0}^{N}(1-\frac{1}{1+(\delta/L)^2})^n).$$

When the model reaches statistical equilibrium, the energy input to the largest scales must match the energy dissipation at the models' micro-scale which scales like $\varepsilon_{small} \simeq \nu(\frac{w_{small}}{\eta_{model}})^2(1+(\frac{\delta}{\eta_{model}})^2)(\sum_{n=0}^{N}(1-\frac{1}{1+(\delta/\eta_{model})^2})^n)$. Thus we have

$$\frac{U^3}{L}(1+(\frac{\delta}{L})^2)(\sum_{n=0}^{N}(1-\frac{1}{1+(\delta/L)^2})^n) \simeq \nu(\frac{w_{small}}{\eta_{model}})^2(1+(\frac{\delta}{\eta_{model}})^2)(\sum_{n=0}^{N}(1-\frac{1}{1+(\delta/\eta_{model})^2})^n).$$

Inserting the above formula for the micro-eddies characteristic velocity w_{small} gives

$$\frac{U^3}{L}(1+(\frac{\delta}{L})^2)(\sum_{n=0}^{N}(1-\frac{1}{1+(\delta/L)^2})^n) \simeq \frac{\nu^3}{\eta_{model}^4}(1+(\frac{\delta}{\eta_{model}})^2)^3(\sum_{n=0}^{N}(1-\frac{1}{1+(\delta/\eta_{model})^2})^n)^{-3}.$$

First note that the expected case in LES is when $(\frac{\delta}{L})^2 << 1$ (otherwise the procedure should be considered a VLES[2]). In this case the LHS simplifies to just $\frac{U^3}{L}$. Next, with this simplification, the solution to this equation depends on which term in the numerator of the RHS is dominant: 1 or $(\frac{\delta}{\eta_{model}})^2$. The former case occurs when the averaging radius δ is so small that the model is very close to the NSE so the latter is the expected case. In this case we have $\eta_{model} \simeq Re^{-\frac{3}{4}}L$, when $\delta < \eta_{model}$. In the expected case, solving for the micro-scale gives

$$\eta_{model} \simeq Re^{-\frac{3}{10}}L^{\frac{2}{5}}\delta^{\frac{3}{5}}(N+1)^{-\frac{3}{10}} \text{ , when } \delta > \eta_{model}.$$

[2]Very Large Eddy Simulation. The estimates of the micro-scale are easily extended to this case too.

5.0 THE JOINT ENERGY-HELICITY CASCADE OF APPROXIMATE DECONVOLUTION MODELS OF TURBULENCE

This analysis is quite clear for the Zeroth Order ADM (3.7) and the *ideas* in the general case are the same as for (3.7). We shall thus focus our analysis on the Zeroth Order ADM (3.7) and then collect the (small but technical) modifications needed for the general case in Section 5.4.

5.1 HELICITY AND ENERGY BALANCES FOR THE ZEROTH ORDER MODEL

The qualitative properties of ADMs flow from their global energy and helicity balance. This balance is derived next for the Zeroth Order Model (3.7). The case of the general, Nth order, model is very similar and treated in Section 5.4. Note that since $\mathbf{w}$ is periodic and divergence free and the filter is given by (3.2)

$$\int_\Omega \nabla\cdot(\overline{\mathbf{w}\mathbf{w}})(-\delta^2\Delta+1)\mathbf{w}\ d\mathbf{x} = \int_\Omega (-\delta^2\Delta+1)^{-1}\nabla\cdot(\mathbf{w}\mathbf{w})(-\delta^2\Delta+1)\mathbf{w}\ d\mathbf{x}$$
$$= \int_\Omega \nabla\cdot(\mathbf{w}\mathbf{w})\mathbf{w}\ d\mathbf{x} = \int_\Omega \mathbf{w}\cdot\nabla\mathbf{w}\cdot\mathbf{w}\ d\mathbf{x} = 0. \quad (5.1)$$

Thus, multiplying (3.7) by $(-\delta^2\Delta+1)\mathbf{w} = (-\delta^2\Delta+1)G_0\mathbf{w}$, integrating over Ω, then over $0\le t\le T$ and dividing by L^3 gives

$$\frac{1}{L^3}\int_\Omega \frac{1}{2}|\mathbf{w}(T)|^2 + \frac{\delta^2}{2}|\nabla\mathbf{w}(T)|^2\ d\mathbf{x} + \int_0^T \frac{1}{L^3}\int_\Omega \nu|\nabla\mathbf{w}(t)|^2 + \nu\delta^2|\Delta\mathbf{w}|^2\ d\mathbf{x}\ dt$$
$$= \frac{1}{L^3}\int_\Omega \frac{1}{2}|\mathbf{w}(0)|^2 + \frac{\delta^2}{2}|\nabla\mathbf{w}(0)|^2\ d\mathbf{x} + \int_0^T \frac{1}{L^3}\int_\Omega \mathbf{f}\cdot\mathbf{w}\ d\mathbf{x}\ dt, \quad (5.2)$$

see [36] for the details of the calculation. Equation (5.2) reveals that the zeroth order model (3.7) has a model kinetic energy and model energy dissipation rate (if $\nu \neq 0$):

$$E_{model}(\mathbf{w})(t) := \frac{1}{L^3}\int_\Omega \frac{1}{2}|\mathbf{w}|^2 + \frac{\delta^2}{2}|\nabla \mathbf{w}|^2 \; d\mathbf{x}\,, \tag{5.3}$$

$$\epsilon_{model}(\mathbf{w})(t) := \frac{1}{L^3}\int_\Omega \nu|\nabla \mathbf{w}|^2 + \delta^2\nu|\Delta \mathbf{w}|^2 \; d\mathbf{x}\,. \tag{5.4}$$

The scale truncation in the model is realized mathematically, because the model has an enhanced energy and energy dissipation. Multiplying by $(-\delta^2\Delta+1)(\nabla\times\mathbf{w})$ and proceeding similarly gives the global helicity balance of (3.7), [49]

$$\begin{aligned}
&\frac{1}{L^3}\int_\Omega (\mathbf{w}\cdot\nabla\times\mathbf{w})\;(T) + \delta^2(\nabla\times\mathbf{w}\cdot(\nabla\times)^2\mathbf{w})\;(T)\;d\mathbf{x} \\
&\qquad + \int_0^T \frac{2\nu}{L^3}\int_\Omega (\nabla\times\mathbf{w})\cdot(\nabla\times)^2\mathbf{w} + \delta^2(\nabla\times)^2\mathbf{w}\cdot(\nabla\times)^3\mathbf{w}\; d\mathbf{x}\; dt \\
&= \frac{1}{L^3}\int_\Omega (\mathbf{w}\cdot\nabla\times\mathbf{w})\;(0) + \delta^2(\nabla\times\mathbf{w}\cdot(\nabla\times)^2\mathbf{w})\;(0)\;d\mathbf{x} + \int_0^T \frac{2}{L^3}\int_\Omega f\cdot\nabla\times\mathbf{w}\; d\mathbf{x}\; dt.
\end{aligned} \tag{5.5}$$

This balance equation shows that the model (3.7) has a well-defined model helicity (conserved if $\nu = 0$) and helicity dissipation rate (if $\nu \neq 0$), given by :

$$H_{model}(\mathbf{w})(t) := \frac{1}{L^3}\int_\Omega \mathbf{w}\cdot\nabla\times\mathbf{w} + \delta^2\nabla\times\mathbf{w}\cdot(\nabla\times)^2\mathbf{w}\; d\mathbf{x}\,, \tag{5.6}$$

$$\gamma_{model}(\mathbf{w})(t) := \frac{2\nu}{L^3}\int_\Omega \nabla\times\mathbf{w}\cdot(\nabla\times)^2\mathbf{w} + \delta^2(\nabla\times)^2\mathbf{w}\cdot(\nabla\times)^3\mathbf{w}\; d\mathbf{x}\,. \tag{5.7}$$

To develop the details of the energy and helicity cascade of the model, we must decompose the energy (in a standard way via Parseval's equality for Fourier series, Section 2.1.1) and the helicity (following Chen, Chen and Eyink [11] and Waleffe [59] via a sum over helical modes, Section 2.3.1) into sums over wave-numbers.

5.1.1 Spectral Representation of the Energy and Helicity Statistics for the Zeroth Order Model

The model's kinetic energy (5.3) and energy dissipation rate (5.4) can be decomposed in Fourier modes.

Lemma 5.1. *In Fourier space, (5.3) corresponds to*

$$E_{model}(\mathbf{w})(t) = \frac{2\pi}{L}\sum_{k}(1+\delta^2k^2)E(k,t), \tag{5.8}$$

or equivalently,

$$E_{model}(\mathbf{w})(t) = \frac{2\pi}{L}\sum_{k}E_{model}(k,t), \tag{5.9}$$

where

$$E_{model}(k,t) := (1+\delta^2k^2)E(k,t). \tag{5.10}$$

Proof. Using Parseval's equality, we get

$$\frac{1}{2\,L^3}\|\mathbf{w}(t)\| = \sum_{k}\sum_{|\mathbf{k}|=k}\frac{1}{2}\left|\hat{\mathbf{w}}(\mathbf{k},t)\right|^2 \tag{5.11}$$

and

$$\frac{1}{2\,L^3}\|\nabla\mathbf{w}(t)\| = \sum_{k}\sum_{|\mathbf{k}|=k}\frac{1}{2}\,k^2\,\left|\hat{\mathbf{w}}(\mathbf{k},t)\right|^2. \tag{5.12}$$

Adding (5.11) and (5.12) proves the claim. □

Lemma 5.2. *In wave-number space, we can rewrite (5.4), the model's energy dissipation:*

$$\varepsilon_{model}(\mathbf{w})(t) = \nu\frac{2\pi}{L}\sum_{k}k^2(1+\delta^2k^2)E(k,t). \tag{5.13}$$

Using (5.10), equation (5.13) can be further simplified to

$$\varepsilon_{model}(\mathbf{w})(t) = \nu\frac{2\pi}{L}\sum_{k}k^2E_{model}(k,t), \tag{5.14}$$

with

$$\varepsilon_{model}(k,t) := k^2E_{model}(k,t). \tag{5.15}$$

Proof. Start with equation (5.4) and proceed as in the proof of Proposition 5.1. □

Next, we turn to the spectral representation of helicity.

Lemma 5.3. *In helical decomposition, (5.6) corresponds to*

$$H_{model}(\mathbf{w})(t) = \frac{2\pi}{L}\sum_{k}(1+\delta^2k^2)H(k,t), \tag{5.16}$$

or equivalently,

$$H_{model}(\mathbf{w})(t) = \frac{2\pi}{L}\sum_{k}H_{model}(k,t), \tag{5.17}$$

where

$$H_{model}(k,t) := (1+\delta^2k^2)H(k,t). \tag{5.18}$$

Proof. Using (2.9)-(2.10), we have

$$\frac{1}{L^3}(\mathbf{w}(t), \nabla\times\mathbf{w}(t)) = \sum_{k}\sum_{|\mathbf{k}|=k}\sum_{s=\pm} s\,k\,|a(\mathbf{k},t)|^2$$

and

$$\frac{1}{L^3}(\nabla\times\mathbf{w}(t), (\nabla\times)^2\mathbf{w}(t)) = \sum_{k}\sum_{|\mathbf{k}|=k}\sum_{s=\pm} s\,k^3\,|a(\mathbf{k},t)|^2$$

so that

$$H_{model}(\mathbf{w})(t) = \frac{2\pi}{L}\sum_{k}(1+\delta^2k^2)H(k). \tag{5.19}$$

□

Lemma 5.4. *In wave-number space, we can rewrite (5.7), the model's helicity dissipation:*

$$\gamma_{model}(\mathbf{w})(t) = \nu\sum_{k}\sum_{|\mathbf{k}|=k}\sum_{s=\pm} sk^3(1+\delta^2k^2)\,|a_s(\mathbf{k},t)|^2\,. \tag{5.20}$$

Using (5.19), equation (5.20) can be further simplified to

$$\gamma_{model}(\mathbf{w})(t) = \nu\frac{2\pi}{L}\sum_{k}k^2H_{model}(k,t), \quad \textit{with} \tag{5.21}$$

$$\gamma_{model}(k,t) := k^2H_{model}(k,t). \tag{5.22}$$

Proof. Use (2.9)-(2.11) to write (5.7) in helical modes. □

Remark 5.1. *We would like to stress that helicity and helicity dissipation of the model can have two signs and that when* $H_{model}(\mathbf{w})(t) \geq 0$ *then* $\gamma_{model}(\mathbf{w})(t) \geq 0$ *and when* $H_{model}(\mathbf{w})(t) \leq 0$ *then* $\gamma_{model}(\mathbf{w})(t) \leq 0$ *(as in the case of NSE). This result follows from the above Lemmas 5.3 and 5.4.*

5.2 PHENOMENOLOGY OF THE JOINT ENERGY AND HELICITY CASCADE

Since helicity plays a key role in organizing three dimensional flows, it is important to understand the extent to which statistics of helicity predicted by an LES model are correct. We answer that question in this section by extending the similarity theory of approximate deconvolution models (begun in [39]) to elucidate the details of the model's helicity cascade and its connection to the model's energy. Inspired by the earlier work on helicity cascades in the Navier-Stokes equations of Brissaud, Frisch, Leorat, Lesieur and Mazure [10], Ditlevsen and Giuliani [16, 17], Q. Chen, S. Chen and Eyink [11], we investigate the existence and details of the joint cascade of energy and helicity adapting a dynamic argument of Kraichnan, [34].

Following Kraichnan [34], let $\Pi_{model}(k)$ and $\Sigma_{model}(k)$ denote the total energy and helicity transfer from all wave-numbers below k to all wave-numbers above k.

Definition 5.1. *We say that the model exhibits a joint cascade of energy and helicity if in some inertial range,* $\Pi_{model}(k)$ *and* $\Sigma_{model}(k)$ *are independent of the wave-number, i.e.,* $\Pi_{model}(k) = \varepsilon_{model}$ *and* $\Sigma_{model}(k) = \gamma_{model}$.

Following Kraichnan's formulation of Kolmogorov's ideas of localness of interaction in wave-number space, we assume the following.

Remark 5.1. $\Pi_{model}(k)$ $(\Sigma_{model}(k))$ *is proportional to the ratio of the total energy* $\simeq kE_{model}(k)$ *(total helicity* $\simeq kH_{model}(k)$*) available in wave-numbers of order* k *and to some effective rate of shear* $\sigma(k)$ *which acts to distort flow structures of scale* $1/k$.

The distortion time $\tau(k)$ of flow structures of scale $1/k$ due to the shearing action $\sigma(k)$ of all wave-numbers $\leq k$ is given by:

$$\tau(k) \simeq \frac{1}{\sigma(k)} \qquad \text{with} \qquad \sigma(k)^2 \simeq \int_0^k p^2 E_{model}(p) dp. \tag{5.23}$$

The conjecture of joint cascades of energy and helicity is based on the idea (supported in numerical experiments of Bourne and Orszag [8]) that since energy and helicity are both dissipated by the same mechanism (viscosity), they relax over comparable time scales.

Remark 5.2. *$\tau(k)$ and $\sigma(k)$ are the same for energy and helicity of the model.*

We therefore write

$$\Pi_{model}(k) \simeq k E_{model}(k)/\tau(k) \qquad \text{and} \qquad \Sigma_{model}(k) \simeq k H_{model}(k)/\tau(k). \tag{5.24}$$

In the definition of mean-square shear (5.23) the major contribution is from $p \simeq k$, in accord with Kolmogorov's localness assumption. This gives

$$\tau(k) \simeq k^{-3/2} E_{model}^{-1/2}(k). \tag{5.25}$$

Putting (5.24) and (5.25) together with the fact that $\Sigma_{model}(k) = \gamma_{model}$, it follows that the Zeroth Order ADM's helicity spectrum is given by:

$$H_{model}(k) \simeq \gamma_{model} k^{-5/2} E_{model}^{-1/2}(k)\,. \tag{5.26}$$

The energy spectrum was derived through dimensional considerations in [39] to be

$$E_{model}(k) \simeq \varepsilon_{model}^{2/3} k^{-5/3}. \tag{5.27}$$

Using 5.10 we obtain

$$E(k) = (1 + \delta^2 k^2)^{-1} \varepsilon_{model}^{2/3} k^{-5/3}. \tag{5.28}$$

Thus, considering cases of which term (1 or $\delta^2 k^2$) is dominant gives

$$E(k) \simeq \varepsilon_{model}^{2/3} k^{-5/3}, \text{ for } k \leq \frac{1}{\delta}, \tag{5.29}$$

$$E(k) \simeq \varepsilon_{model}^{2/3} \delta^{-2} k^{-11/3}\,, \text{ for } k \geq \frac{1}{\delta}\,. \tag{5.30}$$

Inserting $E_{model}(k) = \epsilon_{model}^{2/3} k^{-5/3}$ in (5.26) gives

$$H_{model}(k) \simeq \gamma_{model} \varepsilon_{model}^{-1/3} k^{-5/3}. \tag{5.31}$$

Lemma 5.3 gives

$$H(k) \simeq (1 + \delta^2 k^2)^{-1} \gamma_{model} \varepsilon_{model}^{-1/3} k^{-5/3}. \tag{5.32}$$

Depending on which term is dominant (1 or $\delta^2 k^2$), we have the true helicity spectrum of the $N = 0$ model is

$$H(k) \simeq \gamma_{model} \varepsilon_{model}^{-1/3} k^{-5/3}, \text{ for } k \leq \frac{1}{\delta}, \tag{5.33}$$

$$H(k) \simeq \gamma_{model} \varepsilon_{model}^{-1/3} \delta^{-2} k^{-11/3}, \text{ for } k \geq \frac{1}{\delta}. \tag{5.34}$$

The above result is depicted in Figure 4.

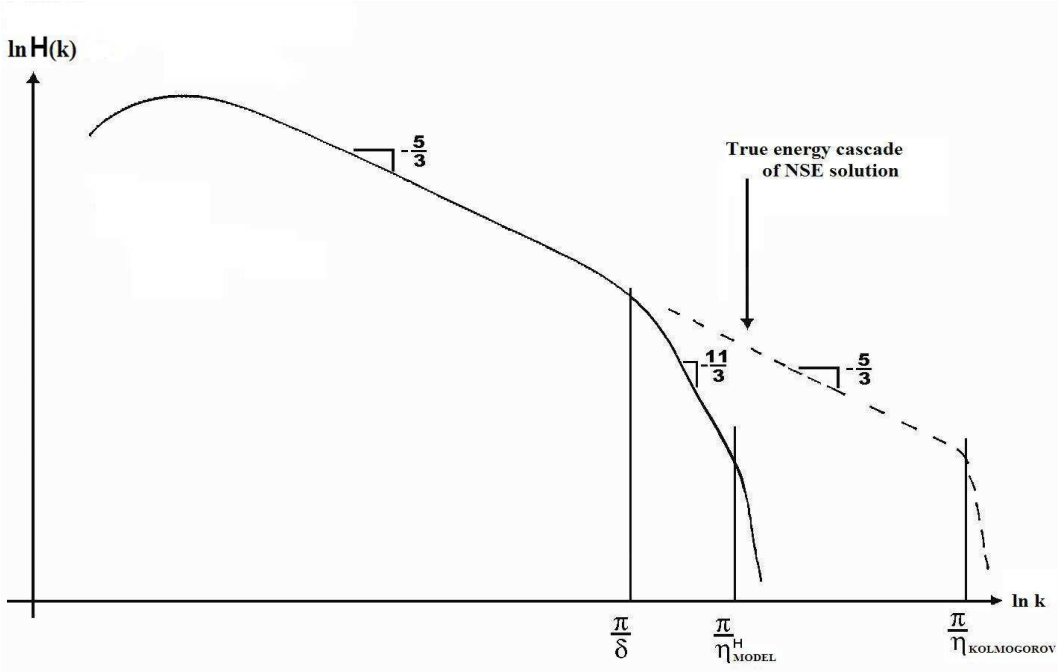

Figure 4: The helicity spectrum of Approximate Deconvolution Models

Thus, one main conclusion is that, down to the cutoff length scale, the Zeroth Order Model predicts the correct energy and helicity cascades.

5.3 ENERGY AND HELICITY MICRO-SCALES IN THE JOINT CASCADE

On a small enough scale, viscosity grinds down all the flow's organized structures (including helicity) and ends all cascades (including the helicity cascade). The length scale, η_H, at which helical structures do not persist and begin to decay exponentially fast is called the helicity micro-scale (in analogy with the Kolmogorov micro-scale for kinetic energy).

In this section, we show that the model's helicity cascade derived in Section 5.2 is consistent up to $k_{E_{model}} (= (\eta^E_{model})^{-1})$, in the sense introduced by Q. Chen, S. Chen and Eyink in [11]. This consistency calculation gives the estimate of the model's helicity micro-scale $\eta^H_{model} = \eta^E_{model}$.

The model's energy and helicity dissipation rates are given by equations (5.4) and (5.7), which are equivalent to

$$\varepsilon_{model}(t) = \nu \int_0^{k_{E_{model}}} k^2 E_{model}(k,t) dk. \tag{5.35}$$

and

$$\gamma_{model}(t) = \nu \int_0^{k_{H_{model}}} k^2 H_{model}(k,t) dk. \tag{5.36}$$

Beginning with (5.35), time averaging both sides and inserting (5.27), $< E_{model}(k,t) >= E_{model}(k) = C_E \epsilon^{2/3}_{model} k^{-5/3}$ in the right hand side gives

$$\epsilon_{model} = \nu \int_0^{k_{E_{model}}} k^2 C_E \epsilon^{2/3}_{model} k^{-5/3}\, dk.$$

Since this can be integrated, it gives an additional consistency equation that can be used to cross check the calculation of η_{model}. Indeed, we have

$$\epsilon_{model} = \nu \frac{3}{4} C_E \epsilon^{2/3}_{model} k^{4/3}_{E_{model}},$$

or $k_{E_{model}} = C\, \nu^{-3/4} \epsilon^{1/4}_{model}$.

The same calculation, beginning with (5.36) instead of (5.35) can be used to calculate the helicity micro-scale. Indeed, time averaging (5.36) gives

$$\gamma_{model} = \nu \int_0^{k_{H_{model}}} k^2 H_{model}(k)\, dk.$$

Inserting (5.31), $H_{model}(k) = C_H \gamma_{model} \epsilon_{model}^{-1/3} k^{-5/3}$ where C_H is just a proportional constant, gives the equation which determines $k_{H_{model}}$.

$$\gamma_{model} = \nu\, C_H \gamma_{model} \epsilon_{model}^{-1/3} \int_0^{k_{H_{model}}} k^{1/3}\, dk.$$

Integration gives

$$k_{H_{model}} = C\, \nu^{-3/4} \epsilon_{model}^{1/4}.$$

Thus the end of the inertial range for helicity is the same as the end of the inertial range of energy, as claimed.

5.4 THE GENERAL, N^{TH} ADM

We begin by recalling the space filtered NSE satisfied by the true flow averages,

$$\overline{\mathbf{u}}_t + \nabla \cdot (\overline{G_N(\overline{\mathbf{u}}) G_N(\overline{\mathbf{u}})}) - \nu \Delta \overline{\mathbf{u}} + \nabla \overline{p} = \overline{f} + \nabla \cdot \overline{\boldsymbol{\tau}} \text{ and } \nabla \cdot \overline{\mathbf{u}} = 0. \tag{5.37}$$

where the residual stresses are given by

$$\boldsymbol{\tau} := G_N(\overline{\mathbf{u}}) G_N(\overline{\mathbf{u}}) - \mathbf{u}\mathbf{u}\,. \tag{5.38}$$

Remark 5.2. *Higher order deconvolution models do contain information about subfiltered scales. Indeed, consider the usual expansion* $\mathbf{u} = \overline{\mathbf{u}} + \mathbf{u}'$. *First we note that for* $N = 0$ *case we have*

$$\overline{\mathbf{u}\,\mathbf{u}} = \overline{\overline{\mathbf{u}}\,\overline{\mathbf{u}}} + \overline{\overline{\mathbf{u}}\,\mathbf{u}' + \mathbf{u}'\,\overline{\mathbf{u}}} + \overline{\mathbf{u}'\,\mathbf{u}'}.$$

Since $N = 0$ *case is equivalent to dropping the last two terms* $\overline{\overline{\mathbf{u}}\,\mathbf{u}' + \mathbf{u}'\,\overline{\mathbf{u}}}$ *and* $\overline{\mathbf{u}'\,\mathbf{u}'}$ *(that are formally of order* δ^2 *for smooth solutions), it is not the most interesting and practical case. However, already the* $N = 1$ *case incorporates approximations of the subfilter scale terms. Indeed, since*

$$G_1\overline{\mathbf{u}} = 2\overline{\mathbf{u}} - \overline{\overline{\mathbf{u}}} = \overline{\mathbf{u}} + (\overline{\mathbf{u}} - \overline{\overline{\mathbf{u}}}),$$

we have for the $N = 1$ *deconvolution closure*

$$\begin{aligned}
\overline{\mathbf{u}\,\mathbf{u}} &\simeq \overline{G_1\overline{\mathbf{u}}\,G_1\overline{\mathbf{u}}} \\
&= \overline{\{\overline{\mathbf{u}} + (\overline{\mathbf{u}} - \overline{\overline{\mathbf{u}}})\}\,\{\overline{\mathbf{u}} + (\overline{\mathbf{u}} - \overline{\overline{\mathbf{u}}})\}} \\
&= \overline{\overline{\mathbf{u}}\,\overline{\mathbf{u}}} + \overline{\overline{\mathbf{u}}(\overline{\mathbf{u}} - \overline{\overline{\mathbf{u}}}) + (\overline{\mathbf{u}} - \overline{\overline{\mathbf{u}}})\overline{\mathbf{u}}} + \overline{(\overline{\mathbf{u}} - \overline{\overline{\mathbf{u}}})\,(\overline{\mathbf{u}} - \overline{\overline{\mathbf{u}}})}.
\end{aligned}$$

The last line shows a clear approximation of the resolved and cross terms as $\overline{\mathbf{u}} - \overline{\overline{\mathbf{u}}} = \overline{\mathbf{u}}'$ *(and a term that formally resembles the subfilter scales).*

From (5.39) we note that

$$\boldsymbol{\tau} := G_N(\overline{\mathbf{u}})G_N(\overline{\mathbf{u}}) - \mathbf{u}\mathbf{u} = (G_N(\overline{\mathbf{u}}) - \mathbf{u})G_N(\overline{\mathbf{u}}) + \mathbf{u}(G_N(\overline{\mathbf{u}}) - \mathbf{u})\,. \tag{5.39}$$

So, the residual stress or consistency error of the model, is governed by the deconvolution error $\mathbf{u} - G_N(\overline{\mathbf{u}})$. Expanding the deconvolution error in a Fourier series gives

$$\mathbf{u} - G_N(\overline{\mathbf{u}}) = \sum_{\mathbf{k}} \left[1 - \widehat{G_N}(k)(1 + \delta^2 k^2)\right] \hat{\mathbf{u}}(\mathbf{k}) e^{i\mathbf{k}\cdot\mathbf{x}}. \tag{5.40}$$

From (5.40), accuracy is determined by how close $\widehat{G_N}(k)$ is to $\frac{1}{1+\delta^2 k^2}$ (i.e. how close approximate deconvolution is to exact deconvolution).

Figure 1 reveals that (i) the $N = 0$ case is not very accurate (since $G_0(k) = 1$ in Figure 1), (ii) as N increases the accuracy on the large scales (small wave-numbers) increases dramatically and the range of wave-numbers over which G_N is an accurate approximate inverse also increases, and (iii) the ADM truncates scales since $\widehat{G_N}(k)$ is bounded.

5.4.1 Extension of the Analysis to the N^{th} ADM

Lemma 3.4 implies that the deconvolution weighted L^2 norm and inner-products (see Definition 3.1) are (uniformly in δ and k) equivalent to the usual L^2 norms and inner products. This observation is one of the keys in the extension of the energy and helicity cascade analysis to the general, N^{th} ADM. The other two keys are the energy and helicity balance of the N^{th} ADM and the decomposition of the energy and helicity into Fourier modes. The energy balance of the N^{th} is derived in Section 4.1.

To derive helicity balance, [49], multiply (3.6) by $\nabla \times (-\delta^2\Delta + 1)G_N(\mathbf{w})$ and integrate over Ω. The nonlinear term vanishes, as in (5.1), because the overbar is $(-\delta^2\Delta + 1)^{-1}$ and all operators commute. Treating the remaining terms exactly as the N=0 case reveals the model helicity and helicity dissipation respectively to be

$$H_{model}(\mathbf{w})(t) := \frac{1}{L^3}\{\mathbf{w}(t), \nabla \times \mathbf{w}(t))_N + \delta^2(\nabla \times \mathbf{w}(t), (\nabla\times)^2\mathbf{w}(t))_N\}, \tag{5.41}$$

$$\gamma_{model}(\mathbf{w})(t) := \frac{2\nu}{L^3}\{(\nabla \times \mathbf{w}(t), (\nabla\times)^2\mathbf{w}(t))_N + \delta^2((\nabla\times)^2\mathbf{w}(t), (\nabla\times)^3\mathbf{w}(t))_N\}. \tag{5.42}$$

The above definitions, equations (5.41) and (5.42) are just deconvolution weighted versions of the $N = 0$ case which are uniformly equivalent to the $N = 0$ case. Since N is fixed and of moderate size (typically $N \sim 5$ to 7), these norms slightly overweight the higher frequencies/smaller scales. The same holds for energy and energy dissipation.

The decomposition of all the quantities considered into Fourier modes is also a minor modification of the $N = 0$ case. For example, for the energy we have

$$N = 0: \qquad E_{model}(k) :=< \frac{L}{2\pi}\sum_{|\mathbf{k}|=k}\frac{1}{2}(1+\delta^2k^2)\,|\hat{\mathbf{w}}(\mathbf{k},t)|^2 >, \tag{5.43}$$

$$\text{General case:} \qquad E_{model}(k) :=< \frac{L}{2\pi}\sum_{|\mathbf{k}|=k}\frac{1}{2}(1+\delta^2k^2)\widehat{G_N}(k)\,|\hat{\mathbf{w}}(\mathbf{k},t)|^2 > . \tag{5.44}$$

and for the helicity

$$N = 0: \qquad H_{model}(k) :=< \frac{L}{2\pi}\sum_{|\mathbf{k}|=k}\sum_{s=\pm} sk(1+\delta^2k^2)\,|a_s(\mathbf{k},t)|^2 >, \tag{5.45}$$

$$\text{General case:} \qquad H_{model}(k) :=< \frac{L}{2\pi}\sum_{|\mathbf{k}|=k}\sum_{s=\pm} sk(1+\delta^2k^2)\widehat{G_N}(k)\,|a_s(\mathbf{k},t)|^2 > . \tag{5.46}$$

Note that the only difference is the weighting by $\widehat{G_N}(k)$ in the general case and $1 \leq \widehat{G_N}(k) \leq N+1$.

With these modifications, all the energy and helicity cascade analysis derived for the Zeroth Order Model hold for the general model for N fixed as well.

6.0 TRUNCATION OF SCALES BY TIME RELAXATION

In this chapter we study one model/regularization: a time relaxation operator introduced as a numerical regularization by Stolz and Adams, e.g., Stolz, Adams and Kleiser [4, 56], based on theoretical work on regularizations of Chapman-Enskog expansions in Rosenau [51], Schochet and Tadmor [55]. This operator aims precisely to truncate the small scales in a solution without altering appreciably the solution's large scales. This regularization operator has many attractive features. It is a lower order perturbation and thus (since the equation does not change order or type) questions of well-posedness and boundary conditions are transparent; it ensures sufficient numerical entropy dissipation for numerical solution of conservation laws, Adams and Stolz [1], p.393; in combination with a large eddy simulation model, it has produced positive results for the Navier-Stokes equations at high Reynolds numbers. It can also be used quite independently of any turbulence model (and has been so used in compressible flow calculations). As a stand alone regularization, it has been successful for the Euler equations for shock-entropy wave interaction and other tests, Stolz and Adams [1], Stolz, Adams and Kleiser [4, 52, 56], including aerodynamic noise prediction and control, Geunanff [25]. Because this term has proven to be widely useful, we isolate its effects by studying the sizes of the persistent scales in the Navier-Stokes equations + relaxation term. We focus on the expected case when *the Reynolds number is high enough that all dissipation and scale truncation is created by precisely this relaxation term* (up to negligible effects). In Section 6.2.1 we shall examine this assumption and see that it is satisfied provided (essentially) the filter length-scale δ is larger than the Kolmogorov micro-scale and the relaxation parameter $\chi > O(1)$.

To introduce the time relaxation term which, when added to the Navier-Stokes equations, we consider as a continuum model, let $\Omega = (0, L)^3$ and suppose periodic with zero mean

boundary conditions are imposed on $\partial\Omega$, i.e.

$$\phi(\mathbf{x}+L\mathbf{e}_j,t)=\phi(\mathbf{x},t) \text{ and } \int_\Omega \phi(\mathbf{x},t)d\mathbf{x}=0 \text{ for } \phi=\mathbf{u},p,\mathbf{f},\mathbf{u}_0.$$

The model we consider is

$$\begin{aligned} \mathbf{u}_t+\mathbf{u}\cdot\nabla\mathbf{u}+\nabla p+\nu\triangle\mathbf{u}+\chi(\mathbf{u}-G_N\overline{\mathbf{u}}) &= \mathbf{f}, \text{in } \Omega\times(0,T) \\ \nabla\cdot\mathbf{u} &= 0, \text{in } \Omega\times(0,T) \text{ and} \\ \mathbf{u}(\mathbf{x},0) &= \mathbf{u}_0(\mathbf{x}), \text{ in } \Omega\ . \end{aligned} \tag{6.1}$$

The relaxation coefficient χ must be specified and has units $\frac{1}{time}$. The term $\mathbf{u}-G_N\overline{\mathbf{u}}$ is a generalized fluctuation included to drive fluctuations below $O(\delta)$ to zero rapidly as $t\to\infty$ without affecting the order of accuracy of the model's solution $\mathbf{u}$ as an approximation to the resolved ($\geq O(\delta)$)scales.

The simplest interesting case is $N=0$. Here $G_0\overline{\mathbf{u}}=\overline{\mathbf{u}}$ represents the part of the velocity that can be represented on an $O(\delta)$ mesh, while $\mathbf{u}':=\mathbf{u}-\overline{\mathbf{u}}$ represents the part of the velocity varying over scales $l\leq O(\delta)$. When $N=0$ the above model reduces to

$$\mathbf{u}_t+\mathbf{u}\cdot\nabla\mathbf{u}+\nu\triangle\mathbf{u}+\nabla p+\chi\mathbf{u}'=\mathbf{f}, \text{in } \Omega\times(0,T)\ . \tag{6.2}$$

When $N=0$, $\mathbf{u}'=\mathbf{u}-\overline{\mathbf{u}}=-\delta^2\triangle\overline{\mathbf{u}}$ so the term $\chi\mathbf{u}'$ represents a smoothed viscous term and some sort of scale truncation is plausible.

To use time relaxation, the relaxation parameter χ must be chosen. Analytical guidance concerning its appropriate scaling with respect to other problem parameters is essential. In Schochet and Tadmor [55] asymptotic analysis suggested the scaling $\chi\sim C_0+C_1/\delta$ but this value was found too large in tests reported in Adams and Stolz [1] p. 403. Herein we consider parameter selection for the Navier-Stokes equations as a part of broader issues for the TRM, including: What is the length scale of the smallest persistent eddy in the above model's solution? (This length scale for (6.1) corresponds to the Kolmogorov dissipation length scale for a turbulent flow of an incompressible, viscous, Newtonian fluid.) Do solutions of the Navier-Stokes equations + relaxation term exhibit an energy cascade and, if so, what are the details of their energy cascade? And, How does the relaxation term act to truncate the small eddies? Our work herein has been inspired by Muschinsky's study of the Smagorinsky

model [46] and enlightened by the paper of Foias, Holm and Titi [19] on the Camassa-Holm / Navier-Stokes-alpha model. The answers to these questions will come from two simple but powerful tools: a precise energy balance for the models themselves together with Kolmogorov's similarity theory, suitably adapted. Interestingly, similarity theory yields $\chi \sim C\delta^{-\frac{2}{3}}$ which is smaller than the above value but consistent with it within the accuracy of an asymptotic expansion.

6.1 ENERGY BALANCE OF TIME RELAXATION MODEL

The theory of (6.1) begins, like the Leray theory of the Navier-Stokes equations, with a clear global energy balance.

Proposition 6.1. *Let $\mathbf{u}_0 \in L^2(\Omega)$, $\mathbf{f} \in L^2(\Omega \times (0,T))$. For $\delta > 0$, let the averaging be $(-\delta^2\triangle + 1)^{-1}$. There exists a weak solution to (6.1) which is unique if it is additionally a strong solution. If $\mathbf{u}$ is a strong solution of (6.1), $\mathbf{u}$ satisfies*

$$\frac{1}{L^3}\frac{1}{2}\left\|\mathbf{u}(\mathbf{x},t)\right\|^2 + \int_0^t \frac{1}{L^3}\int_\Omega \left\{\nu|\nabla\mathbf{u}(\mathbf{x},t')|^2 + \chi(\mathbf{u}(\mathbf{x},t') - H_N\mathbf{u}(\mathbf{x},t'))\cdot\mathbf{u}(\mathbf{x},t')\right\}\, d\mathbf{x}dt' = \frac{1}{L^3}\frac{1}{2}\left\|\mathbf{u}_0\right\|^2 + \int_0^t \frac{1}{L^3}\int_\Omega \mathbf{f}(\mathbf{x},t')\cdot\mathbf{u}(\mathbf{x},t')\, d\mathbf{x}dt'. \quad (6.3)$$

The above energy bound with equality replaced by "$\leq$" is also satisfied by weak solutions.

Proof. The model (6.1) is a lower order, linear perturbation of the Navier-Stokes equations so this follows the Navier-Stokes case very closely, e.g., Galdi [21, 22] for a clear and beautiful presentation. For example, for the energy equality, multiply (6.1) by $\mathbf{u}$, integrate over the domain Ω, then integrate from 0 to t. □

Remark 6.1. *By the Lemma 3.5 and energy estimate (6.3), the model's relaxation term thus extracts energy from resolved scales. Hence, we can define an energy dissipation rate induced by time relaxation for (6.1) as*

$$\varepsilon_{model}(\mathbf{u})(t) := \frac{1}{L^3}\int_\Omega \chi(\mathbf{u}(\mathbf{x},t) - H_N\mathbf{u}(\mathbf{x},t))\cdot\mathbf{u}(\mathbf{x},t)\, d\mathbf{x}\,. \quad (6.4)$$

The models kinetic energy is the same as for the Euler equations

$$E_{model}(\mathbf{u})(t) := \frac{1}{L^3}\frac{1}{2}\int_\Omega |\mathbf{u}(\mathbf{x},t)|^2 \,. \tag{6.5}$$

The following analytic estimate of the effect of the relaxation term follows easily from the above energy estimate.

Theorem 6.1. *Let* $\mathbf{u}$ *be a weak solution of (6.1). If* $\mathbf{u}_0 \in L^2(\Omega)$ *and* $\mathbf{f} \in L^2(0,T;L^2(\Omega))$ *then there is a* $C = C(\mathbf{u}_0, \mathbf{f}, T)$ *such that*

$$\int_{\Omega\times(0,T)} |(I - \Pi_N)\mathbf{u}(\mathbf{x},t)|^2 \, d\mathbf{x}dt \leq \frac{C}{\chi}, \tag{6.6}$$

and thus $(I - \Pi_N)\mathbf{u} \to 0$ *in* $L^2(\Omega \times (0,T))$ *as* $\chi \to \infty$.

Proof. With the stated regularity of the body force, we may use the Cauchy-Schwarz inequality in the RHS of the energy inequality and apply Gronwall's inequality. After this, drop every term on the LHS except the time relaxation term giving

$$\int_0^T \int_\Omega \chi(\mathbf{u}(\mathbf{x},t') - H_N\mathbf{u}(\mathbf{x},t')) \cdot \mathbf{u}(\mathbf{x},t') \, d\mathbf{x}dt' \leq C(\mathbf{u}_0, \mathbf{f}, T).$$

The result follows from this and the Proposition 3.1. □

Theorem 6.1 tells us that as $\chi \to 0$ the fluctuations of the flow tend to 0 too, but does not give us any insight into the parameter selection of χ. Therefore, we continue to develop a similarity theory for TRM with the aim to find the optimal value of time relaxation parameter χ, i.e., the value that maintains a small consistency error of the model and truncates scales at the same time.

6.2 A SIMILARITY THEORY OF TIME RELAXATION

We consider now the Navier-Stokes equations with time relaxation at a high enough Reynolds number and large enough relaxation coefficient that viscous dissipation is negligible. The first question is: *Does the time relaxation term induce a truncation of persistent solution scales?* This question is linked to another: *Does the NSE + time relaxation share the common features of the Navier-Stokes equations which make existence of an energy cascade likely?* Since (6.1) has the same nonlinearity as the Navier-Stokes equations, the conditions remaining are that (i) the solution satisfies an energy equality in which its kinetic energy and energy dissipation are readily discernible, and (ii) in the absence of relaxation (for $\chi = 0$) the model's kinetic energy is conserved through a large ranger of scales/wave-numbers. Since both conditions are satisfied we are proceed to develop a quantitative similarity theory of (6.1), along the lines of the K-41 theory of turbulence.

Since the time relaxation term is not scale invariant, it is critical to formulate the problem in a way that is as simple, clear and physically correct as possible. The first step is to find the model's equivalent of the large scales' Reynolds number of the Navier-Stokes equations. Recall the Reynolds number for the Navier-Stokes equations is, in simplest terms, the ratio of nonlinearity to viscous terms action on the largest scales:

$$\text{for the NSE: } Re \simeq \frac{|\mathbf{u}\cdot\nabla\mathbf{u}|}{|\nu\triangle\mathbf{u}|} \simeq \frac{U\frac{1}{L}U}{\nu\frac{1}{L^2}U} = \frac{UL}{\nu}.$$

The NSE's Reynolds numbers with respect to the smallest scales is obtained by replacing the large scales velocity and length by their small scales equivalent as in $Re_{small} = \frac{u_{small}\eta}{\nu}$. To proceed we must find the physically appropriate and mathematically analogous quantity for the NSE + time relaxation. Again, this derivation is under the assumption that viscous dissipation is negligible compared to dissipation due to time relaxation.

Proceeding analogously, it is clear that the ratio of nonlinearity to dissipative effects should be the analogous quantity, and it should correspond to

$$R_N \simeq \frac{|\mathbf{u}\cdot\nabla\mathbf{u}|}{|\chi(\mathbf{u}-H_N\mathbf{u})|}.$$

For example, if $N = 0$, and keeping in mind that for the large scales $(\frac{\delta}{L})^2 << 1$, then we have

$$\begin{aligned} R_0 &\simeq \frac{|\mathbf{u}\cdot\nabla\mathbf{u}|}{|\chi(\mathbf{u}-\overline{\mathbf{u}})|} = \frac{|\mathbf{u}\cdot\nabla\mathbf{u}|}{|\chi\delta^2\triangle\overline{\mathbf{u}}|} = \\ &= \frac{|\mathbf{u}\cdot\nabla\mathbf{u}|}{|\chi\delta^2\triangle(-\delta^2\triangle+1)^{-1}\mathbf{u}|} \simeq \frac{U\frac{1}{L}U}{\chi\delta^2\frac{1}{L^2}(\frac{\delta^2}{L^2}+1)^{-1}U} \\ &= \frac{LU}{\chi\delta^2}(\frac{\delta^2}{L^2}+1) \simeq \frac{LU}{\chi\delta^2} \end{aligned}$$

In the general case, and using Lemma 3.1, we have

$$\begin{aligned} R_N &\simeq \frac{|\mathbf{u}\cdot\nabla\mathbf{u}|}{|\chi(\mathbf{u}-H_N\mathbf{u})|} \simeq \frac{U^2\frac{1}{L}}{\chi\delta^{2N+2}(\frac{1}{L^2})^{N+1}(\frac{\delta^2}{L^2}+1)^{-(N+1)}U} \\ &= \frac{L^{2N+1}U}{\chi\delta^{2N+2}}(\frac{\delta^2}{L^2}+1)^{N+1} \simeq \frac{L^{2N+1}U}{\chi\delta^{2N+2}}. \end{aligned}$$

This parameter definition can also be obtained by non-dimensionalization. For example, for $N = 0$, denoting the non-dimensionalized quantities with a symbol $\hat{}$ over, we non-dimensionalize in the usual manner and obtain the following system. The term R_0 is $O(1)$ for the large scales-as it should be after non-dimensionalization.

$$\widehat{\mathbf{u}}_t + \widehat{\mathbf{u}}\cdot\widehat{\nabla}\widehat{\mathbf{u}} + \widehat{\nabla}\widehat{p} + \widehat{\nu}\widehat{\triangle}\widehat{\mathbf{u}} + R_0^{-1}(\frac{\widehat{\mathbf{u}}-\widehat{\overline{\mathbf{u}}}}{(\frac{\delta}{L})^2}) = \widehat{\mathbf{f}}, \text{in } \Omega\times(0,T) \ .$$

Definition 6.1. *The non-dimensionalized time relaxation parameter for the NSE + time relaxation is*

$$R_N = \frac{L^{2N+1}U}{\chi\delta^{2N+2}} \ , \textit{for } N = 0,1,2,\ldots. \tag{6.7}$$

Next we must form the small scales parameters which measure the ratio of nonlinearity to dissipation at the smallest persistent scales. Let u_{small} denote a characteristic velocity of the smallest persistent eddies and let η_{model} denote the length scale associated with them. Then, exactly as above we calculate

$$\begin{aligned} R_{N-small} &\simeq \frac{|u_{small}\cdot\nabla u_{small}|}{|\chi(u_{small}-H_N u_{small})|} \\ &\simeq \frac{u_{small}^2\frac{1}{\eta_{model}}}{\chi\delta^{2N+2}(\frac{1}{\eta_{model}^2})^{N+1}(\frac{\delta^2}{\eta_{model}^2}+1)^{-(N+1)}u_{small}} \\ &= \frac{\eta_{model}^{2N+1}u_{small}}{\chi\delta^{2N+2}}(\frac{\delta^2}{\eta_{model}^2}+1)^{N+1}. \end{aligned}$$

For the small scales it is no longer reasonable to suppose δ is small with respect to η_{model}.

Definition 6.2. *Let η_{model}, u_{small} denote, respectively, a characteristic length and velocity of the smallest persistent structures in the flow. The non-dimensionalized parameter associated with the smallest persistent scales of the NSE equations + time relaxation is*

$$R_{N-small} = \frac{\eta_{model}^{2N+1} u_{small}}{\chi \delta^{2N+2}} (\frac{\delta^2}{\eta_{model}^2} + 1)^{N+1} \tag{6.8}$$

The estimate of the smallest resolved scales is based upon two principles:

$$R_{N-small} = O(1) \text{ at length-scale } \eta_{model}$$

and statistical equilibrium in the form *energy input at large scales = dissipation at small scales*. As in the Navier-Stokes equations, the NSE equations + relaxation term's energy cascade is halted by dissipation caused by the time relaxation effects grinding down eddies exponentially fast when $R_{N-small} = O(1)$ at length-scale η_{model}. The largest eddies have energy which scales like $O(U^2)$ and associated time scale $\tau = O(\frac{L}{U})$. The rate of energy transfer/energy input is thus $O(\frac{U^2}{\tau}) = O(\frac{U^3}{L})$ exactly as in the Navier-Stokes case. The dissipation at the smallest resolved scales, estimated carefully, is

$$\begin{aligned} \text{dissipation at small scales} &\simeq \chi(\mathbf{u} - H_N\mathbf{u})\mathbf{u} \text{ (by Lemma 3.1)} \\ &\simeq \chi\delta^{2N+2}(\triangle^{N+1}A^{-(N+1)}\mathbf{u})\mathbf{u} \text{ (at the smallest scales)} \\ &\simeq \chi\delta^{2N+2}(\frac{1}{\eta_{model}^2})^{N+1}(1+\frac{\delta^2}{\eta_{model}^2})^{-(N+1)}u_{small}^2. \end{aligned}$$

These two conditions thus give the pair of equations

$$\begin{aligned} \frac{\eta_{model}^{2N+1}u_{small}}{\chi\delta^{2N+2}}(\frac{\delta^2}{\eta_{model}^2}+1)^{N+1} &\simeq 1 \text{ , and} \\ \frac{U^3}{L} \simeq \chi\delta^{2N+2}(\frac{1}{\eta_{model}^2})^{N+1}(1+\frac{\delta^2}{\eta_{model}^2})^{-(N+1)}u_{small}^2 &\text{ .} \end{aligned} \tag{6.9}$$

The first equation gives an estimate of the characteristic velocity of the smallest eddy in terms of the other parameters; solving for u_{small} gives

$$u_{small} \simeq \frac{\chi\delta^{2N+2}}{\eta_{model}^{2N+1}(1+\frac{\delta^2}{\eta_{model}^2})^{N+1}}.$$

Inserting this value into the second equation gives the following equation determining the model's micro-scale

$$\frac{U^3}{L} \simeq \chi\delta^{2N+2}(\frac{1}{\eta_{model}^2})^{N+1}(1+\frac{\delta^2}{\eta_{model}^2})^{-(N+1)}[\frac{\chi\delta^{2N+2}}{\eta_{model}^{2N+1}(1+\frac{\delta^2}{\eta_{model}^2})^{N+1}}]^2. \tag{6.10}$$

This is the fundamental equation determining the model's micro-scale. There are three cases: $\delta < \eta_{model}$, $\delta > \eta_{model}$ and $\delta = \eta_{model}$.

Case 1: Fully resolved. In this case $\delta < \eta_{model}$ so that $1 + \frac{\delta^2}{\eta_{model}^2} \simeq 1$.

In this case the equation for the micro-scale reduces to

$$\frac{U^3}{L} \simeq \chi\delta^{2N+2}(\frac{1}{\eta_{model}^2})^{N+1}[\frac{\chi\delta^{2N+2}}{\eta_{model}^{2N+1}}]^2,$$

which implies

$$\eta_{model} \simeq (\frac{\chi^3 L}{U^3})^{\frac{1}{6N+4}}\delta^{1+\frac{1}{3N+2}}. \tag{6.11}$$

Case 2: Under resolved. In this case $\delta > \eta_{model}$ so that $1 + \frac{\delta^2}{\eta_{model}^2} \simeq \frac{\delta^2}{\eta_{model}^2}$.

In this case we have

$$\frac{U^3}{L} \simeq \chi\delta^{2N+2}(\frac{1}{\eta_{model}^2})^{N+1}(\frac{\delta^2}{\eta_{model}^2})^{-(N+1)}[\frac{\chi\delta^{2N+2}}{\eta_{model}^{2N+1}(\frac{\delta^2}{\eta_{model}^2})^{N+1}}]^2, \tag{6.12}$$

which gives, after simplification,

$$\eta_{model} \simeq (\frac{U^3}{\chi^3 L})^{\frac{1}{2}}. \tag{6.13}$$

At this point, we do not know how to interpret this estimate because it predicts that in this case increasing χ *decreases* the model's micro-scale. However, this case is not the expected one in practical computations so perhaps the simple interpretation is that solution scales should be resolved.

Case 3: Perfect resolution. In this case $\delta = \eta_{model}$ so that $1 + \frac{\delta^2}{\eta_{model}^2} \simeq 2$.

In this case the interesting question is to determine the choice of relaxation parameter that enforces $\delta = \eta_{model}$. Setting $\delta = \eta_{model}$ and solving for χ gives

$$\chi \simeq \frac{U}{L^{\frac{1}{3}}}2^{N+1}\delta^{-\frac{2}{3}}. \tag{6.14}$$

We want to stress that the above parameter selection agrees with the Lemma 6.1. As $\chi \to \infty$ we must have that $\delta \to 0$, i.e. the fluctuations of the flow tend to 0 as predicted by the result of the Theorem 6.1. When perfectly resolved, the consistency error of the relaxation term (evaluated for smooth flow fields) is, for this scaling of relaxation parameter,

$$|\chi(\mathbf{u} - G_N\overline{\mathbf{u}})| = O(\chi\delta^{2N+2}) = O(\delta^{2N+\frac{4}{3}}).$$

6.2.1 Interpreting the Assumption that Viscous Dissipation is Negligible

Our assumption that viscous dissipation is negligible compared to dissipation caused by time relaxation holds provided the Kolmogorov micro-scale for the Navier-Stokes equations is smaller than the model's micro-scale induced by the relaxation term. This is because the K41 theory is asymptotic at infinite Reynolds number meaning that viscous dissipation is considered negligible at scales above the micro-scale. Thus, one tenant of K41 is that above the Kolmogorov micro-scale the NSE acts like the Euler equations. At high enough Reynolds number and large enough relaxation parameter, it is certainly plausible that relaxation dominates viscosity and that the latter is negligible. The estimates derived in this section give some insight into how large "large enough" is.

The first interpretation of "large enough" is that $\eta_{model} >> \eta_{Kolmogorov}$. If $\eta_{model} >> \eta_{Kolmogorov}$ then practical considerations suggest that we are most commonly in the fully-resolved case or the perfectly resolved case. In the latter, $\eta_{model} = \delta$ and the condition is that $\delta >> \eta_{Kolmogorov}$, i.e., computational resources are insufficient for a DNS. In the fully-resolved case $\eta_{model} > \eta_{Kolmogorov}$ is equivalent to

$$\begin{aligned} (\frac{\chi^3 L}{U^3})^{\frac{1}{6N+4}}\delta^{1+\frac{1}{3N+2}} &> \eta_{Kolmogorov} = Re^{-\frac{3}{4}}L, \text{ which implies} \\ \chi &> (Re^{-\frac{3}{4}}L)^{2N+\frac{4}{3}}\frac{U}{L^{\frac{1}{3}}}\delta^{-2(N+1)} \end{aligned} \tag{6.15}$$

In the typical case of $\delta >> \eta_{Kolmogorov}$ and χ large this places almost no constraint upon the relaxation parameter.

The second interpretation is that at $\eta = \eta_{Kolmogorov}$, $Re_{small} >> R_{N-small}$; this also gives the following mild condition, satisfied by any reasonable scaling of χ, including those derived herein,

$$\chi > \nu(\frac{\delta}{\eta})^{-2N}\delta^{-2}(1+(\frac{\delta}{\eta})^2)^{N+1}.$$

6.3 NONLINEAR TIME RELAXATION

Nonlinear time relaxation mechanisms endeavor to focus the dissipative effects further on smaller scales by localization in physical as well as wave-number space. Nonlinear relaxation, especially quadratic relaxation, is also a more physical realization due to the connection to friction (which is quadratic being proportional to the square of the speed and acting to oppose the direction of motion). For this reason we focus on the quadratic case; the extension to a more general nonlinearity is immediate. In the quadratic case, the following is the correct frictional relaxation model

$$\begin{aligned} \mathbf{u}_t + \mathbf{u}\cdot\nabla\mathbf{u} + \nabla p + \nu\triangle\mathbf{u} + \chi^{\frac{3}{2}}(I-H_N)\{|\mathbf{u}-H_N\mathbf{u}|(\mathbf{u}-H_N\mathbf{u})\} &= \mathbf{f}, \text{in } \Omega\times(0,T), \\ \nabla\cdot\mathbf{u} &= 0, \text{in } \Omega\times(0,T). \end{aligned} \tag{6.16}$$

The dissipation in the above is given by

$$\begin{aligned} \varepsilon_{model}(\mathbf{u})(t) &= \frac{1}{L^3}\int_\Omega \chi^{\frac{3}{2}}(I-H_N)\{|\mathbf{u}-H_N\mathbf{u}|(\mathbf{u}-H_N\mathbf{u})\}\cdot\mathbf{u}\,d\mathbf{x} \\ &= \frac{1}{L^3}\int_\Omega \chi^{\frac{3}{2}}|\mathbf{u}-H_N\mathbf{u}|(\mathbf{u}-H_N\mathbf{u})\cdot(\mathbf{u}-H_N\mathbf{u})\,d\mathbf{x} \\ &= \frac{1}{L^3}\int_\Omega (\chi^{\frac{1}{2}}|\mathbf{u}-H_N\mathbf{u}|)^3\,d\mathbf{x}. \end{aligned}$$

Note that $\varepsilon_{model} \geq 0$ precisely because of the form chosen for the nonlinear term[1].

[1] The choice of relaxation parameter ($\chi^{\frac{3}{2}}$ instead of χ) is motivated by the resemblance of this last expression with the one arising in the linear case.

6.3.1 Parameter Determination via $\varepsilon = \varepsilon_{model}$

The derivation of Lilly [42] for the Smagorinsky model can be adapted to nonlinear time relaxation. This derivation is heuristic but gives another useful indication of the scaling of the relaxation parameter with respect to the other model parameters. Since this analysis is very well known in large eddy simulation, e.g., Pope [47], Sagaut [54], Berselli, Iliescu and Layton [6], we give an abbreviated summary here. The idea of Lilly is to equate $\varepsilon = \varepsilon_{model}$, i.e. the true time averaged energy dissipation rate with the time averaged dissipation rate of the model, and evaluate the RHS by assuming (among other things) that the velocity field arises from homogeneous isotropic turbulence. To use energy spectrum information a further assumption is needed that the following two are of comparable orders of magnitude

$$< ||\mathbf{u} - H_N\mathbf{u}||^3_{L^3(\Omega)} > \simeq < ||\mathbf{u} - H_N\mathbf{u}||^2_{L^2(\Omega)} >^{\frac{3}{2}} .$$

Under these assumptions we calculate

$$\begin{aligned} \varepsilon_{model} &= (\chi)^{3/2}[\int_{k_{\min}}^{k_{\max}} (1 - \widehat{H_N(k)})^2 E(k)\, dk]^{\frac{3}{2}}, \text{ where} \\ E(k) &= \alpha\varepsilon^{\frac{2}{3}}k^{-\frac{5}{3}} \text{ , } \alpha = \text{ Kolmogorov constant.} \end{aligned}$$

With the change of variable $z = \delta k$ this reduces to

$$\varepsilon_{model} = \chi^{\frac{3}{2}}\alpha^{\frac{3}{2}}\varepsilon\delta[\int_{z_{\min}}^{z_{\max}} (\frac{z^2}{1+z^2})^{2N+2} z^{-\frac{5}{3}} dz]^{\frac{3}{2}}.$$

Setting $\varepsilon = \varepsilon_{model}$ thus gives the following value of the relaxation parameter (after simplification)

$$\begin{aligned} \chi &= [\alpha\delta^{\frac{2}{3}}\beta_N]^{-1} \text{ , where} \\ \beta_N &= \int_{z_{\min}}^{z_{\max}} (\frac{z^2}{1+z^2})^{2N+2} z^{-\frac{5}{3}} dz. \end{aligned}$$

The value of β_N can be estimated by the value of the integral $\beta_N \simeq \int_0^\infty (\frac{z^2}{1+z^2})^{2N+2} z^{-\frac{5}{3}} dz$. By considering N to be a continuous variable, we calculate $\frac{d\beta_N(N)}{dN}$ which is negative. Thus,

β_N is decreasing function of N. It is clear that $\beta_N = O(1)$ and some estimates of values of β_N, obtained by numerical integration, are given below.

N =	0	1	2	3	4	5	6	7	8
$\beta_N \simeq$	1.21	0.895	0.766	0.689	0.635	0.596	0.564	0.538	0.517

In all cases these calculations reiterate the scaling

$$\chi = (\alpha\beta_N)^{-1}\delta^{-\frac{2}{3}} \sim O(\delta^{-\frac{2}{3}}). \tag{6.17}$$

7.0 NUMERICAL ANALYSIS OF A HIGHER ORDER TIME RELAXATION MODEL OF FLUIDS

Our goal in this report is to connect the work studying Time Relaxation Model (6.1) as a continuum model with the computational experiments by a numerical analysis of discretizations of (6.1). We thus consider stability and convergence of finite element discretizations of (6.1) with the goal to elucidate the interconnections between δ, h, χ and ν.

7.1 ANALYSIS OF THE TIME RELAXATION MODEL

The following function spaces are used in the analysis:

$$\begin{aligned}
\text{Velocity Space} \quad &: \quad X := H_0^1(\Omega)\,, \\
\text{Pressure Space} \quad &: \quad P := L_0^2(\Omega) = \left\{ q \in L^2(\Omega) \,:\, \int_\Omega q \, d\Omega = 0 \right\}\,, \\
\text{Divergence} - \text{free Space} \quad &: \quad Z := \left\{ v \in X : \int_\Omega q \nabla \cdot \mathbf{v} \, d\Omega \,=\, 0,\ \forall\, q \in P \right\}.
\end{aligned}$$

We denote the dual space of X as X', with norm $\|\cdot\|_{-1}$.

A variational solution of the Navier-Stokes equations may be stated as: *Find* $\mathbf{w} \in L^2(0,T;X) \cap L^\infty(0,T;L^2(\Omega))$, $r \in L^2(0,T;P)$ *with* $\mathbf{w}_t \in L^2(0,T;X')$ *satisfying*

$$(\mathbf{w}_t, \mathbf{v}) + (\mathbf{w} \cdot \nabla \mathbf{w}, \mathbf{v}) - (r, \nabla \cdot \mathbf{v}) + \nu(\nabla \mathbf{w}, \nabla \mathbf{v}) \;=\; (\mathbf{f}, \mathbf{v})\ ,\ \forall \mathbf{v} \in X\,, \tag{7.1}$$

$$(q, \nabla \cdot \mathbf{w}) \;=\; 0\ ,\ \forall q \in P\,, \tag{7.2}$$

$$\mathbf{w}(0, \mathbf{x}) \;=\; \mathbf{w}_0(\mathbf{x})\ ,\ \forall \mathbf{x} \in \Omega\,. \tag{7.3}$$

We consider in comparison to (7.1)-(7.3) the problem: *Find* $\mathbf{u} \in L^2(0,T;X) \cap L^\infty(0,T;L^2(\Omega))$, $p \in L^2(0,T;P)$ *with* $\mathbf{u}_t \in L^2(0,T;X')$ *satisfying*

$$
\begin{aligned}
(\mathbf{u}_t, \mathbf{v}) + (\mathbf{u}\cdot\nabla\mathbf{u}, \mathbf{v}) - (p, \nabla\cdot\mathbf{v}) + \nu(\nabla\mathbf{u}, \nabla\mathbf{v}) + \chi(\mathbf{u} - G_N\bar{\mathbf{u}}, \mathbf{v}) &= (\mathbf{f}, \mathbf{v}),\ \forall \mathbf{v} \in X, && (7.4)\\
(q, \nabla\cdot\mathbf{u}) &= 0,\ \forall q \in P, && (7.5)\\
\mathbf{u}(0, \mathbf{x}) &= \mathbf{w}_0(\mathbf{x}),\ \forall \mathbf{x} \in \Omega. && (7.6)
\end{aligned}
$$

As the operator $(I - G_N G)$ is symmetric positive semi-definite, by Lemma 3.5, the operator $B : L^2(\Omega) \to L^2(\Omega)$ satisfying

$$
B^2\phi := \delta^{-(2N+2)}(I - G_N G)\phi = \delta^{-(2N+2)}(\phi - G_N\bar{\phi}) \tag{7.7}
$$

is bounded and well defined, (i.e. $B = \delta^{-(N+1)}\sqrt{I - G_N G}$).

$$
\text{Let} \qquad \phi^* := \delta^{(N+1)}\, B\phi \quad (\approx \phi - \bar{\phi}). \tag{7.8}
$$

Then, using Lemma 3.1 we have

$$
\begin{aligned}
\|\phi^*\| &= (\phi - G_N\bar{\phi},\, \phi)^{1/2} = \left(\delta^{2N+2}(B\phi,\, B\phi)\right)^{1/2}\\
&= \delta^{N+1}\|B\phi\|\,.
\end{aligned}
$$

Letting $\mathbf{e}(\mathbf{x},t) := \mathbf{w}(\mathbf{x},t) - \mathbf{u}(\mathbf{x},t)$, subtracting (7.4) from (7.1) we have that

$$
\begin{aligned}
(\mathbf{e}_t, \mathbf{v}) + (\mathbf{e}\cdot\nabla\mathbf{w}, \mathbf{v}) + (\mathbf{u}\cdot\nabla\mathbf{e}, \mathbf{v}) + \nu(\nabla\mathbf{e}, \nabla\mathbf{v}) + \chi(\mathbf{e} - G_N\bar{\mathbf{e}}, \mathbf{v})&\\
= \chi(\mathbf{w} - G_N\bar{\mathbf{w}}, \mathbf{v})\ ,\ \forall \mathbf{v} \in Z\,.&
\end{aligned}
$$

With the choice $\mathbf{v} = \mathbf{e}$ we obtain (using $(\mathbf{u}\cdot\nabla\mathbf{e}, \mathbf{e}) = 0$)

$$
\begin{aligned}
\frac{1}{2}\frac{d}{dt}\|\mathbf{e}\|^2 + (\mathbf{e}\cdot\nabla\mathbf{w}, \mathbf{e}) + \nu\|\nabla\mathbf{e}\|^2 + \chi\,(\mathbf{e} - G_N\bar{\mathbf{e}}, \mathbf{e}) &= \chi\,(\mathbf{w} - G_N\bar{\mathbf{w}}, \mathbf{e}),\\
\frac{1}{2}\frac{d}{dt}\|\mathbf{e}\|^2 - |(\mathbf{e}\cdot\nabla\mathbf{w}, \mathbf{e})| + \nu\|\nabla\mathbf{e}\|^2 + \chi\,\|\mathbf{e}^*\|^2 &\le \chi\,\delta^{2N+2}\|B\mathbf{w}\|\,\|B\mathbf{e}\|\,. \qquad (7.9)
\end{aligned}
$$

With the estimate (using Young's inequality),

$$
\begin{aligned}
|(\mathbf{e}\cdot\nabla\mathbf{w}, \mathbf{e})| &\le C\sqrt{\|\mathbf{e}\|\,\|\nabla\mathbf{e}\|}\,\|\nabla\mathbf{w}\|\,\|\nabla\mathbf{e}\| = C\|\mathbf{e}\|^{1/2}\,\|\nabla\mathbf{w}\|\,\|\nabla\mathbf{e}\|^{3/2}\\
&\le \frac{1}{2}\nu\|\nabla\mathbf{e}\|^2 + C_1\nu^{-3}\|\nabla\mathbf{w}\|^4\,\|\mathbf{e}\|^2\,,
\end{aligned}
$$

equation (7.9) becomes

$$\frac{d}{dt}\|\mathbf{e}\|^2 \,-\, C_1\,\nu^{-3}\|\nabla\mathbf{w}\|^4\,\|\mathbf{e}\|^2 \,+\, \nu\|\nabla\mathbf{e}\|^2 \,+\, \chi\,\|\mathbf{e}^*\|^2 \;\leq\; C_2\,\chi\,\delta^{2N+2}\|B\mathbf{w}\|^2.$$

Proceeding as in Gronwall's Lemma, multiplying through by the integrating factor $\exp(-\,C_1\,\nu^{-3}\int_0^{t'}\|\nabla\mathbf{w}\|^4\,ds)$ and using $\|\mathbf{e}\|(0)=0$, we obtain

$$\begin{aligned}\|\mathbf{e}\|^2 \;\;&+\;\; \int_0^t e^{(C_1\,\nu^{-3}\int_{t'}^t\|\nabla\mathbf{w}\|^4\,ds)}\left(\nu\|\nabla\mathbf{e}\|^2 \,+\, \chi\,\|\mathbf{e}^*\|^2\right)\,dt'\\ &\leq\;\; \int_0^t e^{(C_1\,\nu^{-3}\int_{t'}^t\|\nabla\mathbf{w}\|^4\,ds)}\left(C_2\,\chi\,\delta^{2N+2}\|B\mathbf{w}\|^2\right)\,dt'\,,\end{aligned}$$

i.e.,

$$\|\mathbf{e}\|^2 \,+\, \nu\int_0^t\|\nabla\mathbf{e}\|^2\,dt' \,+\, \int_0^t\chi\,\|\mathbf{e}^*\|^2\,dt' \;\leq\; C_2e^{C_1\,\nu^{-3}\,\|\mathbf{w}\|_{4,1}^4}\,\chi\,\delta^{2N+2}\int_0^t\|B\mathbf{w}\|^2\,dt'\,,$$

from which the following lemma follows.

Lemma 7.1. *With* $\mathbf{w}\in L^4(0,T;W_4^1)$ *satisfying (7.1)-(7.3) and* $\mathbf{u}$ *given by (7.4)-(7.6) we have that there exists constants* C_1, $C_2>0$, *such that*

$$\begin{aligned}\|\mathbf{w}\,-\,\mathbf{u}\|^2 \;\;&+\;\; \nu\int_0^t\|\nabla(\mathbf{w}\,-\,\mathbf{u})\|^2\,dt' \,+\, \chi\int_0^t\|(\mathbf{w}\,-\,\mathbf{u})^*\|^2\,dt'\\ &\leq\;\; C_2e^{C_1\,\nu^{-3}\,\|\mathbf{w}\|_{4,1}^4}\,\chi\,\delta^{2N+2}\int_0^t\|B\mathbf{w}\|^2\,dt'\,.\end{aligned}\tag{7.10}$$

□

7.2 NUMERICAL APPROXIMATION OF THE NAVIER-STOKES EQUATIONS USING TIME RELAXATION

In this section we address the error between the *stabilized* approximation computed using equations (7.4)-(7.6) and the solution to the Navier-Stokes equations. In view of estimate (7.10), and with the aid of the triangle inequality, the desired error estimate reduces to finding the error between the numerical approximation of (7.4)-(7.6) and its true solution.

We begin by describing the finite element approximation framework and listing the approximating properties used in the analysis.

Let $\Omega \subset \mathbb{R}^{\acute{d}}$ $(\acute{d} = 2, 3)$ be a polygonal domain and let T_h be a triangulation of Ω made of triangles (in $\mathbb{R}^2$) or tetrahedrons (in $\mathbb{R}^3$). Thus, the computational domain is defined by

$$\Omega = \cup K; \quad K \in T_h.$$

We assume that there exist constants c_1, c_2 such that

$$c_1 h \leq h_K \leq c_2 \rho_K$$

where h_K is the diameter of triangle (tetrahedron) K, ρ_K is the diameter of the greatest ball (sphere) included in K, and $h = \max_{K \in T_h} h_K$. Let $P_k(A)$ denote the space of polynomials on A of degree no greater than k. Then we define the finite element spaces as follows.

$$\begin{aligned} X_h &:= \left\{ \mathbf{v} \in X \cap C(\bar{\Omega})^2 : \mathbf{v}|_K \in P_k(K),\ \forall K \in T_h \right\}, \\ P_h &:= \left\{ q \in P \cap C(\bar{\Omega}) : q|_K \in P_s(K),\ \forall K \in T_h \right\}, \\ Z_h &:= \left\{ \mathbf{v} \in X_h : (q, \nabla \cdot \mathbf{v}) = 0,\ \forall q \in P_h \right\}. \end{aligned}$$

We assume that the spaces X_h, P_h satisfy the discrete inf-sup condition, namely there exists $\gamma \in \mathbb{R}$, $\gamma > 0$,

$$\gamma \leq \inf_{q_h \in P_h} \sup_{\mathbf{v}_h \in X_h} \frac{\int_\Omega q_h \nabla \cdot \mathbf{v}_h \, dA}{\|q_h\|_P \, \|\mathbf{v}_h\|_X}. \tag{7.11}$$

Let $\triangle t$ be the step size for t so that $t_n = n\triangle t$, $n = 0, 1, 2, \ldots, N_T$, with $T := N_T \triangle t$, and $d_t f^n := \frac{f(t_n) - f(t_{n-1})}{\triangle t}$. We define the following additional norms:

$$
\begin{aligned}
|||v|||_{\infty,k} &:= \max_{0\le n\le N_T} \|v^n\|_k\,, & |||v_{1/2}|||_{\infty,k} &:= \max_{1\le n\le N_T} \|v^{n-1/2}\|_k\,,\\
|||v|||_{m,k} &:= \left(\sum_{n=0}^{N_T} \|v^n\|_k^m \triangle t\right)^{1/m}, & |||v_{1/2}|||_{m,k} &:= \left(\sum_{n=1}^{N_T} \|v^{n-1/2}\|_k^m \triangle t\right)^{1/m}.
\end{aligned}
$$

In addition, we make use of the following approximation properties, Brenner and Scott [9]:

$$
\begin{aligned}
\inf_{\mathbf{v}\in X_h} \|\mathbf{u}-\mathbf{v}\| &\le Ch^{k+1}|\mathbf{u}|_{k+1}, \quad \mathbf{u}\in H^{k+1}(\Omega)^{\acute{d}},\\
\inf_{\mathbf{v}\in X_h} \|\mathbf{u}-\mathbf{v}\|_1 &\le Ch^{k}|\mathbf{u}|_{k+1}, \quad \mathbf{u}\in H^{k+1}(\Omega)^{\acute{d}},\\
\inf_{r\in P_h} \|p-r\| &\le Ch^{s+1}|p|_{s+1}, \quad p\in H^{s+1}(\Omega).
\end{aligned}
\tag{7.12}
$$

We define the *skew-symmetric trilinear form* $b^*(\cdot,\cdot,\cdot) : X\times X\times X \to \mathbb{R}$ as

$$
b^*(\mathbf{u},\mathbf{v},\mathbf{w}) := \frac{1}{2}(\mathbf{u}\cdot\nabla\mathbf{v},\mathbf{w}) - \frac{1}{2}(\mathbf{u}\cdot\nabla\mathbf{w},\mathbf{v})\,. \tag{7.13}
$$

Note that for $\mathbf{u}$, $\mathbf{v}$, $\mathbf{w}$, $\in X$, with $\int_\Omega q\,\nabla\cdot\mathbf{u}\,dA = 0$, $\forall q\in P$,

$$
b^*(\mathbf{u},\mathbf{v},\mathbf{w}) = b(\mathbf{u},\mathbf{v},\mathbf{w}) := (\mathbf{u}\cdot\nabla\mathbf{v},\mathbf{w})\,.
$$

For ease of notation in discussion the Crank-Nicolson temporal discretization we let

$$
\breve{\mathbf{u}}^n = \frac{u^n + u^{n-1}}{2}\,.
$$

The time relaxed, discrete approximation to (7.4)-(7.6) on the time interval $(0,T]$, is given by:

For $n = 1, 2, \ldots, N_T$, find $\mathbf{u}_h^n \in X_h$, $p_h^n \in P_h$, such that

$$
\begin{aligned}
(\mathbf{u}_h^n,\mathbf{v}) + \triangle t\, b^*(\breve{\mathbf{u}}_h^n,\breve{\mathbf{u}}_h^n,\mathbf{v}) - \triangle t\,(\breve{p}_h^n,\nabla\cdot\mathbf{v}) &+ \triangle t\,\nu(\nabla\breve{\mathbf{u}}_h^n,\nabla\mathbf{v}) + \triangle t\,\chi\,(\breve{\mathbf{u}}_h^n - G_N\bar{\breve{\mathbf{u}}}_h^n,\mathbf{v})\\
&= (\mathbf{u}_h^{n-1},\mathbf{v}) + \triangle t\,(\breve{\mathbf{f}}^n,\mathbf{v}),\ \forall\mathbf{v}\in X_h\,, && (7.14)\\
(q,\nabla\cdot\mathbf{u}_h^n) &= 0\,,\ \forall q\in P_h\,, && (7.15)\\
(\mathbf{u}_h^0,\mathbf{v}) &= (\mathbf{w}_0,\mathbf{v})\,,\ \forall\mathbf{v}\in X_h\,. && (7.16)
\end{aligned}
$$

As the spaces X_h and P_h satisfy the discrete inf-sup condition (7.11), we can equivalently consider the problem:

For $n = 1, 2, \ldots, N_T$ *find* $\mathbf{u}_h^n \in Z_h$, $p_h \in P_h$, *such that*

$$\begin{aligned}(\mathbf{u}_h^n, \mathbf{v}) \;&+\; \triangle t\, b^*(\breve{\mathbf{u}}_h^n, \breve{\mathbf{u}}_h^n, \mathbf{v}) \;+\; \triangle t\, \nu(\nabla \breve{\mathbf{u}}_h^n, \nabla \mathbf{v}) \;+\; \triangle t\, \chi\, (\breve{\mathbf{u}}_h^n - G_N \bar{\breve{\mathbf{u}}}_h^n, \mathbf{v}) \\ &=\; (\mathbf{u}_h^{n-1}, \mathbf{v}) \;+\; \triangle t\, (\breve{\mathbf{f}}^n, \mathbf{v}),\;\; \forall \mathbf{v} \in Z_h\,. \end{aligned} \tag{7.17}$$

The discrete Gronwall's lemma plays an important role in the following analysis (Heywood and Rannacher [28]).

Lemma 7.2 (Discrete Gronwall's Lemma)**.** *Let* Δt, H, *and* a_n, b_n, c_n, γ_n *(for integers* $n \geq 0$*) be nonnegative numbers such that*

$$a_l \;+\; \Delta t \sum_{n=0}^{l} b_n \;\leq\; \Delta t \sum_{n=0}^{l} \gamma_n\, a_n \;+\; \Delta t \sum_{n=0}^{l} c_n \;+\; H \quad \textit{for } l \geq 0\,.$$

Suppose that $\Delta t\, \gamma_n < 1$, *for all* n, *and set* $\sigma_n = (1 - \Delta t\, \gamma_n)^{-1}$. *Then,*

$$a_l \;+\; \Delta t \sum_{n=0}^{l} b_n \;\leq\; \exp\left(\Delta t \sum_{n=0}^{l} \sigma_n\, \gamma_n\right) \left\{\Delta t \sum_{n=0}^{l} c_n \;+\; H\right\} \quad \textit{for } l \geq 0\,. \tag{7.18}$$

For the approximation scheme given by (7.17) we have that the iteration is computable and satisfies the following a priori estimate.

Lemma 7.3. *For the approximation scheme (7.17) we have that a solution* $\mathbf{u}_h^l$, $l = 1, \ldots N_T$, *exists at each iteration and, for* $\triangle t < 1$, *satisfies the following a priori bounds:*

$$\|\mathbf{u}_h^l\|^2 \;+\; 2\triangle t\, \chi \sum_{n=1}^{l} \|\breve{\mathbf{u}}_h^{n\,*}\|^2 \;+\; 2\triangle t\, \nu \sum_{n=1}^{l} \|\nabla \breve{\mathbf{u}}_h^n\|^2 \;\leq\; C\left(|||f|||_{2,0}^2 \;+\; \|\mathbf{u}_h^0\|^2\right). \tag{7.19}$$

Proof. To obtain the a priori estimate, in (7.17) setting $\mathbf{v} = \breve{\mathbf{u}}_h^n$ we have

$$\|\mathbf{u}_h^n\|^2 \, - \, \|\mathbf{u}_h^{n-1}\|^2 \, + \, 2\triangle t\, \nu \|\nabla \breve{\mathbf{u}}_h^n\|^2 \, + \, 2\triangle t\, \chi \, \|\breve{\mathbf{u}}_h^{n\,*}\|^2 \, \leq \, \triangle t\, \|\breve{\mathbf{u}}_h^n\|^2 \, + \, \triangle t\, \|\breve{\mathbf{f}}^n\|^2 \, . \tag{7.20}$$

Summing (7.20) from $n = 1$ to l, implies

$$\begin{aligned} \|\mathbf{u}_h^l\|^2 \, + \, 2\triangle t\, \chi \sum_{n=1}^{l} \|\breve{\mathbf{u}}_h^{n\,*}\|^2 \quad + \quad & 2\triangle t\, \nu \sum_{n=1}^{l} \|\nabla \breve{\mathbf{u}}_h^n\|^2 \\ & \leq \quad \|\mathbf{u}_h^0\|^2 \, + \, \triangle t \sum_{n=1}^{l} \|\breve{\mathbf{u}}_h^n\|^2 \, + \, \triangle t \sum_{n=1}^{l} \|\breve{\mathbf{f}}^n\|^2 \, , \\ & \leq \quad \|\mathbf{u}_h^0\|^2 \, + \, \triangle t \sum_{n=0}^{l} \|\mathbf{u}_h^n\|^2 \, + \, \triangle t \sum_{n=0}^{l} \|\mathbf{f}^n\|^2 \, . \end{aligned} \tag{7.21}$$

Applying (7.18) we obtain (7.19), with C explicitly given by $C = \exp(T/(1 - \triangle t))$.

The existence of a solution $\mathbf{u}_h^n$ to (7.17) follows from the Leray-Schauder Fixed Point Theorem, see Layton [35] and Zeidler [63]. We reformulate (7.17) as a fixed point problem, insert a parameter γ and adapt the proof of the a priori bound to give a bound uniform in γ. For this, let $A : X' \to Z_h$ be the solution operator of the modified Stokes problem. Specifically, $T(\mathbf{g}) = \mathbf{w}$ where $\mathbf{w} \in Z_h$ solves

$$\nu(\nabla(\mathbf{w} + \mathbf{u}_h^{n-1})/2, \nabla \mathbf{v}) \, + \, \chi((\mathbf{w} + \mathbf{u}_h^{n-1})/2 - G_N(\bar{\mathbf{w}} + \bar{\mathbf{u}}_h^{n-1})/2, \mathbf{v}) \, = \, (\mathbf{g}, \mathbf{v}) \text{ for all } \mathbf{v} \in Z_h.$$

The Lax-Milgram theorem (see Layton [35]) gives that T exists and it is bounded. Also, T is linear.

Now, we define the nonlinear operator $N : Z_h \to X'$ by the Riesz Representation theorem using

$$(N(\mathbf{w}), v) = (\breve{\mathbf{f}}^n, \mathbf{v}) \, - \, b^*(\frac{\mathbf{w} + \mathbf{u}_h^{n-1}}{2}, \frac{\mathbf{w} + \mathbf{u}_h^{n-1}}{,}\mathbf{v}) \, + \, \frac{1}{\triangle t}(\mathbf{u}_h^{n-1} - \mathbf{w}, \mathbf{v}) \text{ for all } \mathbf{v} \in Z_h.$$

This way defined, N is a continuous and bounded operator. Finally, define $F : Z_h \to Z_h$ by $F(\mathbf{w}) = T(N(\mathbf{w}))$ as being a compact operator (based on the result that in finite dimensional space any continuous function is compact). We note that $\mathbf{w}$ is a solution of (7.17) if and only if $\mathbf{w}$ is a fixed point of F.

Now, it is left to show that a fixed point $\mathbf{w}$ of $F(\mathbf{w}) = \mathbf{w}$, in Z_h, exists. Consider

$$\mathbf{w}_\gamma = \gamma\, F(\mathbf{w}_\gamma) \text{ in } Z_h \tag{7.22}$$

By the Leray-Schauder Fixed Point Theorem we need only to prove an a priori bound on $\|\nabla \mathbf{w}_\gamma\|$ independent of γ. We start by rewriting (7.22) as

$$\begin{aligned} &\nu(\nabla(\mathbf{w}_\gamma + \mathbf{u}_h^{n-1})/2, \nabla \mathbf{v}) \;+\; \chi((\mathbf{w}_\gamma + \mathbf{u}_h^{n-1})/2 - G_N(\bar{\mathbf{w}}_\gamma + \bar{\mathbf{u}}_h^{n-1})/2, \mathbf{v}) \\ =\; &\gamma\,(\breve{\mathbf{f}}^n, \mathbf{v}) \;-\; \gamma\, b^*(\frac{\mathbf{w}_\gamma + \mathbf{u}_h^{n-1}}{2}, \frac{\mathbf{w}_\gamma + \mathbf{u}_h^{n-1}}{,}\mathbf{v}) \;+\; \gamma\,\frac{1}{\triangle t}(\mathbf{u}_h^{n-1} - \mathbf{w}_\gamma, \mathbf{v}) \text{ for all } \mathbf{v} \in Z_h. \end{aligned}$$

Setting $\mathbf{v} = \frac{\mathbf{w}_\gamma + \mathbf{u}_h^{n-1}}{2}$, using that $0 < \gamma \leq 1$ and proceeding as in the a priori bound we obtain the necessary bound for $\|\nabla \mathbf{w}_\gamma\|$, i.e. the existence of the solution of (7.17).

□

For the approximation error between $\mathbf{u}_h^n$ satisfying (7.17) and $\mathbf{u}^n$ satisfying (7.4) we have the following.

Theorem 7.1. *For $\mathbf{u} \in L^\infty(0,T;W_4^{k+1}) \cap W_2^3(0,T;L^2) \cap W_4^2(0,T;W_2^1)$, $p \in L^4(0,T;W_4^{s+1}) \cap W_2^2(0,T;L^2)$, $f \in L^2(0,T;W_2^2)$, $\mathbf{w}_0 \in W_2^{k+1}$ satisfying (7.4)-(7.6), and $\mathbf{u}_h$ given by (7.14)-(7.16) we have that for $\triangle t$ sufficiently small*

$$|||\mathbf{u} - \mathbf{u}_h|||_{\infty,0} \;\leq\; \mathbf{F}(\triangle t, h, \delta, \chi) \;+\; Ch^{k+1}|||\mathbf{u}|||_{\infty,k+1}\,, \tag{7.23}$$

$$\begin{aligned} \left(\nu\triangle t \sum_{n=1}^{l} \|\nabla(\mathbf{u}^{n+1/2} - (\mathbf{u}_h^n + \mathbf{u}_h^{n-1})/2)\|^2\right)^{1/2} &\leq \mathbf{F}(\triangle t, h, \delta, \chi) \;+\; C\nu^{1/2}(\triangle t)^2 \|\nabla \mathbf{u}_{tt}\|_{2,0} \\ &\quad + C\nu^{1/2} h^k |||\mathbf{u}|||_{2,k+1}\,, \text{ for } 1 \leq l \leq N_T \end{aligned} \tag{7.24}$$

where

$$\begin{aligned} \mathbf{F}(\triangle t, h, \delta, \chi) \;:=\; & C\nu^{-1/2}\left(h^k |||\mathbf{u}|||_{4,k+1}^2 \;+\; h^{k+1/2}|||\nabla \mathbf{u}|||_{4,0}^2 \;+\; h^{s+1}|||p_{1/2}|||_{2,s+1}\right) \\ & + C\nu^{-1/2}\, h^k \left(|||\mathbf{f}|||_{2,0} \;+\; \|\mathbf{u}_h^0\|\right) \;+\; C\nu^{1/2}\, h^k |||u|||_{2,k+1} \\ & + C\chi^{1/2}\, h^{k+1}|||u|||_{2,k+1} \;+\; C(\triangle t)^2\left(\|\mathbf{u}_{ttt}\|_{2,0} \;+\; \nu^{-1/2}\|p_{tt}\|_{2,0} \;+\; \|\mathbf{f}_{tt}\|_{2,0}\right. \\ & \qquad + \nu^{1/2}\|\nabla \mathbf{u}_{tt}\|_{2,0} \;+\; \nu^{-1/2}\|\nabla \mathbf{u}_{tt}\|_{4,0}^2 \\ & \qquad + \nu^{-1/2}|||\nabla \mathbf{u}|||_{4,0}^2 \;+\; \nu^{-1/2}|||\nabla \mathbf{u}_{1/2}|||_{4,0}^2 \\ & \qquad \left. + \;\chi^{1/2}\,\delta^{2N+2}\|\mathbf{u}_{tt}\|_{2,0} + \chi^{1/2}\,\|\mathbf{u}_{tt}\|_{2,0}\right)\,. \end{aligned}$$

Proof. Let $\mathcal{A} : X \times X \to \mathbb{R}$ be defined by

$$\mathcal{A}(\mathbf{u}, \mathbf{v}) \;:=\; \nu(\nabla \mathbf{u}\,, \nabla \mathbf{v}) \,+\, \chi(\mathbf{u} - G_N \bar{\mathbf{u}}\,,\, \mathbf{v})\;, \tag{7.25}$$

and note that

$$\mathcal{A}(\mathbf{u}, \mathbf{u}) \;=\; \nu \|\nabla \mathbf{u}\|^2 + \chi \|\mathbf{u}^*\|^2\;. \tag{7.26}$$

Then, (7.17) may be written as

$$(\mathbf{u}_h^n - \mathbf{u}_h^{n-1}, \mathbf{v}) \,+\, \Delta t\, \mathcal{A}(\breve{\mathbf{u}}_h^n, \mathbf{v}) \,+\, \Delta t\, b^*(\breve{\mathbf{u}}_h^n, \breve{\mathbf{u}}_h^n, \mathbf{v}) \;=\; \Delta t\, (\breve{\mathbf{f}}, \mathbf{v})\;, \quad \forall \mathbf{v} \in Z_h\,. \tag{7.27}$$

Also, at time $t = (n - 1/2)\Delta t$, $\mathbf{u}$ given by (7.4)-(7.5) satisfies

$$\begin{aligned}(\mathbf{u}^n - \mathbf{u}^{n-1}, \mathbf{v}) \,+\, \Delta t\, \mathcal{A}(\breve{\mathbf{u}}^n, \mathbf{v}) \,+\, \Delta t\, b^*(\breve{\mathbf{u}}^n, \breve{\mathbf{u}}^n, \mathbf{v}) \,-\, \Delta t\, (\breve{p}^n, \nabla \cdot \mathbf{v}) \\ = \;\Delta t\, (\breve{\mathbf{f}}, \mathbf{v}) \,+\, \Delta t\, Intp(\mathbf{u}^n, p^n; \mathbf{v})\;,\end{aligned} \tag{7.28}$$

for all $\mathbf{v} \in Z_h$, where $Intp(\mathbf{u}^n, p^n; \mathbf{v})$, representing the interpolating error, denotes

$$\begin{aligned}Intp(\mathbf{u}^n, p^n; \mathbf{v}) \;=\; &\left(d_t \mathbf{u}^n - \mathbf{u}_t^{n-1/2}, \mathbf{v}\right) + \mathcal{A}(\breve{\mathbf{u}}^n \,-\, \mathbf{u}^{n-1/2}, \mathbf{v}) \,+\, b^*(\breve{\mathbf{u}}^n, \breve{\mathbf{u}}^n, \mathbf{v}) \\ &- b^*(\mathbf{u}^{n-1/2}, \mathbf{u}^{n-1/2}, \mathbf{v}) \,-\, (\breve{p}^n - p^{n-1/2}, \nabla \cdot \mathbf{v}) \,+\, (\mathbf{f}^{n-1/2} - \breve{\mathbf{f}}, \mathbf{v}).\end{aligned} \tag{7.29}$$

Subtracting (7.27) from (7.28), we have for $\mathbf{e}^n \;=\; \mathbf{u}^n \,-\, \mathbf{u}_h^n$,

$$\begin{aligned}(\mathbf{e}^n - \mathbf{e}^{n-1}, \mathbf{v}) \,+\, \Delta t \mathcal{A}(\breve{\mathbf{e}}^n, \mathbf{v}) \,+\, \Delta t\, (b^*(\breve{\mathbf{e}}^n, \breve{\mathbf{u}}^n, \mathbf{v}) \,+\, b^*(\breve{\mathbf{u}}_h^n, \breve{\mathbf{e}}^n, \mathbf{v})) \\ = \;\Delta t(\breve{p}^n, \nabla \cdot \mathbf{v}) \,+\, \Delta t\, Intp(\mathbf{u}^n, p^n; \mathbf{v})\;,\; \text{for all } \mathbf{v} \in Z_h.\end{aligned} \tag{7.30}$$

Let $\mathbf{e}^n \;=\; \mathbf{u}^n \,-\, \mathbf{u}_h^n \;=\; (\mathbf{u}^n - \mathbf{U}^n) \,+\, (\mathbf{U}^n - \mathbf{u}_h^n) := \Lambda^n \,+\, E^n$, where $\mathbf{U}^n$ is the L^2 projection of $\mathbf{u}$ in Z_h.

With the choice $\mathbf{v} = \breve{E}^n$, and using $(q, \nabla \cdot \breve{E}^n) = 0, \;\; \forall q \in P_h$, equation (7.30) becomes

$$\begin{aligned}(E^n - E^{n-1}, \breve{E}^n) \;+\; &\Delta t \mathcal{A}(\breve{E}^n, \breve{E}^n) \,+\, \Delta t \left(b^*(\breve{E}^n, \breve{\mathbf{u}}^n, \breve{E}^n) \,+\, b^*(\breve{\mathbf{u}}_h^n, \breve{E}^n, \breve{E}^n)\right) \\ = \;&-(\Lambda^n - \Lambda^{n-1}, \breve{E}^n) \,-\, \Delta t \mathcal{A}(\breve{\Lambda}^n, \breve{E}^n) \\ &-\Delta t \left(b^*(\breve{\Lambda}^n, \breve{\mathbf{u}}^n, \breve{E}^n) \,+\, b^*(\breve{\mathbf{u}}_h^n, \breve{\Lambda}^n, \breve{E}^n)\right) \\ &+\Delta t(\breve{p}^n - q, \nabla \cdot \breve{E}^n) \,+\, \Delta t\, Intp(\mathbf{u}^n, p^n; \breve{E}^n)\;,\end{aligned}$$

i.e.,

$$\begin{aligned}\frac{1}{2}\left(\|E^n\|^2 - \|E^{n-1}\|^2\right) &+ \Delta t\left(\nu\|\nabla\breve{E}^n\|^2 + \chi\|\breve{E}^{n*}\|^2\right)\\ &= -\Delta t\, b^*(\breve{E}^n, \breve{\mathbf{u}}^n, \breve{E}^n) - (\Lambda^n - \Lambda^{n-1}, \breve{E}^n) - \Delta t\mathcal{A}(\breve{\Lambda}^n, \breve{E}^n)\\ &\quad - \Delta t\left(b^*(\breve{\Lambda}^n, \breve{\mathbf{u}}^n, \breve{E}^n) + b^*(\breve{\mathbf{u}}_h^n, \breve{\Lambda}^n, \breve{E}^n)\right)\\ &\quad + \Delta t(\breve{p}^n - q, \nabla\cdot\breve{E}^n) + \Delta t\, Intp(\mathbf{u}^n, p^n; \breve{E}^n)\,. \end{aligned} \tag{7.31}$$

Next we estimate the terms on the RHS of (7.31).

Because of the choice of $\mathbf{U}$ we obtain

$$(\Lambda^n - \Lambda^{n-1}, \breve{E}^n) = 0\,. \tag{7.32}$$

Using $b^*(\mathbf{u},\mathbf{v},\mathbf{w}) \le C(\Omega)\sqrt{\|\mathbf{u}\|\,\|\nabla\mathbf{u}\|}\,\|\nabla\mathbf{v}\|\,\|\nabla\mathbf{w}\|$, for $\mathbf{u}$, $\mathbf{v}$, $\mathbf{w} \in X$, and Young's inequality,

$$\begin{aligned} b^*(\breve{E}^n, \breve{\mathbf{u}}^n, \breve{E}^n) &\le C\|\breve{E}^n\|^{1/2}\,\|\nabla\breve{E}^n\|^{3/2}\,\|\nabla\breve{\mathbf{u}}^n\|\\ &\le \frac{\nu}{10}\|\nabla\breve{E}^n\|^2 + C\,\nu^{-3}\|\breve{E}^n\|^2\|\nabla\breve{\mathbf{u}}^n\|^4\,. \end{aligned} \tag{7.33}$$

$$\begin{aligned} \mathcal{A}(\breve{\Lambda}^n, \breve{E}^n) &= \nu(\nabla\breve{\Lambda}^n, \nabla\breve{E}^n) + \chi\,(\breve{\Lambda}^n - G_N\bar{\breve{\Lambda}}^n, \breve{E}^n)\\ &\le \frac{\nu}{10}\|\nabla\breve{E}^n\|^2 + C\,\nu\|\nabla\breve{\Lambda}^n\|^2 + \chi\delta^{2N+2}\|B\breve{\Lambda}^n\|\|B\breve{E}^n\|\\ &\le \frac{\nu}{10}\|\nabla\breve{E}^n\|^2 + C\,\nu\|\nabla\breve{\Lambda}^n\|^2 + \chi\frac{1}{2}(\breve{\Lambda}^n - G_N\bar{\breve{\Lambda}}^n, \breve{\Lambda}^n) + \chi\,\frac{1}{2}\|\breve{E}^{n*}\|^2\\ &\le \frac{\nu}{10}\|\nabla\breve{E}^n\|^2 + C\,\nu\|\nabla\breve{\Lambda}^n\|^2 + \chi\,\frac{1}{4}\|\breve{\Lambda}^n - G_N\bar{\breve{\Lambda}}^n\|^2\\ &\quad + \chi\,\frac{1}{4}\|\breve{\Lambda}^n\|^2 + \chi\,\frac{1}{2}\|\breve{E}^{n*}\|^2. \end{aligned} \tag{7.34}$$

$$\begin{aligned} b^*(\breve{\Lambda}^n, \breve{\mathbf{u}}^n, \breve{E}^n) &\le C\sqrt{\|\breve{\Lambda}^n\|\,\|\nabla\breve{\Lambda}^n\|}\,\|\nabla\breve{\mathbf{u}}^n\|\,\|\nabla\breve{E}^n\|\\ &\le \frac{\nu}{10}\|\nabla\breve{E}^n\|^2 + \nu^{-1}\,C\,\|\breve{\Lambda}^n\|\,\|\nabla\breve{\Lambda}^n\|\,\|\nabla\breve{\mathbf{u}}^n\|^2\,. \end{aligned} \tag{7.35}$$

$$b^*(\breve{\mathbf{u}}_h^n, \breve{\Lambda}^n, \breve{E}^n) \le \frac{\nu}{10}\|\nabla\breve{E}^n\|^2 + \nu^{-1}\,C\,\|\breve{\mathbf{u}}_h^n\|\,\|\nabla\breve{\mathbf{u}}_h^n\|\,\|\nabla\breve{\Lambda}^n\|^2\,. \tag{7.36}$$

$$
\begin{aligned}
(\breve{p}^n - q, \nabla \cdot \breve{E}^n) &\leq \|\breve{p}^n - q\| \, \|\nabla \cdot \breve{E}^n\| \\
&\leq \frac{\nu}{10} \|\nabla \breve{E}^n\|^2 \, + \, \nu^{-1} \, C \, \|\breve{p} - q\|^2 \, . \qquad (7.37)
\end{aligned}
$$

Substituting (7.32)-(7.37) into (7.31), and summing from $n = 1$ to l (assuming that $\|E^0\| = 0$), we have

$$
\begin{aligned}
\|E^l\|^2 \;+\; & \triangle t \sum_{n=1}^{l} \nu \|\nabla \breve{E}^n\|^2 \; + \triangle t \chi \sum_{n=1}^{l} \|\breve{E}^{n\,*}\|^2 \\
\leq \; & \triangle t \sum_{n=1}^{l} C \, (\nu^{-3} \|\nabla \breve{\mathbf{u}}^n\|^4) \|\breve{E}^n\|^2 \\
& + \triangle t \sum_{n=1}^{l} \|\Lambda^n - \Lambda^{n-1}\|^2 + \; 2 \triangle t \sum_{n=1}^{l} C \, \nu \|\nabla \breve{\Lambda}^n\|^2 \\
& + \triangle t \, \chi \, \frac{1}{2} \left(\sum_{n=1}^{l} \|\breve{\Lambda}^n - G_N \bar{\breve{\Lambda}}^n\|^2 + \sum_{n=1}^{l} \|\breve{\Lambda}^n\|^2 \right) \\
& + 2 \triangle t \sum_{n=1}^{l} C \, \nu^{-1} \left(\|\breve{\Lambda}^n\| \, \|\nabla \breve{\Lambda}^n\| \, \|\nabla \breve{\mathbf{u}}^n\|^2 \; + \; \|\breve{\mathbf{u}}_h^n\| \, \|\nabla \breve{\mathbf{u}}_h^n\| \, \|\nabla \breve{\Lambda}^n\|^2 \right) \\
& + 2 \triangle t \sum_{n=1}^{l} C \, \nu^{-1} \|\breve{p}^n - q\|^2 \\
& + 2 \triangle t \sum_{n=1}^{l} |Intp(\mathbf{u}^n, p^n; \breve{E}^n)| \, . \qquad (7.38)
\end{aligned}
$$

The next step in the proof is to bound the terms on the RHS of (7.38). We have that

$$
\begin{aligned}
2 \triangle t \sum_{n=1}^{l} C \, \nu \|\nabla \breve{\Lambda}^n\|^2 \;\leq\; & 2 \triangle t \, C \, \nu \sum_{n=0}^{l} \|\nabla \Lambda^n\|^2 \;\leq\; 2C \, \nu \, \triangle t \sum_{n=0}^{l} h^{2k} |\mathbf{u}^n|_{k+1}^2 \\
\leq \; & 2C \, \nu \, h^{2k} |||\mathbf{u}|||_{2,k+1}^2 \, . \qquad (7.39)
\end{aligned}
$$

Also,

$$
\begin{aligned}
\triangle t \sum_{n=1}^{l} \|\Lambda^n - \Lambda^{n-1}\|^2 \;\leq\; & 4 \, \triangle t \sum_{n=0}^{l} \|\Lambda^n\|^2 \;\leq\; 4 \, \triangle t \sum_{n=0}^{l} C \, h^{2k+2} |u^n|_{k+1}^2 \\
\leq \; & C h^{2k+2} |||u|||_{2,k+1}^2 \, . \qquad (7.40)
\end{aligned}
$$

Using Lemma 3.1, and that $G_N G$ is a bounded operator from $L^2(\Omega) \to L^2(\Omega)$,

$$\begin{aligned}
\triangle t\,\chi\,\frac{1}{2}\left(\sum_{n=1}^{l}\|\breve{\Lambda}^n - G_N\bar{\breve{\Lambda}}^n\|^2 + \sum_{n=1}^{l}\|\breve{\Lambda}^n\|^2\right) &\leq C\triangle t\,\chi\sum_{n=1}^{l}\|\breve{\Lambda}^n\|^2 \;+\; \triangle t\,\chi\sum_{n=1}^{l}\|G_N G\breve{\Lambda}^n\|^2 \\
&\leq C\triangle t\,\chi\sum_{n=0}^{l}\|\Lambda^n\|^2 \;+\; \triangle t\,\chi\sum_{n=1}^{l}C_N\|\breve{\Lambda}^n\|^2 \\
&\leq C\triangle t\,\chi\sum_{n=0}^{l}C\,h^{2k+2}|u^n|_{k+1}^2 \;+\; \triangle t\,\chi\,C_N\sum_{n=0}^{l}\|\Lambda^n\|^2 \\
&\leq C\,\chi\,h^{2k+2}\triangle t\sum_{n=0}^{l}|u^n|_{k+1}^2 \\
&\leq C\,\chi\,h^{2k+2}|||u|||_{2,k+1}^2\,. \qquad (7.41)
\end{aligned}$$

For the term

$$\begin{aligned}
2\triangle t\sum_{n=1}^{l}C\,\nu^{-1}\|\breve{\Lambda}^n\|\,\|\nabla\breve{\Lambda}^n\|\,\|\nabla\breve{\mathbf{u}}^n\|^2 &\leq C\,\nu^{-1}\,\triangle t\sum_{n=1}^{l}\big(\|\Lambda^n\|\,\|\nabla\Lambda^n\| \;+\; \|\Lambda^{n-1}\|\,\|\nabla\Lambda^{n-1}\| \\
&\qquad + \|\Lambda^{n-1}\|\,\|\nabla\Lambda^n\| + \;\|\Lambda^n\|\,\|\nabla\Lambda^{n-1}\|\big)\,\|\nabla\breve{\mathbf{u}}^n\|^2 \\
&\leq C\,\nu^{-1}\,h^{2k+1}\left(\triangle t\sum_{n=1}^{l}|\mathbf{u}^n|_{k+1}^2\,\|\nabla\breve{\mathbf{u}}^n\|^2\right. \\
&\qquad + \;\triangle t\sum_{n=1}^{l}|\mathbf{u}^n|_{k+1}|\mathbf{u}^{n-1}|_{k+1}\,\|\nabla\breve{\mathbf{u}}^n\|^2 \\
&\qquad \left. + \;\triangle t\sum_{n=1}^{l}|\mathbf{u}^{n-1}|_{k+1}^2\,\|\nabla\breve{\mathbf{u}}^n\|^2\right) \\
&\leq C\,\nu^{-1}\,h^{2k+1}\left(\triangle t\sum_{n=0}^{l}|\mathbf{u}^n|_{k+1}^4 + \triangle t\sum_{n=0}^{l}\|\nabla\mathbf{u}^n\|^4\right) \\
&= C\,\nu^{-1}\,h^{2k+1}\left(|||\mathbf{u}|||_{4,k+1}^4 \;+\; |||\nabla\mathbf{u}|||_{4,0}^4\right)\,. \qquad (7.42)
\end{aligned}$$

Using the a priori estimate for $\|\mathbf{u}_h^n\|$, (7.19),

$$
\begin{aligned}
& 2\triangle t \sum_{n=1}^{l} C\,\nu^{-1} \left(\|\breve{\mathbf{u}}_h^n\| \, \|\nabla \breve{\mathbf{u}}_h^n\| \, \|\nabla \breve{\Lambda}^n\|^2 \right) \leq C\,\nu^{-1}\,\triangle t \sum_{n=1}^{l} \|\nabla \breve{\mathbf{u}}_h^n\| \, \|\nabla \breve{\Lambda}^n\|^2 \\
\leq \;& C\,\nu^{-1}\,\triangle t \sum_{n=1}^{l} \left(\|\nabla \Lambda^n\|^2 \,+\, \|\nabla \Lambda^{n-1}\|^2 \right) \|\nabla \breve{\mathbf{u}}_h^n\| \\
\leq \;& C\,\nu^{-1}\,h^{2k}\,\triangle t \sum_{n=1}^{l} \left(|\mathbf{u}^n|_{k+1}^2 \,+\, |\mathbf{u}^{n-1}|_{k+1}^2 \right) \|\nabla \breve{\mathbf{u}}_h^n\| \\
\leq \;& C\,\nu^{-1}\,h^{2k} \left(\triangle t \sum_{n=0}^{l} \|\mathbf{u}^n\|_{k+1}^4 \,+\, \triangle t \sum_{n=1}^{l} \|\nabla \breve{\mathbf{u}}_h^n\|^2 \right) \\
\leq \;& C\,\nu^{-1}\,h^{2k} \left(|||\mathbf{u}|||_{4,k+1}^4 \,+\, \nu^{-1} \left(|||\mathbf{f}|||_{2,0}^2 \,+\, \|\mathbf{u}_h^0\|^2 \right) \right). \qquad (7.43)
\end{aligned}
$$

From (.1),

$$
\begin{aligned}
& 2\triangle t \sum_{n=1}^{l} C\,\nu^{-1} \|\breve{p}^n - q\|^2 \leq C\,\nu^{-1}\,\triangle t \sum_{n=1}^{l} \|p^{n-1/2} - q\|^2 \,+\, \|\breve{p}^n - p^{n-1/2}\|^2 \\
\leq \;& C\,\nu^{-1} \left(h^{2s+2}\,\triangle t \sum_{n=1}^{l} \|p^{n-1/2}\|_{s+1}^2 \,+\, \triangle t \sum_{n=1}^{l} \frac{1}{48} (\triangle t)^3 \int_{t_{n-1}}^{t_n} \|p_{tt}\|^2 \, dt \right) \\
\leq \;& C\,\nu^{-1} \left(h^{2s+2} \, |||p_{1/2}|||_{2,s+1}^2 \,+\, (\triangle t)^4 \, \|p_{tt}\|_{2,0}^2 \right) \qquad (7.44)
\end{aligned}
$$

We now bound the terms in $Intp(\mathbf{u}^n, p^n; \breve{E}^n)$. Using (.1), (.2), (.3),

$$
\begin{aligned}
\left(d_t \mathbf{u}^n - \mathbf{u}_t^{n-1/2}, \breve{E}^n \right) \;&\leq\; \frac{1}{2} \|\breve{E}^n\|^2 \,+\, \frac{1}{2} \|d_t \mathbf{u}^n - \mathbf{u}_t^{n-1/2}\|^2 \\
&\leq\; \frac{1}{2} \|E^n\|^2 \,+\, \frac{1}{2} \|E^{n-1}\|^2 \,+\, \frac{1}{2} \frac{(\Delta t)^3}{1280} \int_{t_{n-1}}^{t_n} \|\mathbf{u}_{ttt}\|^2 \, dt \,, \qquad (7.45)
\end{aligned}
$$

$$
\begin{aligned}
(\breve{p}^n - p^{n-1/2}, \nabla \cdot \breve{E}^n) \;&\leq\; \epsilon_1 \nu \|\nabla \breve{E}^n\|^2 \,+\, C\,\nu^{-1} \|\breve{p}^n - p^{n-1/2}\|^2 \\
&\leq\; \epsilon_1 \nu \|\nabla \breve{E}^n\|^2 \,+\, C\,\nu^{-1} \frac{(\Delta t)^3}{48} \int_{t_{n-1}}^{t_n} \|p_{tt}\|^2 \, dt \,, \qquad (7.46)
\end{aligned}
$$

$$
\begin{aligned}
(\mathbf{f}^{n-1/2} - \breve{\mathbf{f}}^n, \breve{E}^n) \;&\leq\; \frac{1}{2} \|\breve{E}^n\|^2 \,+\, \frac{1}{2} \|\mathbf{f}^{n-1/2} - \breve{\mathbf{f}}^n\|^2 \\
&\leq\; \frac{1}{2} \|E^n\|^2 \,+\, \frac{1}{2} \|E^{n-1}\|^2 \,+\, \frac{(\Delta t)^3}{48} \int_{t_{n-1}}^{t_n} \|\mathbf{f}_{tt}\|^2 \, dt \,, \qquad (7.47)
\end{aligned}
$$

$$
\begin{aligned}
\mathcal{A}(\breve{\mathbf{u}}^n - \mathbf{u}^{n-1/2}, \breve{E}^n) &= \nu(\nabla(\breve{\mathbf{u}}^n - \mathbf{u}^{n-1/2}), \nabla \breve{E}^n) \\
&\quad + \chi\left((\breve{\mathbf{u}}^n - \mathbf{u}^{n-1/2}) - G_N\overline{(\breve{\mathbf{u}}^n - \mathbf{u}^{n-1/2})}, \breve{E}^n\right) \\
&\leq \epsilon_2 \nu \|\nabla \breve{E}^n\|^2 + C\,\nu \|\nabla(\breve{\mathbf{u}}^n - \mathbf{u}^{n-1/2})\|^2 + \chi \frac{1}{4}\|\breve{E}^{n\,*}\|^2 \\
&\quad + \chi\left((\breve{\mathbf{u}}^n - \mathbf{u}^{n-1/2}) - G_N\overline{(\breve{\mathbf{u}}^n - \mathbf{u}^{n-1/2})}, \breve{\mathbf{u}}^n - \mathbf{u}^{n-1/2}\right) \\
&\leq \epsilon_2 \nu \|\nabla \breve{E}^n\|^2 + \frac{\chi}{4}\|\breve{E}^{n\,*}\|^2 + C\,\nu \frac{(\Delta t)^3}{48}\int_{t_{n-1}}^{t_n} \|\nabla \mathbf{u}_{tt}\|^2\, dt \\
&\quad + \chi \frac{1}{2}\delta^{4N+4}\|B^2(\breve{\mathbf{u}}^n - \mathbf{u}^{n-1/2})\|^2 + \chi\frac{1}{2}\|\breve{\mathbf{u}}^n - \mathbf{u}^{n-1/2}\|^2 \\
&\leq \epsilon_2 \nu \|\nabla \breve{E}^n\|^2 + \frac{\chi}{4}\|\breve{E}^{n\,*}\|^2 + C\,\nu \frac{(\Delta t)^3}{48}\int_{t_{n-1}}^{t_n} \|\nabla \mathbf{u}_{tt}\|^2\, dt \\
&\quad + C\,\chi\delta^{4N+4}\,(\Delta t)^3 \int_{t_{n-1}}^{t_n} \|\mathbf{u}_{tt}\|^2\, dt + C\,\chi(\Delta t)^3 \int_{t_{n-1}}^{t_n} \|\mathbf{u}_{tt}\|^2\, dt, \qquad (7.48)
\end{aligned}
$$

where in the estimate for the last term, in the last step, we use that B is a bounded operator from $L^2 \to L^2$ and (.1).

$$
\begin{aligned}
& b^*(\breve{\mathbf{u}}^n, \breve{\mathbf{u}}^n, \breve{E}^n) - b^*(\mathbf{u}^{n-1/2}, \mathbf{u}^{n-1/2}, \breve{E}^n) \\
&= b^*(\breve{\mathbf{u}}^n - \mathbf{u}^{n-1/2}, \breve{\mathbf{u}}^n, \breve{E}^n) + b^*(\mathbf{u}^{n-1/2}, \breve{\mathbf{u}}^n - \mathbf{u}^{n-1/2}, \breve{E}^n) \\
&\leq C\,\|\nabla(\breve{\mathbf{u}}^n - \mathbf{u}^{n-1/2})\|\,\|\nabla \breve{E}^n\|\,\left(\|\nabla \breve{\mathbf{u}}^n\| + \|\nabla \mathbf{u}^{n-1/2}\|\right) \\
&\leq C\,\nu^{-1}\left(\|\nabla \breve{\mathbf{u}}^n\|^2 + \|\nabla \mathbf{u}^{n-1/2}\|^2\right)\frac{(\Delta t)^3}{48}\int_{t_{n-1}}^{t_n} \|\nabla \mathbf{u}_{tt}\|^2\, dt + \epsilon_3 \nu \|\nabla \breve{E}^n\|^2 \\
&\leq C\,\nu^{-1}\frac{(\Delta t)^3}{48}\left(\int_{t_{n-1}}^{t_n} 2(\|\nabla \breve{\mathbf{u}}^n\|^4 + \|\nabla \mathbf{u}^{n-1/2}\|^4)\, dt \right. \\
&\qquad \left. + \int_{t_{n-1}}^{t_n} \|\nabla \mathbf{u}_{tt}\|^4\, dt\right) + \epsilon_3 \nu \|\nabla \breve{E}^n\|^2 \\
&\leq C\,\nu^{-1}\,(\Delta t)^4(\|\nabla \breve{\mathbf{u}}^n\|^4 + \|\nabla \mathbf{u}^{n-1/2}\|^4) \\
&\quad + C\,\nu^{-1}\,(\Delta t)^3 \int_{t_{n-1}}^{t_n} \|\nabla \mathbf{u}_{tt}\|^4\, dt + \epsilon_3 \nu \|\nabla \breve{E}^n\|^2\,. \qquad (7.49)
\end{aligned}
$$

Combining (7.45)-(7.49) we have that

$$
\begin{aligned}
2\triangle t \sum_{n=1}^{l} |Intp(\mathbf{u}^n, p^n; \breve{E}^n)| \;\leq\; & \triangle t\, C \sum_{n=0}^{l} \|E^n\|^2 + \triangle t\, \chi \frac{1}{2} \sum_{n=1}^{l} \|\breve{E}^{n\,*}\|^2 \\
& + (\epsilon_1 + \epsilon_2 + \epsilon_3) \triangle t\, \nu \sum_{n=0}^{l} \|\nabla \breve{E}^n\|^2 \\
& + C(\triangle t)^4 \left(\|\mathbf{u}_{ttt}\|_{2,0}^2 + \nu^{-1} \|p_{tt}\|_{2,0}^2 + \|\mathbf{f}_{tt}\|_{2,0}^2 \right. \\
& \quad + \nu \|\nabla \mathbf{u}_{tt}\|_{2,0}^2 + \nu^{-1} \|\nabla \mathbf{u}_{tt}\|_{4,0}^4 \\
& \quad + \nu^{-1} \||\nabla \mathbf{u}|\|_{4,0}^4 + \nu^{-1} \||\nabla \mathbf{u}_{1/2}|\|_{4,0}^4 \\
& \quad \left. + \chi\, \delta^{4N+4} \|\mathbf{u}_{tt}\|_{2,0}^2 + \chi \|u_{tt}\|_{2,0}^2 \right) . \qquad (7.50)
\end{aligned}
$$

Thus, with (7.39)-(7.44) and (7.50), from (7.38) we obtain

$$
\begin{aligned}
& \|E^l\|^2 \;+\; \triangle t \sum_{n=1}^{l} \nu \|\nabla \breve{E}^n\|^2 \;+\; \triangle t\, \chi \frac{1}{2} \sum_{n=1}^{l} \|\breve{E}^{n\,*}\|^2 \\
& \quad \leq \; \triangle t \sum_{n=0}^{l} C(\, \nu^{-3} \|\nabla \breve{\mathbf{u}}^n\|^4 + 1) \|E^n\|^2 \\
& \qquad + C\nu^{-1} \left(h^{2k} \||\mathbf{u}|\|_{4,k+1}^4 + h^{2k+1} \||\nabla \mathbf{u}|\|_{4,0}^4 + h^{2s+2} \||p_{1/2}|\|_{2,s+1}^2 \right) \\
& \qquad + C\nu^{-1}\, h^{2k} (\||\mathbf{f}|\|_{2,0}^2 + \|\mathbf{u}_h^0\|^2) + C\, \chi\, h^{2k+2} \||u|\|_{2,k+1}^2 + C\, \nu\, h^{2k} \||\mathbf{u}|\|_{2,k+1}^2 \\
& \qquad + C(\triangle t)^4 \left(\|\mathbf{u}_{ttt}\|_{2,0}^2 + \nu^{-1} \|p_{tt}\|_{2,0}^2 + \|\mathbf{f}_{tt}\|_{2,0}^2 \right. \\
& \qquad\quad + \nu \|\nabla \mathbf{u}_{tt}\|_{2,0}^2 + \nu^{-1} \|\nabla \mathbf{u}_{tt}\|_{4,0}^4 \\
& \qquad\quad + \nu^{-1} \||\nabla \mathbf{u}|\|_{4,0}^4 + \nu^{-1} \||\nabla \mathbf{u}_{1/2}|\|_{4,0}^4 \\
& \qquad\quad \left. + \chi\, \delta^{4N+4} \|\mathbf{u}_{tt}\|_{2,0}^2 + \chi \|u_{tt}\|_{2,0}^2 \right) . \qquad (7.51)
\end{aligned}
$$

Hence, with $\triangle t$ sufficiently small, i.e. $\triangle t < C(\nu^{-3} \||\nabla \mathbf{u}|\|_{\infty,0}^4 + 1)^{-1}$, from Gronwall's

Lemma (see (7.18), we have

$$
\begin{aligned}
\|E^l\|^2 \;+\; & \triangle t \sum_{n=1}^{l} \nu \|\nabla \breve{E}^n\|^2 \;+\; \triangle t\, \chi \frac{1}{2} \sum_{n=1}^{l} \|\breve{E}^{n\,*}\|^2 \\
\leq\; & C\nu^{-1} \left(h^{2k} |||\mathbf{u}|||^4_{4,k+1} \;+\; h^{2k+1} |||\nabla \mathbf{u}|||^4_{4,0} \;+\; h^{2s+2} |||p_{1/2}|||^2_{2,s+1} \right) \\
& + C\nu^{-1}\, h^{2k} (|||\mathbf{f}|||^2_{2,0} \;+\; \|\mathbf{u}_h^0\|^2) \;+\; C\,\chi\, h^{2k+2} |||u|||^2_{2,k+1} \;+\; C\,\nu\, h^{2k} |||\mathbf{u}|||^2_{2,k+1} \\
& + C(\triangle t)^4 \left(\|\mathbf{u}_{ttt}\|^2_{2,0} \;+\; \nu^{-1} \|p_{tt}\|^2_{2,0} \;+\; \|\mathbf{f}_{tt}\|^2_{2,0} \right. \\
& \qquad + \nu \|\nabla \mathbf{u}_{tt}\|^2_{2,0} \;+\; \nu^{-1} \|\nabla \mathbf{u}_{tt}\|^4_{4,0} \\
& \qquad + \nu^{-1} |||\nabla \mathbf{u}|||^4_{4,0} \;+\; \nu^{-1} |||\nabla \mathbf{u}_{1/2}|||^4_{4,0} \\
& \qquad \left. + \;\chi\, \delta^{4N+4} \|\mathbf{u}_{tt}\|^2_{2,0} + \chi \|u_{tt}\|^2_{2,0} \right) . \qquad (7.52)
\end{aligned}
$$

Estimate (7.23) then follows from the triangle inequality and (7.52).

To obtain (7.24), we use (7.52) and

$$
\begin{aligned}
& \|\nabla \left(\mathbf{u}^{n+1/2} - (\mathbf{u}_h^n + \mathbf{u}_h^{n-1})/2 \right) \|^2 \leq \|\nabla (\mathbf{u}^{n+1/2} - \breve{\mathbf{u}}^n)\|^2 \;+\; \|\nabla \breve{\Lambda}^n\|^2 \;+\; \|\nabla \breve{E}^n\|^2 \\
\leq\; & \frac{(\triangle t)^3}{48} \int_{t_{n-1}}^{t_n} \|\nabla \mathbf{u}_{tt}\|^2 \, dt \;+\; Ch^{2k} |\mathbf{u}^n|^2_{k+1} \;+\; Ch^{2k} |\mathbf{u}^{n-1}|^2_{k+1} \;+\; \|\nabla \breve{E}^n\|^2 .
\end{aligned}
$$

□

Corollary 7.1. *Under the assumptions of Lemma 7.1 and Theorem 7.1 we have that*

$$
\begin{aligned}
|||\mathbf{w} \;-\; \mathbf{u}_h|||_{\infty,0} \;&\leq\; C_2 e^{C_1 \nu^{-3/2} \|\mathbf{w}\|^2_{4,1}} \chi^{1/2}\, \delta^{N+1} \|B\mathbf{w}\|_{2,0} \;+\; \mathbf{F}(\triangle t, h, \delta, \chi) \;+\; Ch^{k+1} |||\mathbf{u}|||_{\infty,k+1} \\
|||\nabla(\mathbf{w} \;-\; \mathbf{u}_h)|||_{2,0} \;&\leq\; C_2 e^{C_1 \nu^{-3/2} \|\mathbf{w}\|^2_{4,1}} \chi^{1/2}\, \delta^{N+1} \|B\mathbf{w}\|_{2,0} \;+\; \mathbf{F}(\triangle t, h, \delta, \chi) \\
& \quad + C\nu^{1/2} (\triangle t)^2 ||\nabla \mathbf{u}_{tt}||_{2,0} \;+\; C\nu^{1/2} h^k |||\mathbf{u}|||_{2,k+1}
\end{aligned}
$$

with $\mathbf{F}(\triangle t, h, \delta, \chi)$ *defined as in Theorem 7.1.*

Proof. : The result follows immediately from Lemma 7.1, Theorem 7.1, and the triangle inequality. □

7.3 MESH REFINEMENT STUDY

In this section, we present a mesh refinement study of the 2D vortex decay problem of Chorin [13]. It was also used by Tafti [57] and John and Layton [31].

We define the domain $\Omega = (0,1)^2$ and specify

$$\begin{aligned} u1 &:= -\cos(n\pi x)\sin(n\pi y)\exp(-2n^2\pi^2 t/\tau), \\ u2 &:= \sin(n\pi x)\cos(n\pi y)\exp(-2n^2\pi^2 t/\tau), \\ p &:= -\frac{1}{4}(\cos(2n\pi x)+\cos(2n\pi y))\exp(-4n^2\pi^2 t/\tau). \end{aligned} \tag{7.53}$$

With the parameter $\tau = Re$ and appropriate (time dependent, Dirichlet) boundary conditions, this is a solution of the Navier-Stokes equations with $\mathbf{f} = 0$. The solution consists of an $n \times n$ array of oppositely signed vortices that decay as $t \to 0$.

h	$\|\|\mathbf{w}-\mathbf{u}_h\|\|_{L^\infty(0,T;L^2)}$	rate	$\|\|\nabla(\mathbf{w}-\mathbf{u}_h)\|\|_{L^\infty(0,T;L^2)}$	rate
1/4	$4.62593 \cdot 10^{-3}$		$2.79577 \cdot 10^{-2}$	
1/8	$5.94747 \cdot 10^{-4}$	2.96	$7.17742 \cdot 10^{-3}$	1.96
1/16	$7.69042 \cdot 10^{-5}$	2.95	$1.8104 \cdot 10^{-3}$	1.98
1/32	$1.84055 \cdot 10^{-5}$	2.06	$4.55369 \cdot 10^{-4}$	1.99
1/64	$1.65968 \cdot 10^{-5}$	0.15	$1.21047 \cdot 10^{-4}$	1.91

Table 2: Finite element convergence estimates for the TRM with $\delta = h^2$ and at $Re = 1$

For our purposes, we take (7.53) as the solution of (7.1)-(7.3) to illustrate the error estimates of Corollary 7.1, presented in Tables 2 and 4. Also, since $(u1, u2)$ is the eigenvector for the filter problem (3.2) we are able to exactly calculate the right hand side of TRM given by (7.4)-(7.6). Therefore, we also illustrate the error estimates given in Theorem 7.1 in Tables 3 and 5 . We specify the following parameters: $n = 1$, time step $\triangle t = 0.005$, final time $T = 0.5$, time relaxation parameter $\chi = 0.1$, order of deconvolution $N = 0$ and $\tau = Re$ with $Re = 1$ in Tables 2 and 3 and $Re = 10^4$ in Tables 4 and 5. For our computations, we assume $n = 1$, i.e. a 1×1 array of vortices and study the finite element convergence rates

h	$\|\|\mathbf{u}-\mathbf{u}_h\|\|_{L^\infty(0,T;L^2)}$	rate	$\|\|\nabla(\mathbf{u}-\mathbf{u}_h)\|\|_{L^\infty(0,T;L^2)}$	rate
1/4	$4.62507 \cdot 10^{-3}$		$2.79575 \cdot 10^{-2}$	
1/8	$5.94787 \cdot 10^{-4}$	2.96	$7.17747 \cdot 10^{-3}$	1.96
1/16	$7.73426 \cdot 10^{-5}$	2.94	$1.8106 \cdot 10^{-3}$	1.99
1/32	$1.93074 \cdot 10^{-5}$	2.00	$4.55615 \cdot 10^{-4}$	1.99
1/64	$1.68549 \cdot 10^{-5}$	0.19	$1.21286 \cdot 10^{-4}$	1.91

Table 3: Finite element convergence estimates for the TRM, with $\delta = h$ and at $Re = 1$

for fixed $\triangle t$, $\delta = h^2$ for Tables 2 and 4, $\delta = h$ for Tables 3 and 5, and as $h \to 0$. For the spatial discretization we chose the Taylor-Hood finite elements, i.e second order polynomial approximation for velocity and first order polynomial approximation for pressure.

h	$\|\|\mathbf{w}-\mathbf{u}_h\|\|_{L^\infty(0,T;L^2)}$	rate	$\|\|\nabla(\mathbf{w}-\mathbf{u}_h)\|\|_{L^\infty(0,T;L^2)}$	rate
1/4	$2.10541 \cdot 10^{-1}$		2.13246	
1/8	$4.32355 \cdot 10^{-2}$	2.28	$9.72472 \cdot 10^{-1}$	1.13
1/16	$8.65877 \cdot 10^{-3}$	2.31	$4.19813 \cdot 10^{-1}$	1.21
1/32	$1.26752 \cdot 10^{-3}$	2.77	$1.37417 \cdot 10^{-1}$	1.61
1/64	$9.92257 \cdot 10^{-5}$	3.67	$2.85818 \cdot 10^{-2}$	2.26

Table 4: Finite element convergence estimates for the TRM with $\delta = h^2$ and at $Re = 10^4$

The incompressibility constraint $\nabla \cdot \mathbf{u}$ in TRM is relaxed by setting

$$\alpha p_\alpha + \nabla \cdot \mathbf{u}_\alpha = 0\,, \tag{7.54}$$

where α is a small parameter. Now, the incompressibility constraint is no longer satisfied, but it can be proven (e.g. formula (5.16) in [26])

$$|\mathbf{u} - \mathbf{u}_\alpha|_1 + \|p - p_\alpha\|_0 \leq C\,\alpha\,. \tag{7.55}$$

h	$\|\|\mathbf{u}-\mathbf{u}_h\|\|_{L^\infty(0,T;L^2)}$	rate	$\|\|\nabla(\mathbf{u}-\mathbf{u}_h)\|\|_{L^\infty(0,T;L^2)}$	rate
1/4	$2.08249 \cdot 10^{-1}$		2.11457	
1/8	$4.2445 \cdot 10^{-2}$	2.29	$9.6155 \cdot 10^{-1}$	1.13
1/16	$8.49152 \cdot 10^{-3}$	2.32	$4.14752 \cdot 10^{-1}$	1.21
1/32	$1.25264 \cdot 10^{-3}$	2.76	$1.36138 \cdot 10^{-1}$	1.61
1/64	$1.02615 \cdot 10^{-4}$	3.61	$2.84635 \cdot 10^{-2}$	2.26

Table 5: Finite element convergence estimates for the TRM, with $\delta = h$ and at $Re = 10^4$

Therefore, as $\alpha \to 0$, the solution of the penalized problem converges to that of the unpenalized problem. For our computations, we used $\alpha = 10^{-6}$ and that restricts the L^2 errors to stope decreasing as we refine the mesh and thus the rates deteriorate. Tables 4 and 5 show the results of the convergence rates for higher $Re = 10^4$ for which the errors are bigger and therefore the rates are not affected by the penalization of the incompressibility condition.

7.4 A NUMERICAL ILLUSTRATION

We study herein a simple, underresolved flow with recirculation: the flow across a step. The most distinctive feature of this flow is a recirculating vortex behind the step, see Figure 5 for illustration. A discussion of this test problem can be also found in Gunzburger [26] and John and Liakos [32].

Thus, we will study a flow in the transition via shedding of eddies behind the step using Navier-Stokes equations + Time Relaxation, i.e. (7.4)-(7.6) with $N = 0$ (NSE + TR0), (7.4)-(7.6) with $N = 1$ (NSE + TR1) and NSE + nonlinear Time Relaxation with $N = 0$ (NSE + NTR0). We will compare these models with a LES model - the Smagorinsky model. Since NSE does not give good or even any vortex recirculation behind the step on coarser mesh, see Figure 6 and 7, there is a need to find models that can represent the shedding of the eddies correctly on a very coarse mesh so that the computational time is much more

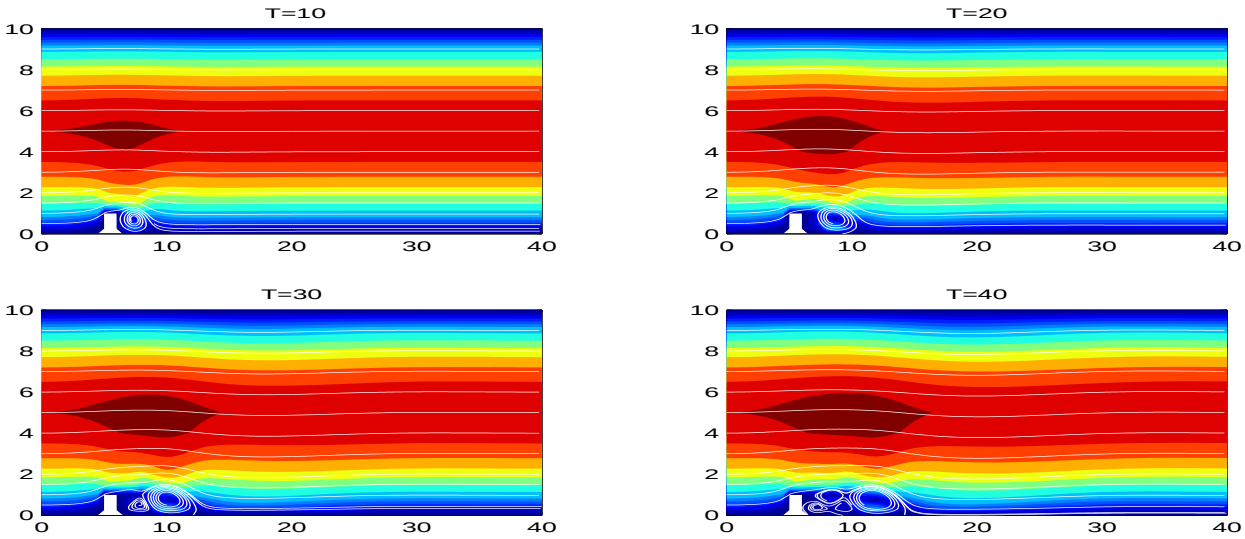

Figure 5: NSE at $\nu = 1/600$ and level 3 grid

shorter but the important properties of the flow are still captured.

The difference between NSE + TR0 and NSE + NTR0 is in the time relaxation term which has the form:

$$\chi|\mathbf{u} - \overline{\mathbf{u}}|(\mathbf{u} - \overline{\mathbf{u}})$$

in the NSE + NTR0. In this notation, by $|\cdot|$ we mean the Euclidean norm of the corresponding vector. We used $\chi = 0.01$ in the computations presented in this section. The only difference between the Navier-Stokes equations (NSE) and the Smagorinsky model (NSE + SMA) is in the viscous term, which has the following form:

$$\nabla \cdot ((2\nu + c_s\delta^2||\mathbb{D}(\mathbf{u})||_F)\mathbb{D}(\mathbf{u}))\,.$$

Here, c_s is a positive constant (usually $c_s \sim 0.01$, see Sagaut [54]), $\mathbb{D}(\mathbf{u})$ is the deformation tensor and $||\cdot||_F$ denotes the Frobenius norm of a tensor. We used $c_s = 0.01$ in the computations presented in this section. Although the Smagorinsky model is widely used, it has some drawbacks. These are well documented in the literature, e.g. see Zang, Street and Koseff

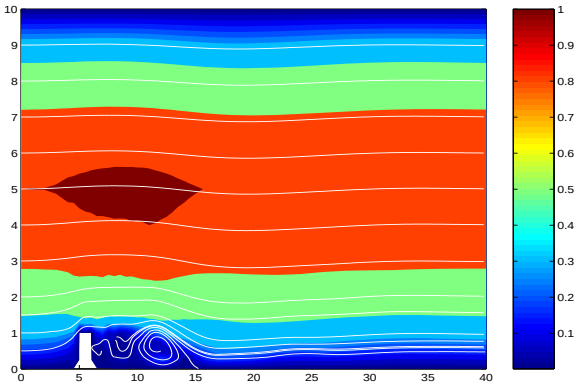

Figure 6: NSE at at $\nu = 1/600$, $T = 40$ and level 1 grid

[62]. For instance, the Smagorinsky model constant c_s is an á priori input and this single constant is not capable of representing correctly various turbulent flows. Another drawback of this model is that it introduces too much diffusion into the flow, e.g., see Iliescu, John, Matthies and Tobiska [29] or Figure 10.

The domain of the two-dimensional flow across a step is presented in Figure 8. We present results for a parabolic inflow profile, which is given by $\mathbf{u} = (u_1, u_2)^T$, with $u_1 = y(10-y)/25$, $u_2 = 0$. No-slip boundary condition is prescribed on the top and bottom boundary as well as on the step. At the outflow we have "do nothing" boundary condition (i.e. $\mathbf{n}\cdot(-\nu\nabla\mathbf{u}+p\mathbb{I}) = 0$ where $\mathbf{n}$ is the outward normal vector), an accepted outflow condition in computational fluid dynamics (CFD).

The computations were performed on various grids. For instance, for the fully resolved NSE simulation, which is our "truth" solution, we used a fine grid level 3, with number of degrees of freedom $N_{dof} = 41502$, whereas much coarser grids (level 0 with $N_{dof} = 2072$ and level 1 with $N_{dof} = 6903$) have been used for the investigation of NSE + TR0, NSE + TR1, NSE + NTR0 and NSE + SMA. The point is obviously to compare the performance of the various options in underresolved simulations by comparison against a "truth"/fully-resolved solution.

The computations were performed with the software FreeFem++; see [27] for its descrip-

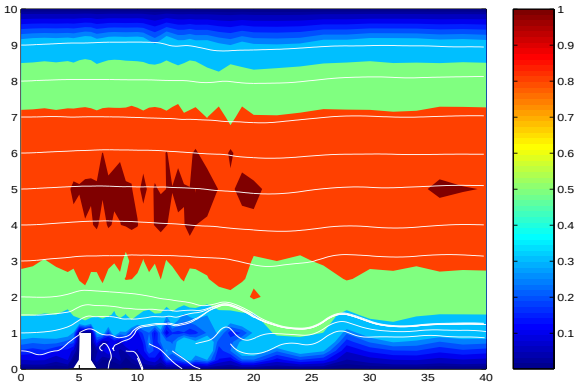

Figure 7: NSE at at $\nu = 1/600$, $T = 40$ and level 0 grid

tion. The models were discretized in time with the Crank Nicolson (an implicit scheme of second order) and in space with the Taylor Hood finite-element method, i.e., the velocity is approximated by continuous piecewise quadratics and the pressure by continuous piecewise linears. The coarse grid level 0 which was used in the computations is given in Figure 9. The background color represents the norm of the velocity vectors.

Comparing the Figures 10, 11, 12, 13 with 5 we conclude that the NSE + TR0, NSE + TR1 and NSE + NTR0 tests replicate the shedding of eddies and the Smagorinsky eddy remains attached. Clearly, the Smagorinsky model is too stabilizing: eddies which should separate and evolve remain attached and attain steady state. However, regarding the main point of study, the effects of the Time Relaxation on the truncation of scales, it is clear that this approach of regularization of NSE improved the simulation results for this transition problem. On the coarsest grid level 0 (see Figure 14) we obtained that NSE+NTR0 gives the best results out of all time relaxation forms and NSE. Further studies and tests of this approach are thus well merited!

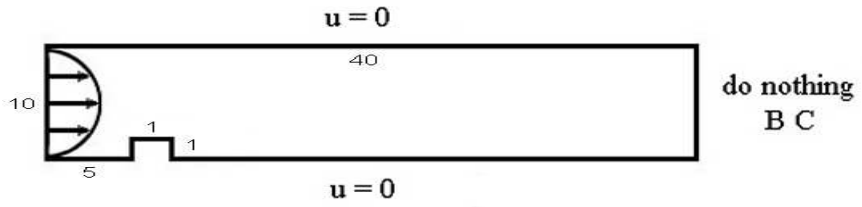

Figure 8: Boundary conditions

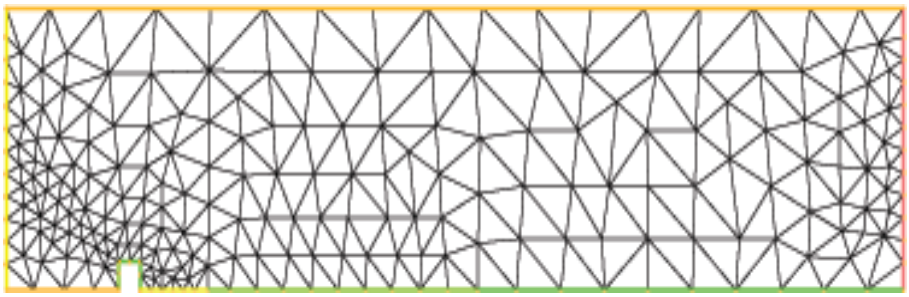

Figure 9: Mesh at level 0

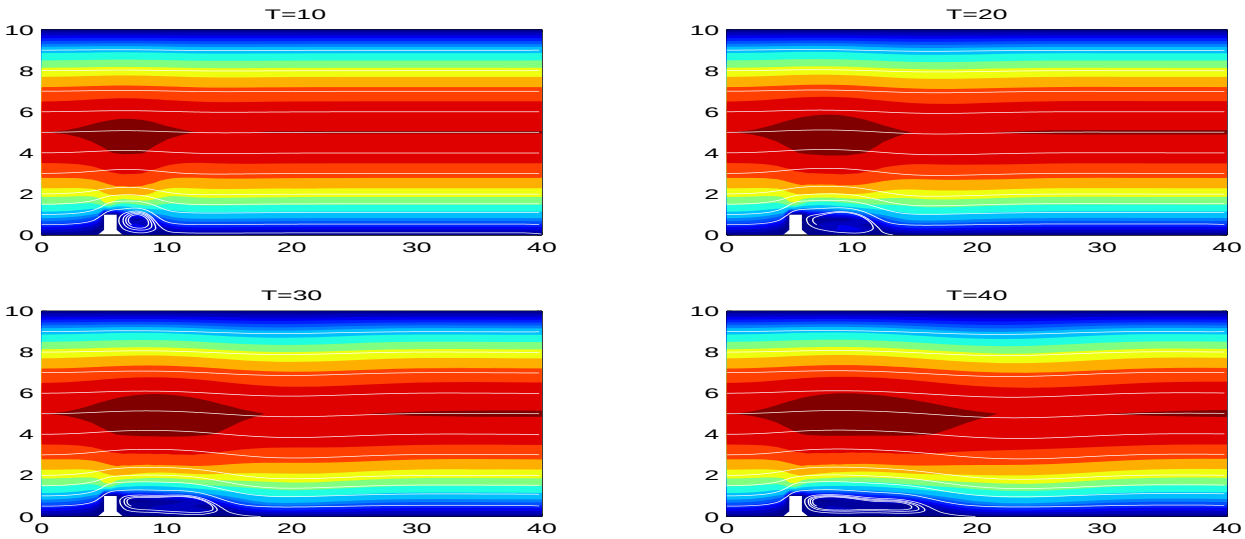

Figure 10: NSE + SM at $\nu = 1/600$, $\delta = 1.5$ and level 1 grid

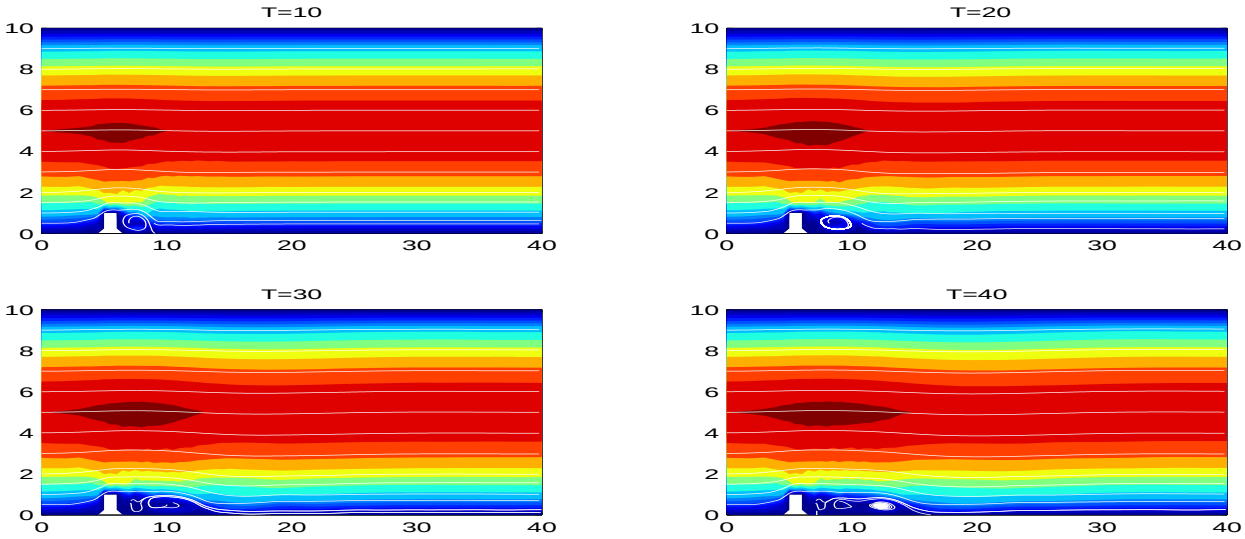

Figure 11: NSE + TR0 at $\nu = 1/600$, $\delta = 1.5$ and level 1 grid

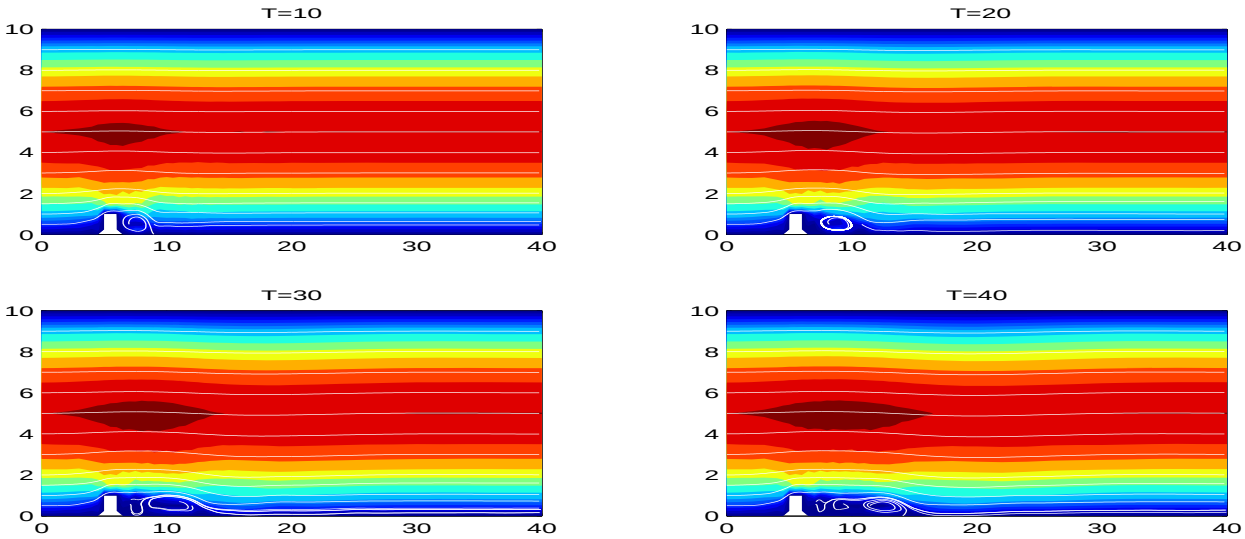

Figure 12: NSE + TR1 at $\nu = 1/600$, $\delta = 1.5$ and level 1 grid

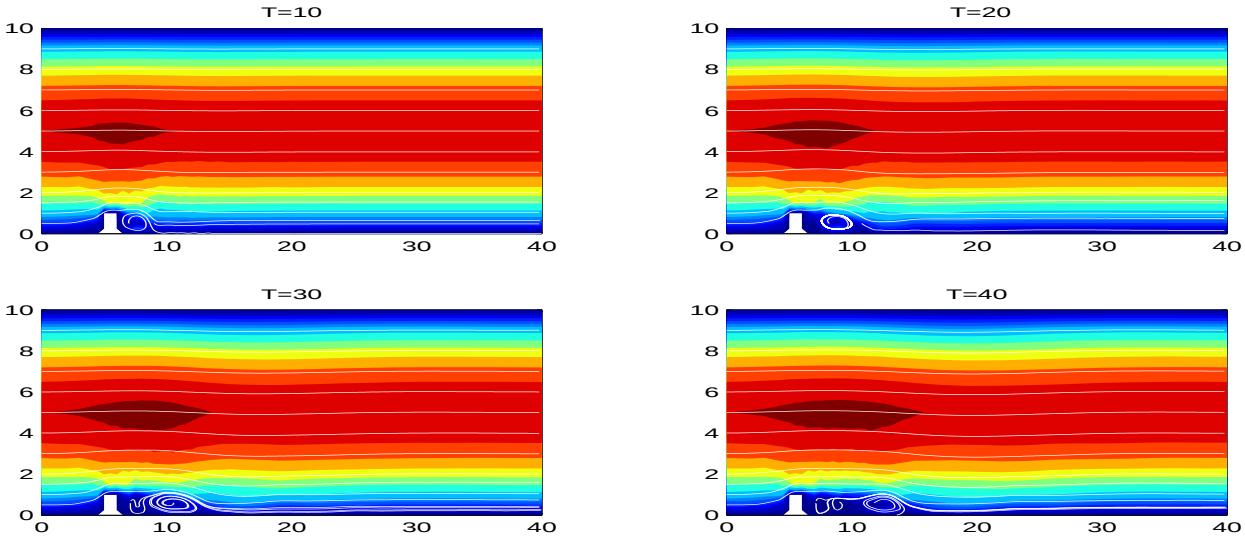

Figure 13: NSE + NTR0 at $\nu = 1/600$, $\delta = 1.5$ and level 1 grid

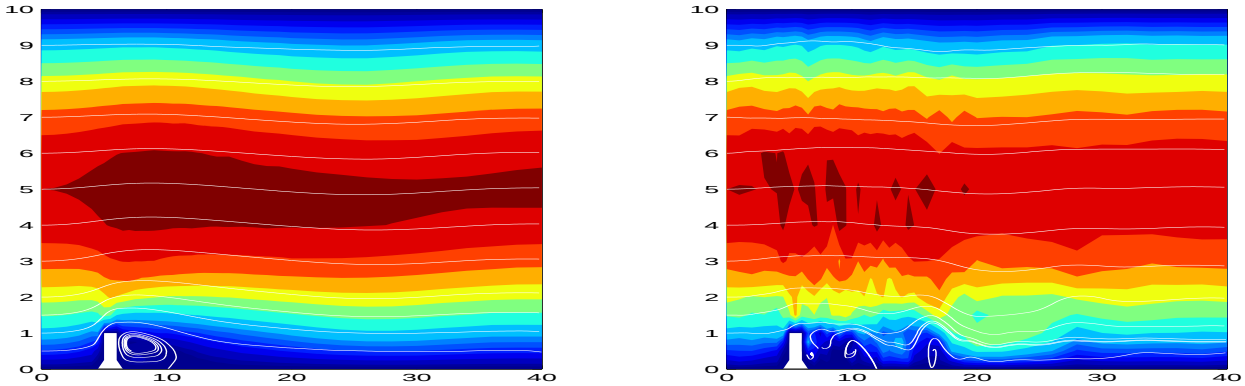

Figure 14: NSE+SM (left) and NSE+NTR0 (right) at $\nu = 1/600$, $\delta = 3.0$, level 0 grid

8.0 CONCLUSIONS AND FUTURE RESEARCH

Turbulence models should have a faithful representation of the mean effects of the unresolved scales on the resolved scales, a deep condition that is related to the physical fidelity of the flow statistics of energy and helicity predicted by the models. One way to obtain useful insights is to develop similarity theory of the models. Turbulent statistics predicted by the models should be compared to those of the NSE through the filter length-scale, i.e. on the large/resolved scales since the models are used to predict these scales. Each such test of the models gives evidence that, in the mean, the representation of the mean effects of the unresolved scales is accurate and the important flow statistics are correctly predicted.

In Chapter 4 we showed that Approximate Deconvolution Models possesses an energy cascade that truncates the true energy spectrum in two ways. First, there is an enhanced viscosity acting in the model. This enhanced viscosity does not dissipate energy for laminar shear flows and its amount is related to the local curvature of the velocity field. Further, it disappears when $\nu = 0$. The action of this enhanced viscosity is to trigger exponential decay of eddies at the models' micro-scale The second way the ADM truncates the scales of motion is through an energy sponge in the models' kinetic energy. The extra term triggers an accelerated energy decay of $O(k^{-\frac{11}{3}})$ at the cutoff length scale. *Above the cutoff length scale the ADM predicts the correct energy cascade!*

The main open question not resolved in the similarity theory of ADM pertains to the unknown, non-dimensional function $f(\Pi_2)$. The principle of economy of explanation suggests that $f(\Pi_2)$ is constant, and this is supported, strongly by Kraichnan's dynamic theory of turbulence, subsection 4.2.1. This question can be resolved by numerical experiments on the model itself (not on the Navier-Stokes equations) establishing the curve between the Π 's. Having this curve we can get complete quantitative information. Suppose that the

E_{model} is desired for conditions k_a and δ_a. The dimensionless group $(\Pi_2)_a$ can be immediately evaluated as $k_a\delta_a$. Corresponding to this value of $(\Pi_2)_a$, the value of $(\Pi_1)_a$ is read off the plot. $(E_{model})_a$ is then computed.

Kolmogorov theory enables us to determine the behavior of small scale motion in the inertial range but does not determine a function of $\eta\mathbf{k}$ for large wave-numbers where dissipation occurs. To resolve this problem various transfer theories developed for Navier-Stokes equations have been proposed by Heisenberg, Pao and others (see [60]). Thus another open question is to understand the dissipation subrange of ADM by using the transfer theories suitably adapted.

In Chapter 5 a joint energy and helicity cascade has been shown to exist for homogeneous, isotropic turbulence generated by ADM. The models' energy and helicity both cascade at the correct $O(k^{-5/3})$ rate for inertial range wave-numbers up to the cutoff wave-number of $O(\frac{1}{\delta})$, and at $O(k^{-11/3})$ afterward until the models' energy and helicity micro-scale. This establishes consistency of the model's helicity and energy cascades with the corresponding cascades of the true, underlying turbulent flow. Furthermore, we show the consistency of the ADM joint cascade up to the $k_{E_{model}}$, i.e. the inertial range for helicity is the same as for the energy.

Approximate Deconvolution Models have high accuracy in the large scales and give approximations of all resolved scales of high physical fidelity and with the correct statistics. The main drawback is that their micro-scale is substantially beyond the cutoff length-scale δ. This can be corrected by adding an appropriate time relaxation term analyzed in Chapter 6 or by using a different filter.

Tracking the effects of the choice of filter backward through the analysis of energy cascade and joint energy-helicity cascade leads to a very simple conclusion. The secondary cascade $(k^{-11/3})$ of the models' solution results because the filter decays like

$$\widehat{G}(k) \simeq k^{-2} \quad \text{and} \quad -5/3 + (-2) = -11/3$$

It is easy to check, for example, tracking forward that if the filter arises from $4th$ order (hyperviscosity like) operator with symbol decaying like k^{-4} then the secondary cascade will have exponent $k^{-17/3}$ (i.e. $-17/3 = -5/3 + (-4)$). Continuing, if a gaussian filter (which

has exponential decay in wave-number space) is used, then exponential decay of the energy spectrum begins at the cutoff frequency. This immediate truncation might compensate in some calculation for its extra complexity.

In Chapter 6 was shown that the Time Relaxation Model possesses an energy cascade that truncates the energy spectrum at a point that depends upon the relaxation parameter, the global velocity and length scale and the averaging radius δ. The time relaxation term does not dissipate energy for the resolved scales of the flow. The action of this time relaxation term is to induce a micro-scale, analogous to the Kolmogorov micro-scale in turbulence, and to trigger decay of eddies at the model's micro-scale. The extra dissipation at the cutoff length scale induced by time relaxation must reduce the number of degrees of freedom needed (per time step) for a 3D turbulent flow simulation. With proper scaling of χ this extra dissipation will also balance the transfer of energy to those scales from the flow's power input and thus prevent a non-physical accumulation of energy around the cutoff length scale as well as force the model's micro-scale to coincide with the averaging radius δ.

With the formula derived herein, $\chi \simeq \frac{U}{L^{\frac{1}{3}}} 2^{N+1} \delta^{-\frac{2}{3}}$, the model's micro-scale is δ and the number of degrees of freedom (per time step) needed for a 3d turbulent flow simulation with the model (6.1) is

$$N_{dof} \simeq (\frac{L}{\delta})^3, \text{ independent of } Re \text{ !}$$

This leads to a *huge* computational speedup using (1.1) over a DNS of

$$(\frac{N_{dof}^{NSE}}{N_{dof}})^{\frac{4}{3}} \simeq (\frac{Re^{\frac{9}{4}}}{L^3 \delta^{-3}})^{\frac{4}{3}} = (\frac{\delta}{L})^4 \, Re^3.$$

Finally, the time relaxation studied herein, since it is a lower order term, is ideal for use with many other models (e.g., the ADM, the NSE-alpha model) to reduce further their computational complexity by accelerating the truncation of scales without altering a model's accuracy on the resolved scales. The above value of χ is derived for fully developed, turbulent flow. While it is smaller than other theoretical values, it is also possible that other flow settings, such as transition, would require other, still smaller values - an important open problem.

There are many open problems connected to finding rigorous proofs of this description directly from the Navier-Stokes equations and without assumptions of homogeneity or isotropy.

There are also other possible scale-dependent relaxation strategies which should be developed and compared to find the best tool for a given flow problem. It is also important to study the time relaxation operator used in a synthesis with other good models of turbulence. There does not seem to be a clear strategy of developing a general theory of such mixed models so the effect of such combinations must be investigated on a case by case basis.

Another interesting question is the parameter selection for time relaxation inside turbulent boundary layer, i.e. part of the flow into which the vorticity originally generated at the surface has spread. Another striking characteristic of turbulent boundary layers is the existence of coherent structures. These are vortical structures that retain their identity for many eddy-turnover times and which appear again and again in approximately the same shape. There are different criteria, such as the Q-criterion, λ_2-criterion (see [15]) that characterize convex low-pressure tubes which are generally associated with coherent vortices. Since turbulence models are used for the simulation of turbulent flows and the real engineering problems appear in complicated bounded domains, an interesting topic is the identification of these vortices in the boundary layers that get created by turbulence models.

Lastly, in Chapter 7 we have studied a continuous finite element discretization of the Time Relaxation Model. Thus understanding the effects of the time relaxation, when discretized, and performing a rigorous numerical analysis of the combination is a very important step that we performed. The successful simulations on the 2D step problem showed that that the extra stabilization induced by time relaxation does not retard the transition of the flow. Further experiments such as the $2D$ turbulent mixing layer problem (see [30]) are the next step. Then, other $3D$ benchmark problems are the topic of future investigation too.

In Section 7.4 we showed some preliminary experiments of the 2D step problem for a specific nonlinear time relaxation term. Future work on this topic will include a detail numerical study of a finite element scheme for the Nonlinear Time Relaxation Model (6.16) followed by numerical computations. Then the exploration of physical fidelity of (6.16) will continue through investigations of the fundamental physical quantities, such as kinetic energy and enstrophy in 2D and a deeper study of the important role of helicity in 3D.

Because of the lack of continuity constraint between elements, the Discontinuous Galerkin (DG) finite element methods offer several advantages over the classical continuous finite

element methods:

local mesh refinement and derefinement are easily implemented (several hanging nodes per edge are allowed)

the incompressibility condition is satisfied locally on each mesh element

unstructured meshes and domains with complicated geometries are easily handled.

Therefore, an interesting future work is to investigate theoretically and computationally the DG methods for the time relaxation.

Turbulence models have an enormous promise towards the improvement of prediction and understanding of turbulent flows. Thus, there is a need to advance the models from the mathematical point of view by investigating statistics of energy and helicity, developing better numerical algorithms and performing tests to validate them.

A.1 APPENDIX

Lemma .1.

$$\|\breve{\mathbf{u}}^n - \mathbf{u}^{n-1/2}\|^2 \;\leq\; \frac{1}{48}(\Delta t)^3 \int_{t_{n-1}}^{t_n} \|\mathbf{u}_{tt}\|^2 \, dt \,. \tag{.1}$$

Proof of Lemma .1:

$$\begin{aligned}
& \|\breve{\mathbf{u}}^n - \mathbf{u}^{n-1/2}\|^2 = \|\frac{1}{2}(\mathbf{u}^n + \mathbf{u}^{n-1}) - \mathbf{u}^{n-1/2}\|^2 \\
= \;& \frac{1}{4}\int_\Omega \left[\int_{t_{n-1/2}}^{t_n} \mathbf{u}_{tt}(\cdot,t)\,(t_n - t)\,dt \;+\; \int_{t_{n-1}}^{t_{n-1/2}} \mathbf{u}_{tt}(\cdot,t)\,(t - t_{n-1})\,dt \right]^2 d\mathbf{x} \\
\leq \;& \frac{1}{4}\int_\Omega 2\left[\left(\int_{t_{n-1/2}}^{t_n} \mathbf{u}_{tt}(\cdot,t)\,(t_n - t)\,dt \right)^2 + \left(\int_{t_{n-1}}^{t_{n-1/2}} \mathbf{u}_{tt}(\cdot,t)\,(t - t_{n-1})\,dt \right)^2 \right] d\mathbf{x} \\
\leq \;& \frac{1}{2}\int_\Omega \left[\int_{t_{n-1/2}}^{t_n} (\mathbf{u}_{tt}(\cdot,t))^2 \, dt \int_{t_{n-1/2}}^{t_n} (t_n - t)^2 \, dt \right. \\
& \left. + \int_{t_{n-1}}^{t_{n-1/2}} (\mathbf{u}_{tt}(\cdot,t))^2 \, dt \int_{t_{n-1}}^{t_{n-1/2}} (t - t_{n-1})^2 \, dt \right] d\mathbf{x} \\
= \;& \frac{1}{2}\int_\Omega \left[\frac{1}{3}\left(\frac{\Delta t}{2}\right)^3 \int_{t_{n-1/2}}^{t_n} (\mathbf{u}_{tt}(\cdot,t))^2 \, dt \;+\; \frac{1}{3}\left(\frac{\Delta t}{2}\right)^3 \int_{t_{n-1}}^{t_{n-1/2}} (\mathbf{u}_{tt}(\cdot,t))^2 \, dt \right] d\mathbf{x} \\
= \;& \frac{1}{48}(\Delta t)^3 \int_\Omega \int_{t_{n-1}}^{t_n} (\mathbf{u}_{tt}(\cdot,t))^2 \, dt \, d\mathbf{x} \\
= \;& \frac{1}{48}(\Delta t)^3 \int_{t_{n-1}}^{t_n} \|\mathbf{u}_{tt}\|^2 \, dt \,.
\end{aligned}$$

□

Lemma .2.

$$\|d_t\mathbf{u}^n - \mathbf{u}_t^{n-1/2}\|^2 \;\leq\; \frac{1}{1280}(\Delta t)^3 \int_{t_{n-1}}^{t_n} \|\mathbf{u}_{ttt}\|^2 \, dt \,. \tag{.2}$$

Proof of Lemma .2:

$$
\begin{aligned}
& \|d_t\mathbf{u}^n - \mathbf{u}_t^{n-1/2}\|^2 = \|\frac{1}{\Delta t}(\mathbf{u}^n - \mathbf{u}^{n-1}) - \mathbf{u}_t^{n-1/2}\|^2 \\
= \; & \left(\frac{1}{4\,\Delta t}\right)^2 \int_\Omega \left[\int_{t_{n-1/2}}^{t_n} \mathbf{u}_{ttt}(\cdot,t)\,(t_n - t)^2\,dt \;+\; \int_{t_{n-1}}^{t_{n-1/2}} \mathbf{u}_{ttt}(\cdot,t)\,(t - t_{n-1})^2\,dt\right]^2 d\mathbf{x} \\
\leq \; & \left(\frac{1}{4\,\Delta t}\right)^2 \int_\Omega 2\left[\left(\int_{t_{n-1/2}}^{t_n} \mathbf{u}_{ttt}(\cdot,t)\,(t_n - t)^2\,dt\right)^2 \;+\; \left(\int_{t_{n-1}}^{t_{n-1/2}} \mathbf{u}_{ttt}(\cdot,t)\,(t - t_{n-1})^2\,dt\right)^2\right] d\mathbf{x} \\
\leq \; & 2\left(\frac{1}{4\,\Delta t}\right)^2 \int_\Omega \left[\int_{t_{n-1/2}}^{t_n} (\mathbf{u}_{ttt}(\cdot,t))^2\;dt \;\int_{t_{n-1/2}}^{t_n} (t_n - t)^4\,dt\right. \\
& \left. + \int_{t_{n-1}}^{t_{n-1/2}} (\mathbf{u}_{ttt}(\cdot,t))^2\;dt \;\int_{t_{n-1}}^{t_{n-1/2}} (t - t_{n-1})^4\,dt\right] d\mathbf{x} \\
= \; & 2\left(\frac{1}{4\,\Delta t}\right)^2 \int_\Omega \left[\frac{1}{5}\left(\frac{\Delta t}{2}\right)^5 \int_{t_{n-1/2}}^{t_n} (\mathbf{u}_{ttt}(\cdot,t))^2\;dt \;+\; \frac{1}{5}\left(\frac{\Delta t}{2}\right)^5 \int_{t_{n-1}}^{t_{n-1/2}} (\mathbf{u}_{ttt}(\cdot,t))^2\;dt\right] d\mathbf{x} \\
= \; & \frac{1}{1280}(\Delta t)^3 \int_\Omega \int_{t_{n-1}}^{t_n} (\mathbf{u}_{ttt}(\cdot,t))^2\;dt\,d\mathbf{x} \\
= \; & \frac{1}{1280}(\Delta t)^3 \int_{t_{n-1}}^{t_n} \|\mathbf{u}_{ttt}\|^2\,dt\,.
\end{aligned}
$$

□

For the vector $\mathbf{u}$, $\mathbf{u}^{(i)}$, $i = 1, \ldots \acute{d}$, denotes the ith component of the vector.

Lemma .3.

$$
\|\nabla(\breve{\mathbf{u}}^n - \mathbf{u}^{n-1/2})\|^2 \;\leq\; \frac{(\Delta t)^3}{48} \int_{t_{n-1}}^{t_n} \|\nabla \mathbf{u}_{tt}\|^2\,dt\,. \tag{.3}
$$

Proof of Lemma .3:

$$\|\nabla(\breve{\mathbf{u}}^n - \mathbf{u}^{n-1/2})\|^2 = \frac{1}{4}\int_\Omega \nabla\left\{\int_{t_{n-1/2}}^{t_n} \mathbf{u}_{tt}(\cdot,t)\,(t_n - t)\,dt \;+\; \int_{t_{n-1}}^{t_{n-1/2}} \mathbf{u}_{tt}(\cdot,t)\,(t - t_{n-1})\,dt\right\}$$

$$: \;\nabla\left\{\int_{t_{n-1/2}}^{t_n} \mathbf{u}_{tt}(\cdot,t)\,(t_n - t)\,dt \;+\; \int_{t_{n-1}}^{t_{n-1/2}} \mathbf{u}_{tt}(\cdot,t)\,(t - t_{n-1})\,dt\right\}\,d\mathbf{x}$$

interchanging differentiation and integration

$$= \frac{1}{4}\int_\Omega \left\{\int_{t_{n-1/2}}^{t_n} \nabla\mathbf{u}_{tt}(\cdot,t)\,(t_n - t)\,dt \;+\; \int_{t_{n-1}}^{t_{n-1/2}} \nabla\mathbf{u}_{tt}(\cdot,t)\,(t - t_{n-1})\,dt\right\}$$

$$: \left\{\int_{t_{n-1/2}}^{t_n} \nabla\mathbf{u}_{tt}(\cdot,t)\,(t_n - t)\,dt \;+\; \int_{t_{n-1}}^{t_{n-1/2}} \nabla\mathbf{u}_{tt}(\cdot,t)\,(t - t_{n-1})\,dt\right\}\,d\mathbf{x}$$

$$= \sum_{i,j=1}^{\acute{d}} \frac{1}{4}\int_\Omega \left(\int_{t_{n-1/2}}^{t_n} \mathbf{u}^i_{ttx_j}(\cdot,t)\,(t_n - t)\,dt \;+\; \int_{t_{n-1}}^{t_{n-1/2}} \mathbf{u}^i_{ttx_j}(\cdot,t)\,(t - t_{n-1})\,dt\right)^2 d\mathbf{x}$$

$$\le \sum_{i,j=1}^{\acute{d}} \frac{1}{4}\int_\Omega 2\left[\left(\int_{t_{n-1/2}}^{t_n} \mathbf{u}^i_{ttx_j}(\cdot,t)\,(t_n - t)\,dt\right)^2 + \left(\int_{t_{n-1}}^{t_{n-1/2}} \mathbf{u}^i_{ttx_j}(\cdot,t)\,(t - t_{n-1})\,dt\right)^2\right] d\mathbf{x}$$

$$\le \sum_{i,j=1}^{\acute{d}} \frac{1}{4}\int_\Omega 2\left[\int_{t_{n-1/2}}^{t_n} \left(\mathbf{u}^i_{ttx_j}(\cdot,t)\right)^2 dt \int_{t_{n-1/2}}^{t_n} (t_n - t)^2\,dt\right.$$

$$\left. + \int_{t_{n-1}}^{t_{n-1/2}} \left(\mathbf{u}^i_{ttx_j}(\cdot,t)\right)^2 dt \int_{t_{n-1}}^{t_{n-1/2}} (t - t_{n-1})^2\,dt\right] d\mathbf{x}$$

$$= \sum_{i,j=1}^{\acute{d}} \frac{1}{4}\int_\Omega 2\,\frac{1}{3}\left(\frac{\Delta t}{2}\right)^3 \int_{t_{n-1}}^{t_n} \left(\mathbf{u}^i_{ttx_j}(\cdot,t)\right)^2 dt\; d\mathbf{x}$$

$$= \frac{(\Delta t)^3}{48}\int_{t_{n-1}}^{t_n} \|\nabla\mathbf{u}_{tt}\|^2\,dt\,.$$

□

BIBLIOGRAPHY

[1] N. Adams and S. Stolz. A subgrid-scale deconvolution approach for shock capturing. *Journal of Computational Physics*, 178, 2002.

[2] N. A. Adams and S. Stolz. On the Approximate Deconvolution procedure for LES. *Phys. Fluids*, 2:1699–1701, 1999.

[3] N. A. Adams and S. Stolz. Deconvolution methods for subgrid-scale approximation in large eddy simulation. *Modern Simulation Strategies for Turbulent Flow*, 2001.

[4] S. Stolz N. Adams and L. Kleiser. The approximate deconvolution model for large-eddy simulations of compressible flows and its application to shock-turbulent-boundary-layer interaction. *Physics of Fluids*, 13, 2001.

[5] J. C. André and M. Lesieur. Influence of helicity on high Reynolds number isotropic turbulence. *Journal of Fluid Mechanics*, 81:187–207, 1977.

[6] L.C. Berselli, T. Iliescu, and W. J. Layton. *Mathematics of Large Eddy Simulation of Turbulent Flows*. Scientific Computation. Springer, 2006.

[7] M. Bertero and B. Boccacci. *Introduction to Inverse Problems in Imaging*. IOP Publishing Ltd., 1998.

[8] J. Bourne and S. Orszag. Spectra in helical three-dimensional homogeneous isotropic turbulence. *Physics Review Letters E*, 55:7005–7009, 1997.

[9] S. Brenner and L.R. Scott. *The Mathematical Theory of Finite Element Methods*. Springer-Verlag, 1994.

[10] A. Brissaud, U. Frisch, J. Leorat, and A. Mazure M. Lesieur. Helicity cascades in fully developed isotropic turbulence. *Physics of Fluids*, 16(8), 1973.

[11] Q. Chen, S. Chen, and G. Eyink. The joint cascade of energy and helicity in three dimensional turbulence. *Physics of Fluids*, 15(2):361–374, 2003.

[12] Q. Chen, S. Chen, G. Eyink, and D. Holm. Intermittency in the joint cascade of energy and helicity. *Physical Review Letters*, 90: 214503, 2003.

[13] A.J. Chorin. Numerical solution of the navier-stokes equations. *Math. Comp.*, 22:754–762, 1968.

[14] R.L. Daugherty and J.B. Franzini. *Fluid mechanics with engineering application.* McGraw-Hill, New York, 1977.

[15] P.A. Davidson. *Turbulence - An introduction for scientists and engineers.* Oxford University Press, 2004.

[16] P. Ditlevsen and P. Giuliani. Cascades in helical turbulence. *Physical Review E*, 63, 2001.

[17] P. Ditlevsen and P. Giuliani. Dissipation in helical turbulence. *Physics of Fluids*, 13, 2001.

[18] A. Dunca and Y. Epshteyn. On the Stolz-Adams deconvolution model for the large-eddy simulation of turbulent flows. *SIAM J. Math. Anal.*, 37(6):1890–1902, 2006.

[19] C. Foias, D. Holm, and E. Titi. The Navier-Stokes-alpha model of fluid turbulence. *Physica D*, pages 505–519, May 2001.

[20] U. Frisch. *Turbulence.* Cambridge University Press, 1995.

[21] G.P. Galdi. Lectures in mathematical fluid dynamics. *Bikhauser-Verlag*, 2000.

[22] G.P. Galdi. An introduction to the mathematical theory of the navier-stokes equations. *Springer*, I, Berlin, 1994.

[23] M. Germano. Differential filters for the large eddy numerical simulation of turbulent flows. *Phys. Fluids*, 29:1755–1757, 1986.

[24] B.J. Geurts. Inverse modeling for large eddy simulation. *Phys. Fluids*, 9:3585, 1997.

[25] R. Guenanff. *Non-stationary coupling of Navier-Stokes/Euler for the generation and radiation of aerodynamic noises.* PhD thesis, Dept. of Mathematics, Université Rennes 1, Rennes, France, 2004.

[26] M.D. Gunzburger. *Finite Element Methods for Viscous Incompressible Flows - A Guide to Theory, Practices, and Algorithms.* Academic Press, 1989.

[27] F. Hecht and O. Pironneau. Freefem++. webpage: http://www.freefem.org.

[28] J. Heywood and R. Rannacher. Finite element approximation of the nonstationary Navier-Stokes problem. Part IV: Error analysis for the second order time discretization. *SIAM J. Numer. Anal.*, 2:353–384, 1990.

[29] T. Iliescu, V. John, W. J. Layton, G. Matthies, and L. Tobiska. A numerical study of a class of LES models. *Int. J. Comput. Fluid Dyn.*, 17:75 – 85, 2003.

[30] V. John. *Large Eddy Simulation of Turbulent Incompressible Flows.* Springer, Berlin, 2004.

[31] V. John and W. Layton. Analysis of numerical errors in large eddy simulation. *SIAM J. Numer. Anal.*, 40(3):995–1020, 2002.

[32] V. John and A. Liakos. Time dependent flow across a step: the slip with friction boundary condition. *Int. J. Numer. Meth. Fluids*, 50:713–731, 2006.

[33] A. V. Kolmogorov. The local structure of turbulence in incompressible viscous fluids for very large reynolds number. *Dokl. Akad. Nauk SSR*, 30:9–13, 1941.

[34] R. Kraichnan. Inertial-range transfer in two- and three-dimensional turbulence. *Journal of Fluid Mechanics*, 47, 1971.

[35] W. Layton. Introduction to the numerical analysis of incompressible, viscous flow phenomena. Lecture Notes, 2007.

[36] W. Layton and R. Lewandowski. On the leray deconvolution models. *Analysis and Applications*, to appear, 2007.

[37] W. Layton, C. Manica, M. Neda, and L. Rebholz. The joint helicity-energy cascade for homogeneous isotropic turbulence generated by approximate deconvolution models. Technical report, University of Pittsburgh, 2006.

[38] W. Layton and M. Neda. Truncation of scales by time relaxation. *Journal of Mathematical Analysis and Applications*, 325:788–807, 2007.

[39] W. Layton and M. Neda. The energy cascade for homogeneous, isotropic turbulence generated by approximate deconvolution models. *Journal of Mathematical Analysis and Applications*, to appear, 2007.

[40] R. Lewandowski and W. Layton. On a well posed turbulence model. *Discrete and continuous dynamical systems B*, 6(1):111–128, 2006.

[41] R. Lewandowsky and W. Layton. Residual stress of approximate deconvolution large eddy simulation models of turbulence. *Journal of Turbulence*, 46(2):1–21, 2006.

[42] D.K. Lilly. The representation of small-scale turbulence in numerical simulation experiments. *Proceedings IBM Scientific Computing Symposium on Environmental Sciences*, Yorktown Heights, 1967.

[43] H. Moffatt. Simple topological aspects of turbulent vorticity dynamics. In T. Tatsumi, editor, *Proc. IUTAM Symposium on Turbulence and Chaotic Phenomena in Fluids*, pages 223–230. Elsevier, 1984.

[44] H. Moffatt and A. Tsoniber. Helicity in laminar and turbulent flow. *Annual Review of Fluid Mechanics*, 24:281–312, 1992.

[45] J.J. Moreau. Constantes d'unilot tourbilloinnaire en fluide parfait barotrope. *C.R. Acad.Aci. Paris*, 252:2810–2812, 1961.

[46] A. Muschinsky. A similarity theory of locally homogeneous and isotropic turbulence generated by a Smagorinsky-type LES. *Journal of Fluid Mechanics*, 325:239–260, 1996.

[47] S. Pope. *Turbulent Flows*. Cambridge University Press, 2000.

[48] C. Pruett. Temporal large-eddy simulation: Theory and practice. *Theoretical and Computational Fluid Dynamics*, 2006, in press.

[49] L. Rebholz. Conservation laws of turbulence models. *Journal of Mathematical Analysis and Applications*, 326(1):33–45, 2007.

[50] O. Reynolds. On the dynamic theory of incompressible viscous fluids and the determination of the criterium. *Phil. Trans. R. Soc. London*, A 186:123–164, 1895.

[51] P. Rosenau. Extending hydrodynamics via the regularization of the chapman-enskog expansion. *Phys. Rev. A*, 40:7193, 1989.

[52] N. A. Adams S. Stolz and L. Kleiser. *Advances in LES of complex flows*, chapter The approximate deconvolution model for compressible flows: isotropic turbulence and shock-boundary-layer interaction. Kluwer, Dordrecht, 2002.

[53] S.G. Saddoughi and S.V. Veeravalli. Local isotropy in turbulent boundary layers at high reynolds nuber. *J. Fluid Mechanics*, 268:333–372, 1994.

[54] P. Sagaut. *Large Eddy Simulation for Incompressible Flows*. Springer, Berlin, 2001.

[55] S. Schochet and E. Tadmor. The regularized chapman-enskog expansion for scalar conservation laws. *Arch. Rat. Mech. Anal.*, 119:95, 1992.

[56] S. Stolz, N. Adams, and L. Kleiser. An approximate deconvolution model for large-eddy simulation with application to incompressible wall-bounded flows. *Phys. Fluids*, 13:997–1015, 2001.

[57] D. Tafti. Comparison of some upwind-based high order formulations with a second-order central-difference scheme for time integration of the incompressible navier-stokes equations. *Comput. ℘ Fluids*, 25(7):647–665, 1996.

[58] W. Layton V. Ervin and Monika Neda. Numerical analysis of a higher order time relaxation model of fluids. *International Journal of Numerical Analysis and Modeling*, 4:648–670, 2007.

[59] F. Waleffe. The nature of triad interactions in homogeneous turbulence. *Phys. Fluids A*, 1992.

[60] Z.U.A. Warsi. *Fluid Dynamics - Theoretical and Computational Approaches.* CRC Press, 1993.

[61] J.C. Wyngaard and Y.H. Pao. Some measurements of fine structure of large reynolds number turbulence. *Lecture Notes in Physics*, 12:384–401, 1972.

[62] Y. Zang, R. L. Street, and J. R. Koseff. A dynamic mixed subgrid-scale model and its application to turbulent recirculating flows. *Phys. Fluids A*, 5:3186–3196, 1993.

[63] E. Zeidler. *Applied Functional Analysis: Applications to Mathematical Physics.* Springer-Verlag, New York, 1995.